

STATIONARY SPHERICAL OPTICALLY THICK ACCRETION
INTO BLACK HOLES

Thesis by

Richard Alan Flammang

In Partial Fulfillment of the Requirements
for the Degree of
Doctor of Philosophy

California Institute of Technology
Pasadena, California

1982

(Submitted January 4, 1982)

Λαμπαδια εχοντες διαδωσουσιν αλληλοις .

- *Plato*

Χαλεπα τα καλα εστιν οπη εχει μαθειν .

- *ancient, quoted by Socrates in
Plato's "Cratylus"*

Εκ θαμινησ ραθαμιγγος , οπωσ λογος αιεν
ιοισασ , χα λιθοσ εσ βρωχμον κοιλαινεται .

- *Bion*

Η πιθι η απιθι .

- *anonymous*

PREFACE

There are many individuals and organizations who contributed to the successful completion of this thesis. It is a pleasure to extend my thanks to all of them here.

First, thanks are due to Caltech and especially to its Physics Department for admitting a recycled economist to its graduate program, for making available to me sound training in the methods of theoretical physics, and for providing me with a relaxed yet very stimulating place to work. Everyone knows that Caltech is a very special place. For my part, it has been both very rewarding and a privilege to be associated with Caltech.

The Physics Department at Caltech provided a great deal of the financial wherewithal for this thesis by making teaching assistantships available to me. I hope I repaid that account to some extent by my performance in the classroom. The other principal source of financial support for this thesis came in the form of research assistantships from Kip Thorne's National Science Foundation grants. I thank Kip, the National Science Foundation, and the American taxpayer for these. I also received support from the Schlumberger Foundation and the Danforth Foundation. I would particularly like to thank the Danforth Foundation for their support over the years and especially during the difficult time when I was switching from economics to physics.

My advisor for this project has been Kip Thorne. Kip's interest in black holes in stars served as the impetus for this study of

optically thick accretion. I thank Kip for his advice, his implicit faith in my ability to do good science, and for a supply of patience that is simply staggering. I also owe special thanks to G. B. Witham, whose comments on the distinction between high and low order waves in hyperbolic systems led to my understanding of the critical point structure of this problem.

I turned to Yekta Gürsel on countless occasions for guidance and help with the computing involved in this project. He never failed to tell me just what I needed to know. JoAnn Boyd typed up much of this thesis in a frantic rush, working late after hours. Her typing remained impeccable even after a considerable collection of empty Coors cans had piled up beside her typewriter. Thank you JB. Thanks also to Lynn Finger, who did a fine job typing up most of the rest of this thesis via correspondence while I was in Austin, Texas. I thank Carl Caves for a much valued friendship and for his wise counsel on how to cope with the vagaries and vicissitudes of completing a Ph.D. I thank Bill DeCampli and ArieH Königl for the considerable inspiration and encouragement they provided me by showing, by their example, that it was possible to get jobs in astrophysics. I also thank David Payne and Roger Blandford for helpful advice and encouragement.

Throughout the entire period of this study, my family, especially my parents, have provided support, encouragement, and, on many memorable occasions, some much needed diversion from the task. Thanks also go to Frances and Ted at L'Omelette. I would also like to express here my gratitude to Craig Wheeler and

Greg Shields at the University of Texas at Austin for making a postdoctoral position available to me after this work was completed. Finally, I thank Elsje for being there when it was all over with.

ABSTRACT

As its title indicates, this thesis treats the problem of stationary, spherical, optically thick accretion into black holes. By the phrase "optically thick" it is meant that (1) radiative energy transport can be adequately described by the diffusion approximation and (2) the photons are everywhere in local energy equilibrium (LTE) with the accreting gas particles.

In Chapter 1, a general set of equations governing time-independent spherical accretion into black holes is formulated. The equations are fully general relativistic and are applicable to optically thick regions, optically thin regions, and the transition regions which join them. The radiation is treated using frequency-integrated moments. The full, infinite series of moment equations is given, together with the limiting forms the equations take in the optically thick regime.

In Chapter 2, we present the mathematical theory of stationary spherical optically thick accretion. We analyze the integral curves of the differential equations describing the problem. We find a one-parameter family of critical points, where the inflow velocity equals the isothermal sound speed. Physical solutions must pass through one of these critical points. We obtain a complete set of boundary conditions which the solution must satisfy at the horizon of the black hole, and show that these, plus the requirement that the solution pass through a critical point, determine a unique solution to the problem. This analysis leads to a generalization

of the well-known Bondi critical point **constraint**, which arises in the adiabatic accretion problem and which is effective at the point where the inflow velocity equals the adiabatic sound speed. We show that this point can be regarded as a "diffused critical point" in our problem. The analysis also yields a simple expression for the diffusive luminosity at radial infinity. Finally, we find a satisfying explanation for the rather peculiar critical point structure of this problem in an analysis of the characteristics and subcharacteristics present in the problem and in a "hierarchical" analysis of the waves which propagate along them.

In Chapter 3, we apply the theory of optically thick accretion developed in Chapter 2 to a wide range of physically different accretion regimes. Numerical solutions are presented and their physical properties are discussed. For solutions in which radiation pressure P_R dominates gas pressure P_G , but in which gas energy density (including its rest-mass) ρ_G dominates radiation energy density ρ_R , we pay particular attention to the adabaticity of the flow. Our quantitative results in this regime agree very well with Begelman's (1978) theory. We find the dimensionless number which governs the importance of heat diffusion in our problem and show that it reduces to the idea of "trapping of photons" and to the Péclet number in the appropriate limits. We find that solutions with $P_R > P_G$ and $\rho_R > \rho_G$ are always essentially adiabatic, owing in part to a relativistic suppression of heat flux which becomes important in this regime. The diffusive luminosity at infinity for these solutions is the Eddington limit of the black hole; with the adiabatic accretion rate, "efficiencies" of up to order unity are possible. We give preliminary

consideration to the question of the stability of our solutions against convection and conclude that the Schwarzschild criterion is applicable, even for our non-static accretion flows. We show that solutions with $P_R > P_G$ are everywhere stable against convection. On the other hand, solutions which start out at radial infinity with $P_G > P_R$ are unstable to convection (if the adiabatic index of the gas γ_G exceeds 17/12) from radial infinity down to the point where $P_R \sim P_G$ and the radiation-gas mixture has attained an adiabatic index of 17/12. Inside this point, the solution is stable against convection. The diffusive luminosity at infinity for these solutions is reduced from the Eddington limit of the black hole by the factor $(\gamma_G - 1)4P_{R\infty}/\gamma_G P_{G\infty}$; it is further reduced by the ratio of the electron scattering opacity to the actual opacity at infinity, if this differs from unity. In most cases, energy diffusion has a negligible effect on the accretion rate of these solutions.

TABLE OF CONTENTS

Chapter 1.	Stationary Spherical Accretion into Black Holes:	
	Equations of Structure	1
	Abstract	2
	1. Introduction	2
	2. The Equations	3
	3. Discussion	9
	References	11
	Appendix. A Note on Units	11
Chapter 2.	The Theory of Optically Thick Accretion	12
	Abstract	13
	1. Introduction	13
	2. The Basic Equations	18
	3. The Adiabatic Problem	23
	4. Discussion of Basic Equations	26
	5. The Quasi-Exponential Behavior of the Luminosity	29
	6. Construction of Solutions	32
	7. Behavior near the Sonic Surface	37
	8. Behavior at Large Radii	41
	9. The Theory of Critical and Subcritical Points	45

10. Example of Numerical Solution	58
11. Conclusion	59
Acknowledgements	62
References	63
Appendix A. Derivation of Basic Equations	65
Appendix B. Derivation of First-Order Derivatives	68
Appendix C. Two Integral Curves through Each Critical Point	72
Appendix D. The Growth Rate k Governing the Quasi-Exponential Behavior of the Luminosity	73
Appendix E. Formal Solution for the Luminosity	75
Appendix F. Derivation of the Basic Perturbation Equation	79
Table	85
Figure Captions	86
Figures	89
Chapter 3. Optically Thick Accretion in Specific Cases	100
Abstract	101
1. Introduction	103
2. Numerical Method	105
3. Solutions with $P_R > P_G$, $\rho_G > \rho_R$	107

4. The Dimensional-Analysis Approach to the Question of Adiabaticity	114
5. Relativistic Accretion: The Case $\rho_R > \rho_G$	118
6. Stability Against Convection	121
7. Solutions with $P_{G\infty} > P_{R\infty}$	127
8. Conclusion	134
Acknowledgement	136
References	137
Appendix. Derivation of the Dimensionless Number which Characterizes the Importance of Energy Diffusion	138
Tables	139
Figure Captions	141
Figures	142

Chapter 1

Stationary Spherical Accretion into Black Holes:
Equations of Structure

This chapter is a paper by Kip S. Thorne, Richard A. Flammang, and Anna N. Żytkow. It was published in the February, 1981, issue of the Monthly Notices of the Royal Astronomical Society, Volume 194, pages 475-484.

Mon. Not. R. astr. Soc. (1981) 194, 475–484

Stationary spherical accretion into black holes – I. Equations of structure*

Kip S. Thorne and Richard A. Flammang

*W. K. Kellogg Radiation Laboratory, California Institute of Technology,
Pasadena, California 91125, USA*

Anna N. Żytkow *Copernicus Astronomical Center, Polish Academy of Sciences,
Warsaw, Poland*

Received 1980 June 20; in original form 1980 March 31

Summary. A general set of equations governing time-independent spherical accretion into black holes is formulated. The equations are fully general relativistic and are applicable to optically thick regions, optically thin regions, and the transition regions which join them. The radiation is treated using frequency-integrated moments. The full, infinite series of moment equations is given; the user of the formalism can truncate the series wherever he wishes.

1 Introduction

There is an extensive literature on the theory of stationary spherical accretion of gas into black holes – including, for example, adiabatic accretion treated general relativistically (e.g. Michel 1972; Blumenthal & Mathews 1976; Begelman 1978a); general relativistic, optically thin accretion with radiation losses to infinity and down the hole (e.g. Schwartzman 1971; Shapiro 1973a, b; Mészáros 1975a, b); optically thick accretion with diffusive heat flow treated using Newtonian gravity (e.g. Kafka & Mészáros 1976; Begelman 1978b, 1979); and accretion with the transition between optically thin and thick regions treated using either a Newtonian moment formalism (Tamazawa *et al.* 1975) or the general-relativistic transfer equation (Schmid-Burgk 1978).

Despite this extensive literature, there are a number of unresolved issues about spherical accretion. For example, it is not yet known whether a black hole of any size (microscopic to macroscopic), residing at the centre of a star, will eat the entire star on a free-fall time-scale ($\lesssim 1$ yr) or on an Eddington-limited time-scale ($\sim 10^8$ yr) or on some intermediate time-scale. Nor is the efficiency for converting gravitational energy of inflowing gas into outflowing radiation known as a function of the mass of the hole and of the properties of the gas far from the hole – except for a few special regimes that have been studied in detail.

This is the first of a series of papers which will analyse these issues. In this paper we formulate a general set of equations governing the hydrodynamics of the accretion and the

* Supported in part by the National Science Foundation (AST79-22012).

476 *K. S. Thorne, R. A. Flammang and A. N. Żytkow*

transfer of radiation through the accreting gas. Subsequent papers will use these equations to study various regimes of accretion.

We have chosen to formulate a new set of equations because all previous sets are either Newtonian (require $v/c \ll 1$, $GM/rc^2 \ll 1$) rather than general relativistic, or are restricted to adiabatic or optically thin flows. The sole exception is the set of equations used by Schmid-Burgk (1978). However, Schmid-Burgk's equations involve three non-trivial coordinates in the photon phase space: radius r , photon 'energy at infinity' E_∞ , and photon angular momentum J – and consequently they are too complex to be useful in a survey study of a wide variety of accretion regimes. Our equations will be made simpler (one non-trivial coordinate, r) by the use of Thorne's (1981) moment formalism for relativistic radiative transfer.

Our equations for the structure of the flow (equations 18 and 19 below) are perfectly general and accurate, so long as the following assumptions are satisfied: (i) the hole is spherical (Schwarzschild geometry with no rotation); (ii) the gas flows radially inward from rest at infinity; (iii) gravity produced by the gas and radiation is negligible compared to the gravity of the hole; (iv) the flow is stationary on time-scales long compared to hydrodynamical and radiative diffusion times; (v) the stress-energy of the gas is describable as a perfect fluid with isotropic pressure (no viscosity except that due to photon transport). The user of the equations can insert whatever physics he wishes, so long as it is compatible with these five assumptions.

The slow growth of the hole due to accretion can be studied by constructing a sequence of stationary solutions of our equations.

The mathematical conventions used in this paper are those of Misner, Thorne & Wheeler (1973) – including the use of geometrized units in which $c = G = 1$. For those readers who feel ill at ease in geometrized units, the translation to cgs units is given in the Appendix.

2 The equations

2.1 LIST OF BASIC VARIABLES

The basic variables, in terms of which our equations are formulated, are the following. For each variable we list the equation in which it first appears and any other equations in which it may be explicated.

Black hole variables

M mass of hole (a constant): (1),
 r Schwarzschild radial coordinate: (1).

Gas-motion variables

v inward velocity of gas as measured by an observer at fixed r in his local proper reference frame: (2),
 $y \equiv (1 - 2M/r)^{1/2} (1 - v^2)^{-1/2}$ 'energy parameter' of the flow: (2), (3),
 $\dot{M}_o \equiv 4\pi r^2 \rho_o v y$ rate of accretion of rest mass into the hole (a constant): (7).

Gas-state variables

ρ_o rest-mass density of gas: (6),
 Π_G specific internal energy of gas: (6),
 p_G pressure of gas: (6).

Radiation-state variables

$w_0 \equiv \rho_R$ zeroth moment of intensity; equal to radiation energy density: (8), (10), (13), (14),
 $w_1 \equiv L/4\pi r^2$ first moment of intensity; L is the outflowing luminosity as measured by an
observer moving with the gas: (8), (11), (13), (14),
 w_2, w_3, \dots second, third and higher-order moments of intensity: (8), (13), (14),
 L_∞ luminosity far from the hole (at ‘radial infinity’; a constant): (12).

Variables characterizing radiation–gas interaction

ϵ_l emissivity into l th moment of radiation: (15),
 κ_l opacity for l th moment of radiation: (15), (16), (17).

2.2 EXPLANATION OF BASIC VARIABLES

We describe the gravitational field of the black hole by the Schwarzschild metric

$$ds^2 = -(1 - 2M/r)dt^2 + (1 - 2M/r)^{-1}dr^2 + r^2(d\theta^2 + \sin^2\theta d\phi^2), \quad (1)$$

where M is the mass of the hole and (t, r, θ, ϕ) are the Schwarzschild spacetime coordinates. Contributions of the inflowing gas to the gravitational field are neglected.

We describe the local flow speed of the gas by its inward velocity v (ordinary velocity, not four-velocity) as measured in the local proper reference frame of an observer at rest in the Schwarzschild coordinate system. The four-velocity of the gas is then

$$\mathbf{u} = y(1 - 2M/r)^{-1} \partial/\partial t - vy \partial/\partial r, \quad (2)$$

where

$$y \equiv -\mathbf{u} \cdot \partial/\partial t = (1 - 2M/r)^{1/2} (1 - v^2)^{-1/2} \quad (3)$$

is the ‘energy-at-infinity per unit rest mass’ (‘energy parameter’ for short). For gas in free-fall (geodesic motion) y is a constant, independent of radius. The flow is assumed to be stationary so that v and y are functions of r but not of t .

The ‘local rest frame of the gas’ has orthonormal basis vectors.

$$\begin{aligned} \mathbf{e}_{\hat{t}} &= \mathbf{u} = y(1 - 2M/r)^{-1} \partial/\partial t - vy \partial/\partial r, \\ \mathbf{e}_{\hat{r}} &= -vy(1 - 2M/r)^{-1} \partial/\partial t + y \partial/\partial r, \\ \mathbf{e}_{\hat{\theta}} &= r^{-1} \partial/\partial \theta, \quad \mathbf{e}_{\hat{\phi}} = (r \sin \theta)^{-1} \partial/\partial \phi. \end{aligned} \quad (4)$$

Expressed in this basis, the flow has four-acceleration $\mathbf{a} = a \mathbf{e}_{\hat{r}}$, expansion Θ , rotation $\boldsymbol{\omega} = 0$, shear $\boldsymbol{\sigma} = \sigma(\mathbf{e}_{\hat{r}} \otimes \mathbf{e}_{\hat{r}} - \frac{1}{2} \mathbf{e}_{\hat{\theta}} \otimes \mathbf{e}_{\hat{\theta}} - \frac{1}{2} \mathbf{e}_{\hat{\phi}} \otimes \mathbf{e}_{\hat{\phi}})$, and extrinsic curvature $\Gamma_{\hat{\theta}\hat{r}\hat{\theta}} = \Gamma_{\hat{\phi}\hat{r}\hat{\phi}} = b$, where

$$a = y', \quad \Theta = -r^{-2}(r^2 vy)', \quad \sigma = -(2r/3)(vy/r)', \quad b = y/r. \quad (5)$$

(cf. equations 5.2, 5.3, 5.14 of Thorne 1981). Here and throughout this paper a prime denotes derivative with respect to r , d/dr . In our application of Thorne’s (1981) radiative-transfer moment formalism we shall choose the world lines of the gas as our ‘fiducial congruence’, and the local rest frame of the gas (equation 4) as our ‘fiducial reference frame’.

In its local rest frame the gas is described physically by its density of rest mass ρ_o (equal to number density of baryons multiplied by some standard rest mass per baryon), its specific

478 *K. S. Thorne, R. A. Flammang and A. N. Żytkow*

internal energy Π_G , and its pressure p_G – which we assume to be isotropic. The components of the stress-energy tensor of the gas are

$$T_G^{\hat{0}\hat{0}} = \rho_o(1 + \Pi_G), \quad T_G^{\hat{r}\hat{r}} = T_G^{\hat{\theta}\hat{\theta}} = T_G^{\hat{\varphi}\hat{\varphi}} = p_G, \quad (6)$$

all other $T_G^{\hat{\alpha}\hat{\beta}}$ vanish.

Rest-mass conservation and stationarity of the flow guarantee that the rest-mass accretion rate is independent of radius:

$$\dot{M}_o \equiv -4\pi r^2 \rho_o u^r = 4\pi r^2 \rho_o v y = \text{constant, independent of } r. \quad (7)$$

(Here u^r is the radial component of the four-velocity in the Schwarzschild coordinate frame.)

The radiation is described by its frequency-integrated moments w_0, w_1, w_2, \dots , which are defined by (*cf.* equation 5.6c of Thorne 1981).

$$w_l \equiv \frac{l!(2l+1)}{(2l+1)!!} \int_{-1}^1 I(\mu) P_l(\mu) 2\pi d\mu. \quad (8)$$

Here I is the radiation intensity ($\text{erg cm}^{-2} \text{s}^{-1} \text{sr}^{-1}$) measured in the local rest frame of the gas (equation 4); it is a function of

$$\mu = \left(\begin{array}{l} \text{cosine of angle between direction of photon} \\ \text{momentum and outward radial direction } e_{\hat{r}} \end{array} \right). \quad (9)$$

The integral (8) is over all photon directions, as measured in the gas's rest frame; $P_l(\mu)$ is the Legendre polynomial of order l ; and $(2l+1)!! \equiv (2l+1) \cdot (2l-1) \cdots (2 \text{ or } 1)$. (Note that $(2l+1)!!/[l!(2l+1)]$ is the coefficient of the μ^l term in $P_l(\mu)$.) We introduce special notations for the zeroth and first moments.

$$\rho_R \equiv w_0, \quad (10)$$

$$L/4\pi r^2 \equiv w_1. \quad (11)$$

One can easily see from equation (8) that ρ_R is the energy density of the radiation, $L/4\pi r^2$ is the outward flux of radiation energy, and L is the local luminosity – all as measured in the local rest frame of the gas. The luminosity measured at radial infinity (where we assume that $v = 0$) will be denoted L_∞ :

$$L_\infty \equiv L(r = \infty). \quad (12)$$

In Newtonian theory a more familiar notation for the first three moments is

$$w_0 = 4\pi J, \quad w_1 = 4\pi H, \quad w_2 = 4\pi(K - \frac{1}{3}J). \quad (13)$$

The stress-energy tensor for the radiation has the following components, as measured in the local rest frame of the gas:

$$\begin{aligned} T_R^{\hat{0}\hat{0}} &= \rho_R, & T_R^{\hat{r}\hat{r}} &= T_R^{\hat{\theta}\hat{\theta}} = L/4\pi r^2, & T_R^{\hat{\varphi}\hat{\varphi}} &= \frac{1}{3}\rho_R + w_2, \\ T_R^{\hat{\theta}\hat{\theta}} &= T_R^{\hat{\varphi}\hat{\varphi}} = \frac{1}{3}\rho_R - \frac{1}{2}w_2, & \text{all other } T_R^{\hat{\alpha}\hat{\beta}} & \text{vanish;} \end{aligned} \quad (14)$$

cf. equation (5.9) of Thorne (1981).

The radiation–gas interaction is characterized by multipole moments, ϵ_l , of the emissivity, and by opacities, κ_l , for each multipole ($l = 0, 1, 2, 3, \dots$). The rigorous defini-

tion of ϵ_l and κ_l is

$$\rho_o(\epsilon_l - \kappa_l w_l) \equiv \frac{l!(2l+1)}{(2l+1)!!} \int_{-1}^1 \int_0^\infty \left(\frac{dI_\nu}{d\tau} \right)_{\text{interaction}} P_l(\mu) d\nu 2\pi d\mu. \quad (15)$$

Here I_ν is the specific intensity ($\text{erg cm}^{-2} \text{s}^{-1} \text{Hz}^{-1} \text{sr}^{-1}$) of the radiation, ν is the radiation frequency, and τ is the proper time – all as measured in the local rest frame of the gas; and $(dI_\nu/d\tau)_{\text{interaction}}$ is the ‘interaction’ (or ‘source’) term in the equation of radiative transfer. (The quantity $\rho_o(\epsilon_l - \kappa_l w_l)$ is denoted s_l in Section 5 of Thorne (1981). In Section 6 of Thorne (1981), from which we obtain expressions (16) and (17) for κ_l , $\rho_o(\epsilon_l - \kappa_l w_l)$ is denoted $\mathcal{S}^{\hat{r}\hat{r}\dots\hat{r}}$ and w_l is denoted $\mathcal{W}^{\hat{r}\hat{r}\dots\hat{r}}$ (l factors of \hat{r} .)

We lump into $-\rho_o \kappa_l w_l$ all parts of the integral (15) which are directly proportional to w_l . For example, Thomson scattering by non-relativistic electrons appears in this term, with

$$(\kappa_0)_T = 0, \quad (\kappa_2)_T = \frac{9}{10} \frac{\sigma_T}{m_p \mu_e}, \quad (\kappa_l)_T = \frac{\sigma_T}{m_p \mu_e} \quad \text{for } l \neq 0 \text{ or } 2 \quad (16)$$

(equation 6.25 of Thorne 1981). Here σ_T is the Thomson cross section, m_p is the proton rest mass, and μ_e is the mean molecular weight per electron. Also, single-photon absorption processes appear here with opacities $\bar{\kappa}_l$ that are approximately the same for all l . (For example, in the diffusion regime with I_ν nearly a blackbody, $\bar{\kappa}_0$ is the Planck mean and $\bar{\kappa}_1$ is the Rosseland mean of κ_ν , the frequency-dependent absorption opacity.) Double-Compton scattering (one photon in and two out), plus Comptonization of the new photon, appears in $-\rho_o \kappa_0 w_0$ with a *negative* opacity

$$(\kappa_0)_{\text{DC}+\text{C}} = -\frac{\sigma_T}{m_p \mu_e} \frac{16\alpha}{\pi} \left(\frac{kT}{m_e c^2} \right)^2 \ln \left[\left(\frac{45}{4\pi^3 \alpha} \frac{m_e c^2}{kT} \frac{aT^4}{\rho_R} \right)^{1/2} \right] \quad (17)$$

(equation 6.43 of Thorne 1981). Here m_e is the electron rest mass, α is the fine-structure constant, T is the temperature of the Comptonizing electrons (assumed to be in local thermodynamic equilibrium with each other), aT^4 is the equilibrium radiation energy density, and this expression is valid only when (i) the expansion time-scale $|1/\theta|$ is long compared to the Comptonization time-scale $t_C = [c(\rho_o/m_p \mu_e)\sigma_T (4kT/m_e c^2)]^{-1}$; (ii) the mean distance $[(\rho_o/m_p \mu_e)\sigma_T]^{-1} [m_e c^2/4kT]^{1/2}$ travelled by a photon during one Comptonization time t_C is short compared to all macroscopic length-scales; (iii) the radiation field is nearly isotropic, $w_0 \gg$ (all other w_l); and (iv) $\rho_R \lesssim \frac{1}{2} aT^4$. For discussion of the regimes $\rho_R \approx aT^4$ and $\rho_R > aT^4$ see Section 6.3.4 of Thorne (1981).

In expression (15), $\rho_o \epsilon_l$ includes all parts of the integral not directly proportional to w_l . For example, isotropic single-photon emission and Comptonization of the emitted photon appear in ϵ_0 ; *cf.* Section 6.3.3 of Thorne (1981). Isotropic emission contributes nothing to ϵ_l for $l \geq 1$.

2.3 EQUATIONS GOVERNING BASIC VARIABLES

Of the basic variables listed in Section 2.1, three are constants (M, \dot{M}_o, L_∞); one is the independent radial coordinate (r); and the rest are functions of r (‘dependent variables’: $v, y, \rho_o, \Pi_G, p_G; \rho_R, L, w_2, w_3, \dots; \epsilon_0, \epsilon_1, \epsilon_2, \dots$; and $\kappa_0, \kappa_1, \kappa_2, \dots$). The user of our equations must supply his own expressions for the emissivities ϵ_l and opacities κ_l , and one ‘equation of state’ for the gas relating ρ_o, Π_G , and p_G to each other. The remaining dependent variables (v, y ; two of ρ_o, Π_G and $p_G; \rho_R, L, w_2, w_3, \dots$) will then be determined by the following equations – in which the mass of the hole M , the accretion rate \dot{M}_o , and the luminosity-at-infinity L_∞ are assumed to have been specified:

480 *K. S. Thorne, R. A. Flammang and A. N. Żytkow*

The energy parameter y is expressed algebraically in terms of density and radius by

$$y(\rho_o, r) = \left[\left(\frac{\dot{M}_o}{4\pi r^2 \rho_o} \right)^2 + 1 - \frac{2M}{r} \right]^{1/2} \quad (18a)$$

(derivable from equations 3 and 7).

The velocity v is expressed algebraically in terms of y , ρ_o and r by the law of *mass conservation* (7):

$$v(y, \rho_o, r) = \frac{\dot{M}_o}{4\pi r^2 \rho_o y}. \quad (18b)$$

The relativistic *Bernoulli equation*, $\nabla \cdot [(\partial/\partial t) \cdot \mathbf{T}] = 0$ where \mathbf{T} is the total stress-energy tensor, can be expressed as $4\pi r^2 T_t^r = \text{constant}$. Here T_t^r is the time-radial component of \mathbf{T} in the Schwarzschild coordinate frame. When the gas stress-energy tensor (6) and radiation stress-energy tensor (14) are inserted into this equation, it becomes the following expression for L in terms of the other variables:

$$L(1+v^2)y^2 = L_\infty + \dot{M}_o y \left(1 + \Pi_G + \frac{p_G}{\rho_o} + \frac{4\rho_R/3 + w_2}{\rho_o} \right) - \dot{M}_o \left(1 + \Pi_G + \frac{p_G}{\rho_o} + \frac{4\rho_R/3 + w_2}{\rho_o} \right)_{\text{at } r = \infty}. \quad (18c)$$

Here in determining the value of the constant we have assumed that at $r = \infty$ $v = 0$ (and hence $y = 1$).

The equation of *radial force balance* $T^{\hat{r}\hat{\beta}}{}_{;\hat{\beta}} = 0$ can be expressed as the following differential equation:

$$y(p_G + \frac{1}{3}\rho_R)' + (\rho_o + \rho_o \Pi_G + p_G + \frac{4}{3}\rho_R)y' = \frac{(Lv^2y^2)'}{4\pi r^2 v y} - \frac{1}{r^3} (r^3 y w_2)' \quad \text{in general} \quad (18d)$$

= 0 in photon-diffusion regime (equations 20 below).

The zeroth moment of the radiative transfer equation (*radiation energy balance*; equation 5.10c of Thorne (1981) with $k = 0$) can be expressed as the following differential equation:

$$v y \rho_R \left(\frac{\rho_R'}{\rho_R} - \frac{4}{3} \frac{\rho_o'}{\rho_o} \right) + \rho_o (\epsilon_o - \kappa_o \rho_R) - \frac{(Ly^2)'}{4\pi r^2 y} = -r \left(\frac{vy}{r} \right)' w_2 \quad \text{in general} \quad (18e)$$

= 0 in photon-diffusion regime (equations 20 below).

In the photon-diffusion regime, if the radiation time-scale $(\rho_o \kappa_o)^{-1}$ is sufficiently short (equations 21 below), then the photons will be very nearly in *radiative energy equilibrium*:

$$\rho_R = \epsilon_o / \kappa_o \quad (18e')$$

= aT^4 if the emitters and absorbers in the gas are in thermodynamic equilibrium with each other at temperature T .

The first moment of the radiative transfer equation (*radiation force balance*; equation

5.10c of Thorne (1981) with $k = 1$) can be expressed as the following differential equation:

$$\begin{aligned} & \frac{1}{3y^3} (\rho_R y^4)' + \rho_o \kappa_1 \frac{L}{4\pi r^2} \\ &= \rho_o \epsilon_1 + \frac{(Lv^2 y^2)'}{4\pi r^2 v y} - \frac{1}{r^3} (r^3 y w_2)' \quad \text{in general} \end{aligned} \quad (18f)$$

= 0 in photon-diffusion regime (equations 20 below).

The *second moment of the radiative transfer equation* (equation 5.10c of Thorne (1981) with $k = 2$) can be expressed as the following equation for the second moment of the radiation field:

$$\begin{aligned} & \rho_o \kappa_2 w_2 - \frac{16}{45} r \left(\frac{vy}{r} \right)' \rho_R + \frac{4}{15} \frac{r}{y^4} \left(\frac{Ly^5}{4\pi r^3} \right)' \\ &= \rho_o \epsilon_2 + vy w_2' + \left[\frac{4}{3r^2} (r^2 vy)' + \frac{10}{21} r \left(\frac{vy}{r} \right)' \right] w_2 - y w_3' - \frac{4}{r} y w_3 \\ & \quad - r \left(\frac{vy}{r} \right)' w_4 \quad \text{in general} \end{aligned} \quad (18g)$$

= 0 in photon-diffusion regime (equations 20 below).

The *lth moment of the radiative transfer equation* (equation 5.10c of Thorne (1981) with $k = l$) can be expressed as the following equation for the *lth* moment of the radiation field:

$$\begin{aligned} & \rho_o \kappa_l w_l - \frac{(l-1)^2 l^2 (l+2)}{(2l-3)(2l-1)^2 (2l+1)} r \left(\frac{vy}{r} \right)' w_{l-2} + \frac{l^2}{(2l-1)(2l+1)} y w_{l-1}' \\ & \quad + \left[\frac{l^2 (l+3) y' - l^2 (l-1) y/r}{(2l-1)(2l+1)} \right] w_{l-1} \\ &= \rho_o \epsilon_l + vy w_l' + \left[\frac{4}{3} \frac{(r^2 vy)'}{r^2} + \frac{5l(l+1)}{3(2l-1)(2l+3)} r \left(\frac{vy}{r} \right)' \right] w_l - y w_{l+1}' \\ & \quad + \left[(l-2) y' - \left(\frac{l+2}{r} \right) y \right] w_{l+1} - (l-1) r \left(\frac{vy}{r} \right)' w_{l+2} \quad \text{in general} \end{aligned} \quad (18h)$$

= 0 in photon diffusion regime (equation 20 below).

2.4 BOUNDARY CONDITIONS

The equations of structure (18) must be solved subject to boundary conditions at $r = \infty$ and at $r = 2M$ (horizon of hole).

We presume that the states of the gas and radiation at infinity are specified by the user of the equations:

$$\begin{aligned} \rho_o(r = \infty) &= \rho_{o\infty}, & \Pi_G(r = \infty) &= \Pi_{G\infty}, & p_G(r = \infty) &= p_{G\infty}, \\ \rho_R(r = \infty) &= \rho_{R\infty}, & L(r = \infty) &= L_\infty, & w_l(r = \infty) &= w_{l\infty}. \end{aligned} \quad (19a)$$

If the gas is optically thin at $r = \infty$, then all photons will be moving precisely radially there

482 *K. S. Thorne, R. A. Flammang and A. N. Żytkow*

$[I(\mu) = (\rho_{R\infty}/\pi)\delta(\mu - 1)]$, and consequently

$$\rho_R = \frac{L_\infty}{4\pi r^2}, \quad w_{l\infty} = \frac{l!(2l+1)L_\infty}{(2l+1)!!4\pi r^2} \quad (\text{optically thin}). \quad (19a')$$

We have presumed throughout that the gas is at rest at infinity:

$$v(r = \infty) = 0, \quad y(r = \infty) = 1. \quad (19b)$$

At the horizon, physical conditions in the rest frame of the gas must be perfectly normal. The most important condition of 'normality' is finiteness of the four-acceleration, $a = y^1$:

$$y'(r = 2M) \quad \text{is finite.} \quad (19c)$$

If acceptable physics (opacities, equations of state, ...) is put into the equations of structure (18), then because those equations are standard physical laws (energy conservation, force balance, etc.), they plus 'finite a ' presumably will guarantee complete 'normality' at the horizon. For example, the relation $y = (1 - 2M/r)^{1/2}(1 - v^2)^{-1/2}$ (which follows from the equations of structure 18a, b), together with finiteness of $a = y^1$, guarantees that

$$v = 1, \quad y \text{ finite and positive} \quad \text{at } r = 2M, \quad (19d)$$

which is a 'condition of normality' corresponding to the gas world lines being time-like and the laws of physics in the rest frame of the gas thereby being 'normal'.

In solving the equations of structure (18), one may well introduce approximations which break the power of 'finite a ' to guarantee normality at the horizon. For example, one may introduce the diffusion approximation in equations (18d)–(18h). The diffusion approximation is notoriously acausal – it permits thermal pulses to travel faster than the speed of light, and thereby permits transfer of information out of the horizon. With such an approximation, one should not be surprised that 'finite a ' is an insufficient boundary condition at the horizon (see Flammang 1981, a sequel to this paper). One must then impose additional normality conditions independently. A sufficient set of additional conditions is that

$$\rho_o, \Pi_G, p_G, \rho_R, L, w_2, w_3; \dots \quad \text{all be finite at } r = 2M, \quad (19e)$$

and – perhaps more crucially – that the radiation intensity $I(\mu)$, as measured in the rest frame of the gas, be non-negative for all μ :

$$I(\mu) = \sum_{l=0}^{\infty} \frac{(2l+1)!!}{4\pi l!} w_l P_l(\mu) \geq 0 \quad \text{for all } -1 \leq \mu \leq 1, \text{ at } r = 2M. \quad (19f)$$

3 Discussion of the equations

Two regimes of our equations of structure (18) deserve special note: The first is the *photon-diffusion regime*, in which (i) the gas is optically thick to the flow of radiation on macroscopic scales:

$$\bar{\lambda} \ll \mathcal{L}, \quad \text{where}$$

$$\bar{\lambda} \equiv \max_{l \geq 1} [(\kappa_l \rho_o)^{-1}], \quad (20a)$$

$$\mathcal{L} \equiv \frac{1}{y} \times \left[\begin{array}{l} \text{minimum of macroscopic length-scales } r, \quad |(\ln y)'|^{-1}, \quad |(\ln v)'|^{-1}, \\ |(\ln \rho_R)'|^{-1}, \quad |(\ln \rho_o)'|^{-1}, \quad |(\ln p_G)'|^{-1} \end{array} \right];$$

and (ii) the emissivity is isotropic

$$\rho_o \epsilon_l \lesssim (\bar{\lambda}/\mathcal{L})^{l(l+1)/2} (v + \bar{\lambda}/\mathcal{L})^{l/2} \rho_R/\mathcal{L} \quad \text{for all } l \geq 1. \quad (20b)$$

Here $[n/2] \equiv$ (the largest integer less than or equal to $n/2$). In this regime photons diffuse through the gas with mean-free paths of order $\bar{\lambda}$, and their diffusion drives the magnitudes of the radiation moments down to

$$\begin{aligned} w_1 &= L/4\pi r^2 \sim (\bar{\lambda}/\mathcal{L})\rho_R, & w_2 &\sim (\bar{\lambda}/\mathcal{L})(v + \bar{\lambda}/\mathcal{L})\rho_R, \\ w_l &\sim (\bar{\lambda}/\mathcal{L})^{l(l+1)/2} (v + \bar{\lambda}/\mathcal{L})^{l/2} \rho_R & \text{for all } l \geq 1. \end{aligned} \quad (20c)$$

(See equations (18f)–(18h), in which we presume that the opacities κ_l are slowly varying functions of ρ_o and p_G : $|(\ln \kappa_l)'| \leq |(\ln \rho_o)'| + |(\ln p_G)'|$.) Note that near the hole, where $v \sim 1$, the second moment w_2 is comparable in magnitude to the first $L/4\pi r^2$, whereas the moments of order $l \geq 3$ are negligible compared to $L/4\pi r^2$ independently of velocity v . It may be interesting to compare this discussion of the photon diffusion regime with that in equations (7.5) of Thorne (1981). The discussions differ because Thorne treats v as of order unity, whereas we make special allowance for the possibility that $v \leq \bar{\lambda}/\mathcal{L}$.

The second special regime is that of *radiative energy equilibrium*. This occurs when the photons are diffusing (equations 20) and when, in addition, the time-scale to build up and maintain an equilibrium radiative energy density is short compared to macroscopic time-scales:

$$\bar{\lambda}_0 \ll \mathcal{L}_0 \quad \text{and} \quad \bar{\lambda}_0 \ll \mathcal{L}^2/\bar{\lambda}, \quad \text{where} \quad (21a)$$

$$\bar{\lambda}_0 \equiv (\kappa_o \rho_o)^{-1}, \quad \mathcal{L}_0 \equiv [\text{minimum of macroscopic time-scales } |\Theta|^{-1}, |d \ln \rho_R/d\tau|^{-1}] \geq \mathcal{L}/v$$

with $d/d\tau =$ (proper time derivative moving with gas). In this regime energy exchange between the photons and the gas (equation 18e) maintains photon energy equilibrium:

$$\begin{aligned} \rho_R &= \epsilon_o/\kappa_o \quad \text{in general,} \\ &= aT^4 \quad \text{if the emitters and absorbers in the gas are in thermodynamic} \\ &\quad \text{equilibrium with each other at temperature } T. \end{aligned} \quad (21b)$$

One will typically have photon diffusion without radiative energy equilibrium whenever (i) scattering opacity (which contributes to $\kappa_1, \kappa_2, \dots$ but not to κ_o) is far greater than absorption opacity, and (ii) the gas is expanding (or compressing) with a time-scale $|1/\theta|$ between $(\rho_o \kappa_1)^{-1}$ and $(\rho_o \kappa_o)^{-1}$.

To make the equations of structure (18) tractable, it will be necessary to truncate the radiation moment expansion – i.e. to ignore all moments above some order l_{\max} and to make some wise guess as to the values of $w_{l_{\max}+1}$ and $w_{l_{\max}+2}$ in the moment equations (18h) of order l_{\max} and $l_{\max}-1$. In the diffusion regime, $l_{\max} = 2$ is a reasonable choice, and setting $w_3 = w_4 = 0$ in the moment equation (18g) is reasonable; *cf.* equation (20c). In optically thin and marginally thick regimes, one may want to compare results using different values of l_{\max} in order to see how small an l_{\max} is viable.

Because the flow is subsonic ($v = 0$) at infinity and supersonic ($v = 1$) at the horizon, it will possess a critical sonic point analogous to that which occurs in models of stellar winds. The sonic point is rather well understood in the case of general relativistic, adiabatic inflow (e.g. Blumenthal & Mathews 1976; Begelman 1978a); there it occurs when v is equal to the adiabatic sound velocity. In a sequel to this paper, Flammang (1981) will analyse optically

thick inflow with local thermodynamic equilibrium (equations 20 and 21 satisfied). He will show that there is a ‘full-fledged’ critical point of the equations when v is equal to the isothermal sound velocity, and in addition there is a ‘latent’ critical point of the equations when v is equal to the adiabatic sound velocity. The requirement that the flow pass smoothly through these two critical points, plus the boundary conditions at infinity and at the horizon, will determine *both* the mass accretion rate \dot{M}_o and the luminosity-at-infinity L_∞ in terms of the mass M of the black hole and the physical state of the gas at infinity.

References

- Begelman, M. C., 1978a. *Astr. Astrophys.*, **70**, 583.
 Begelman, M. C., 1978b. *Mon. Not. R. astr. Soc.*, **184**, 53.
 Begelman, M. C., 1979. *Mon. Not. R. astr. Soc.*, **187**, 237.
 Blumenthal, G. R. & Mathews, W. G., 1976. *Astrophys. J.*, **203**, 714.
 Flammang, R. A., 1981. *Mon. Not. R. astr. Soc.*, to be submitted.
 Kafka, P. & Mészáros, P., 1976. *Gen. Rel. Grav.*, **7**, 841.
 Mészáros, P., 1975a. *Nature*, **258**, 583.
 Mészáros, P., 1975b. *Astr. Astrophys.*, **44**, 59.
 Michel, F. C., 1972. *Astrophys. Space Sci.*, **15**, 153.
 Misner, C. W., Thorne, K. S. & Wheeler, J. A., 1973. *Gravitation*. W. H. Freeman, San Francisco.
 Schmid-Burgk, J., 1978. *Astrophys. Space Sci.*, **56**, 191.
 Schwartzman, V. F., 1971. *Soviet Astr.-A. J.*, **15**, 377.
 Shapiro, S. L., 1973a. *Astrophys. J.*, **180**, 531.
 Shapiro, S. L., 1973b. *Astrophys. J.*, **185**, 69.
 Tamazawa, S., Toyama, K., Kaneko, N. & Ono, Y., 1975. *Astrophys. Space Sci.*, **32**, 403.
 Thorne, K. S., 1981. *Mon. Not. R. astr. Soc.*, **194**, 439.

Appendix: Translation of equations into cgs units

The body of this paper uses geometrized units – i.e. units where Newton’s gravitation constant G and the speed of light c are both one. Box 1.8 of Misner *et al.* (1973) explains how to translate geometrized units into cgs units. We list below, as an aid, the translation of the basic variables which are introduced in Section 2.1 and which appear in our fundamental equations (18). To put our equations into cgs units, one must replace the symbol in the left column by the expression in the right column.

M (cm)	$\rightarrow GM/c^2$	(M in g)
r (cm)	$\rightarrow r$	(r in cm)
v (dimensionless)	$\rightarrow v/c$	(v in cm s^{-1})
y (dimensionless)	$\rightarrow y$	(dimensionless)
\dot{M}_o (dimensionless)	$\rightarrow G\dot{M}_o/c^3$	(\dot{M}_o in g s^{-1})
ρ_o (cm^{-2})	$\rightarrow G\rho_o/c^2$	(ρ_o in g cm^{-3})
Π_G (dimensionless)	$\rightarrow \Pi_G/c^2$	(Π_G in erg g^{-1})
p_G (cm^{-2})	$\rightarrow Gp_G/c^4$	(p_G in dyne cm^{-2})
w_l (cm^{-2})	$\rightarrow Gw_l/c^4$	(w_l in $\text{erg cm}^{-3} = \text{dyne cm}^{-2}$)
ρ_R (cm^{-2})	$\rightarrow G\rho_R/c^4$	(ρ_R in erg cm^{-3})
L (dimensionless)	$\rightarrow GL/c^5$	(L in erg s^{-1})
L_∞ (dimensionless)	$\rightarrow GL_\infty/c^5$	(L_∞ in erg s^{-1})
ϵ_l (cm^{-1})	$\rightarrow \epsilon_l/c^3$	(ϵ_l in $\text{erg g}^{-1} \text{s}^{-1}$)
κ_l (cm)	$\rightarrow \kappa_l c^2/G$	(κ_l in $\text{cm}^2 \text{g}^{-1}$)

Chapter 2

The Theory of Optically Thick Accretion

This chapter is a paper published in the June, 1982, issue of the Monthly Notices of the Royal Astronomical Society, Volume 199, Page 833.

Abstract

In this paper, the problem of spherical, steady-state, optically thick accretion into black holes is solved. We analyze the integral curves of the differential equations describing the problem. We find a one-parameter family of critical points, where the inflow velocity equals the isothermal sound speed. Physical solutions must pass through one of these critical points. We obtain a complete set of boundary conditions which the solution must satisfy at the horizon of the black hole, and show that these, plus the requirement that the solution pass through a critical point, determine a unique solution to the problem. This analysis leads to a generalization of the well-known Bondi critical point constraint, which arises in the adiabatic accretion problem and which is effective at the point where the inflow velocity equals the adiabatic sound speed. We show that this point can be regarded as a "diffused critical point" in our problem. The analysis also yields a simple expression for the diffusive luminosity at radial infinity. Finally, we find a satisfying explanation for the rather peculiar critical point structure of this problem in an analysis of the characteristics and subcharacteristics present in the problem and in a "hierarchical" analysis of the waves which propagate along them.

1. Introduction

The purpose of this paper is to understand what happens when a black hole finds itself surrounded by an optically thick cloud of gas. Physically, we expect the black hole to draw matter inward and, at the same time, to compress it. As the inflowing material is compressed,

it will heat up, and this will establish a temperature gradient-- which, in turn, will lead to an outflowing luminosity.

A satisfactory resolution of this problem seems especially important now for two main reasons. First, there are the important astrophysical applications. For example, most quasars lack jets, rapid time variability, and significant polarization and could thus be powered by steady, spherical accretion into a large black hole. In order to produce the enormous luminosities observed in these sources, one must either assume very high efficiencies or one must feed the black hole with a large accretion rate. In the latter instance, conditions will be very optically thick near the black hole, and the results of the present paper will apply. Indeed, we shall find that steady, spherical, optically thick accretion into black holes can effortlessly produce luminosities up to the usual Eddington limit.

There is also the possibility that runaway Roche-lobe overflow in a close binary system could eventually lead to the formation of a "black hole core star" [cf. Taam, Bodenheimer, and Ostriker (1978), and Thorne and Żytkow (1977) for a discussion of the neutron-star case.] Furthermore, recent calculations of core collapse in massive supergiants suggest that the end product may be not a supernova but a "star" with a central black hole [Woosley (1980)].

But there is another, more fundamental, reason to turn our attention to this problem: it is, or can be made, a well-posed problem of mathematical physics; and we shall see that to understand the answer deeply requires the introduction of some new, essentially mathematical, ideas into the standard lore of accretion physics.

Steady, spherical accretion was first studied by Bondi (1952), who considered adiabatic accretion of a polytropic gas using Newtonian gravity. The corresponding general relativistic problem was treated by Michel (1972). The more complicated problem where the effects of radiative transfer are taken into account, has been studied, in the optically thin limit, by Shvartsman (1971), Shapiro (1973a,b), and Mészáros (1975). All of these authors have paid particular attention to the roles played by magnetic fields and synchrotron emission. In the case of optically thin accretion, photon energy densities are so tiny that radiation has a negligible influence on the flow, and the problems of radiative transfer and hydrodynamics effectively decouple. When conditions are optically thick the situation is very different. In this case radiation pressure can build up and decisively alter the accretion flow. Tamazawa et al. (1975) considered a particular accretion problem which went optically thick near the black hole. They found exponentially diverging luminosities when they tried to integrate their equations down into this optically thick inner region. To continue their solution on down to the horizon, they assumed the flow to be exactly adiabatic and then used the resulting temperature gradient to compute a luminosity in the diffusion approximation. The heat lost from each inflowing fluid element as a result of the ensuing luminosity gradient was neglected in their equation of energy conservation. While this procedure is physically justifiable and was entirely satisfactory for the particular problem Tamazawa et al. were considering, it sidesteps, rather than confronts, the issues we wish to investigate here.

The first attempt at a fully self-consistent analysis of optically thick accretion was made by Kafka and Mészáros (1976). They used a highly simplified set of equations, first employed by Maraschi et al. (1974) to study accretion onto a compact star. These equations are Newtonian, neglect the pressure and internal energy of the gas, and include only electron-scattering opacity. Unfortunately, the solutions found by Kafka and Mészáros are unphysical: they all have subsonic velocities at the "horizon" of their Newtonian black hole. Of course, a meaningful description of the flow near the horizon of the black hole can only be given in a fully relativistic treatment. As was pointed out in the first paper of this series [Thorne, Flammang, and Żytkow (1981)--hereafter paper 1], the inflow velocity, as measured by local, static observers, must equal the speed of light at the horizon of the black hole. Thus the flow cannot be subsonic there.

Begelman (1978), using the same equations as Kafka and Mészáros, treated the problem of optically thick accretion by analogy with Bondi's theory of adiabatic Newtonian accretion. Because his equations were Newtonian, Begelman was not able to consider, except in an approximate way, relevant boundary conditions at the horizon of the black hole; he also misidentified the critical points in his problem. Nevertheless, the basic perturbative approach used by Begelman is quite sound. As a result, many of Begelman's approximate analytic results are correct, and these provide some valuable physical insight.

Vitello (1978), who considered spherical, optically thick accretion onto compact stars, seems to have been the first to point out in the literature that, with radiative transfer treated in the

diffusion approximation, the resulting set of basic equations describing the accretion problem have critical points where the inflow velocity equals the isothermal sound speed.

More recently, Gilden and Wheeler (1980), in a fully relativistic treatment, studied the time-dependent behavior of optically thick plasma located within ten Schwarzschild radii of a black hole. They found that the solution quickly relaxed to steady-state "free-fall" regardless of initial conditions. As we shall see later on, this result is obtained because the region Gilden and Wheeler were studying lay well inside of the relevant "critical points" of the corresponding steady-state problem. Their conclusion, that an optically-thick cloud of gas always falls into a central black hole on a free-fall timescale, is valid only for the material in this inner region. Further out, the material is basically in hydrostatic equilibrium and, in particular, can be supported by radiation pressure gradients (luminosity). However, the time-dependent calculations of Gilden and Wheeler provide a valuable demonstration of the stability of the innermost regions of steady, optically-thick accretion flows into black holes. Finally, Gillman and Stellingwerf (1980) reconsidered the problem posed by Kafka and Mészáros in a completely relativistic analysis, this time including gas pressure, but, like Kafka and Mészáros, found only unphysical "solutions".

Obviously, this problem is in dire need of a clean, definitive, understandable solution, and this is what we will attempt to present in the following sections. Specifically, we consider the problem of steady-state, spherically-symmetric accretion into a Schwarzschild black hole in those circumstances where the density is high enough

to ensure (1) that photon transport can be adequately described by the diffusion approximation and (2) that the photons and the gas are in local energy equilibrium (LTE). These two conditions constitute the definition of the phrase "optically thick" as used here. As its title indicates, this paper will focus on the formal, mathematical aspects of the problem. In a sequel paper [Flammang (1982)], specific numerical solutions and their physical character will be discussed.

2. Basic Equations

The equations we shall need are discussed in Thorne, Flammang, and Żytkow (1980) [paper 1]. When specialized to the case of interest here (see Appendix A), they can be written as:

$$4\pi r^2 \rho_0 v Y = \dot{M}_0 = \text{constant} \quad (1a)$$

$$\frac{Y'}{Y} + \frac{P'}{\rho + P} = 0 \quad (1b)$$

$$HY\dot{M}_0 - \hat{L} = \dot{E} = \text{constant} \quad (1c)$$

$$\hat{L} = -4\pi r^2 Y^3 (1+v^2) \frac{4P_R}{\rho_0 \kappa_1} \left[\frac{T'}{T} + \frac{Y'}{Y} \right] \quad (1d)$$

expressing conservation of "rest mass", conservation of radial momentum, Bernoulli's equation (corrected to include heat transfer), and the diffusion of photons, respectively. In these equations, the following variables have the same meaning as in paper 1:

$$r = \text{Schwarzschild radial coordinate} \quad (2a)$$

$$\rho_o = \text{density of "rest mass"} \quad (2b)$$

$$v = \text{radial inflow velocity as measured by local, static observers} \quad (2c)$$

$$Y = \left[\frac{1-2M/r}{1-v^2} \right]^{\frac{1}{2}} = \text{energy, per unit rest mass, at infinity} \quad (2d)$$

Here M is the mass of the black hole.

$$\dot{M}_o = \text{rest mass accretion rate} \quad (2e)$$

$$\kappa_1 = \text{first-moment opacity} \quad (2f)$$

and a prime denotes differentiation with respect to r . In addition, the following new variables appear:

$$P = P_G + P_R = \text{total pressure (gas plus radiation)} \quad (2g)$$

$$P_R = \frac{1}{3} \rho_R = \text{radiation pressure} \quad (2h)$$

$$\rho = \rho_G + \rho_R = \text{total energy density (gas plus radiation), including rest mass} \quad (2i)$$

$$H = \frac{\rho+P}{\rho_o} = \text{total enthalpy, including rest mass, per unit rest mass} \quad (2j)$$

$$T = \text{common temperature of gas and radiation.} \quad (2k)$$

All of the above quantities are as measured by observers moving with the inflowing matter.

$$\begin{aligned} \dot{E} &= \text{total mass-energy accretion rate, including "PdV work", and} \\ &\text{allowing for heat transfer--equals } \dot{M}, \text{ the rate at which the} \\ &\text{black hole gains mass} \end{aligned} \quad (2l)$$

$$\hat{L} = (1 + v^2) Y^2 L \quad (2m)$$

Here $L = 4\pi r^2 w_1$ is the diffusive luminosity measured by observers moving with the inflowing matter; w is the first moment of the photon intensity [cf. equation (10) paper 1].

It is a simple matter to verify that, with M , \dot{M}_0 , and \dot{E} specified, the equations (1) are sufficient to determine a solution to our problem. We presume of course that ρ , P , and κ_1 are some given functions of ρ_0 and T (equations of state, opacity law).

After considerable manipulation (see Appendix B) the following equations for first-order derivatives can be obtained:

$$\frac{r}{\rho_0} \rho_0' = \frac{C - \mathcal{L}}{v^2 - v_c^2} \quad (3a)$$

$$\frac{r}{Y} Y' = -\frac{r}{\rho + P} P' = \frac{v^2 \mathcal{L} - v_c^2 C}{v^2 - v_c^2} \quad (3b)$$

$$\frac{r}{T} T' = \frac{v_c^2 C - (v^2 - a) \mathcal{L} / b}{v^2 - v_c^2} \quad (3c)$$

$$\frac{r}{v} v' = - \frac{(1 - v_c^2) \frac{M}{rY^2} - (1 - v^2) 2v_c^2 - (1 - v^2) \mathcal{L}}{v^2 - v_c^2} \quad (3d)$$

$$\begin{aligned} \frac{r}{H} TS' &= \frac{r}{HY} (HY)' = \frac{r}{HY\hat{M}_0} \hat{L}' = \\ &= - \frac{1}{q} \frac{(v_s^2 - v_c^2)C + (v^2 - v_s^2) \mathcal{L}}{v^2 - v_c^2} \end{aligned} \quad (3e)$$

where

$$C \equiv \frac{M}{rY^2} - 2v^2 \quad (4a)$$

$$\mathcal{L} \equiv \frac{b}{1-b} \frac{\rho_0}{4P_R} \frac{\kappa_1}{4\pi r} \frac{\hat{L}}{Y^3(1+r^2)} = - \frac{b}{1-b} \frac{r}{TY} (TY)' \quad (4b)$$

$$v_c^2 \equiv \frac{a}{1-b} \quad (4c)$$

is the isothermal sound speed squared [cf. (B4)]

$$v_s^2 \equiv qb + a \quad (4d)$$

is the adiabatic sound speed squared [cf. (B11) and (B12)]

$$a \equiv \frac{\rho_o}{\rho + P} \left(\frac{\partial P}{\partial \rho_o} \right)_T \quad (4e)$$

$$b \equiv \frac{T}{\rho + P} \left(\frac{\partial P}{\partial T} \right)_{\rho_o} \quad (4f)$$

$$q \equiv \left(\frac{\partial P}{\partial \rho} \right)_{\rho_o} \quad (4g)$$

[cf. (B10)], and where S is the entropy per unit "rest mass".

These equations will be discussed in the ensuing sections; but, in order to lay some groundwork for that discussion, it is helpful first to consider the adiabatic limit of equations (1) and (3).

3. The Adiabatic Problem

If we adopt a reduced level of description of our problem by forbidding the diffusion of photons altogether, we obtain the adiabatic limit of the equations (1):

$$4\pi r^2 \rho_0 v Y = \dot{M}_0 \quad (5a)$$

$$\frac{Y'}{Y} + \frac{P'}{\rho + P} = 0 \quad (5b)$$

$$HY = H_\infty = \text{constant} \quad (5c)$$

To obtain the adiabatic limit of equations (3), note that (3e) and the adiabatic condition $S' = 0$ tell us that

$$\mathcal{L} = \frac{v_s^2 - v_c^2}{v_s^2 - v^2} C \equiv \mathcal{L}_S \quad (6)$$

Substituting this value of \mathcal{L} in the equation (3) gives

$$\frac{r}{\rho_o} \rho_o' = \frac{C}{v^2 - v_s^2} \quad (7a)$$

$$\frac{r}{Y} Y' = - \frac{r}{\rho + P} P' = - v_s^2 \frac{C}{v^2 - v_s^2} \quad (7b)$$

$$\frac{r}{T} T' = q \frac{C}{v^2 - v_s^2} \quad (7c)$$

$$\frac{r}{v} v' = - \left[\frac{(1 - v_s^2) \frac{M}{rY^2} - (1 - v^2) 2v_s^2}{v^2 - v_s^2} \right] \quad (7d)$$

the adiabatic limit of (3). [It is worth noting here that the isothermal limit of the equations (3) is obtained by putting $\mathcal{L} = 0$ in them.]

Since there is only one differential equation in the system (5), only one of the equations (7) is independent. Thus we may adopt (7d) and plot the trajectories defined by it in the two-dimensional "phase plane" $[r \times v]$. In order to construct such a diagram, it is necessary to fix three parameters, for example M , \dot{M}_o , and H_∞ . The result is shown schematically in Fig. 1 [cf. also Blumenthal and Mathews (1976)]. Since the entropy S is constant along each curve in Fig. 1, we may regard

this figure as a "contour diagram" of the function $S(r,v)$ defined implicitly by equations (5a,c) and an equation of state. The "saddle point" of this figure corresponds to the point where both the numerator and denominator of (7d) vanish:

$$C = 0 \quad (8a)$$

$$v = v_s \quad (8b)$$

This point is a "critical point" of (7d) in the usual mathematical sense of the term [cf. Birkhoff and Rota, Ch. 5, §1]. Equations (8) may be solved for the "sonic radius"

$$r_s = \frac{M}{2} \left(\frac{1}{v_s^2} + 3 \right) \quad (9a)$$

Note that, since a gas of extreme relativistic particles has $v_s^2 = 1/3$, we have

$$r_s \geq 3M \quad (9b)$$

Since the boundary conditions for the accretion problem are

$$v = 1 \quad \text{at} \quad r = 2M \quad (10a)$$

$$v = 0 \quad \text{at} \quad r = \infty \quad (10b)$$

[cf. equations (19b,d) of paper 1], it is clear from Fig. 1 that we must choose the "critical" solution which passes through the sonic point and connects the points (10a) and (10b) (dark curve in the figure). This procedure fixes the entropy of the solution for given

values of M , \dot{M}_0 , and H_∞ . Turning this statement around, for given M , H_∞ , and S_∞ , the value of \dot{M}_0 is uniquely determined.

In view of the great usefulness of the "phase plane" Fig. 1 in understanding and solving the adiabatic problem, we shall employ a generalization of this approach in the succeeding sections where the full problem with photon diffusion is analyzed.

4. Discussion of Basic Equations

In this section we begin an analysis of the equations set forth in §2 describing accretion with photon diffusion. First note that, compared to their adiabatic counterparts in §3, these equations possess one more variable, \hat{L} , and hence one more equation to describe it [(1d), or (3e)]. Thus two of the equations (3) are independent. Second, the critical velocity in this higher level description of the problem is the isothermal sound speed v_c , not the adiabatic sound speed v_s . Third, \hat{L} (via \mathcal{L}) enters the numerators of all of the equations (3), where it competes with C -- except in equation (3d) for v' where its role is nevertheless similar.

Because two of the equations (3) are independent, and because of the especially important roles played by v and \mathcal{L} on the right-hand sides of (3), it is wise to adopt (3d) and (3e) for v' and \hat{L}' and to consider the trajectories or integral curves defined by them in the three-dimensional space $[r \times v \times \hat{L}]$. To do this, it is necessary to fix three parameters, for example M , \dot{M}_0 , and \dot{E} .

First we look at the turning points of r , v , and \hat{L} . The numerator of (3d) vanishes when

$$\mathcal{L} = \frac{1 - v_c^2}{1 - v^2} \frac{M}{rY^2} - 2v_c^2 \equiv \mathcal{L}_v \quad (11a)$$

On this surface in $[r \times v \times \hat{L}]$, integral curves have $dv = 0$. The numerator of (3e) vanishes when

$$\mathcal{L} = \frac{v_s^2 - v_c^2}{v_s^2 - v^2} C \equiv \mathcal{L}_s \quad (11b)$$

[cf. equation (6)]. On this surface the integral curves of (3d,e) have $d\hat{L} = 0$. Finally, the denominators of both (3d) and (3e) vanish when

$$v = v_c \quad (11c)$$

On this surface in $[r \times v \times \hat{L}]$, integral curves have $dr = 0$. Note that

$$\mathcal{L}_v = \mathcal{L}_s = C \quad \text{when} \quad v = v_c \quad (12)$$

This means that the surfaces (11a) and (11b) intersect each other in the surface (11c)--i.e., all three intersect along some common curve in $[r \times v \times \hat{L}]$ which we can characterize simply by

$$\mathcal{L} = C \quad (13a)$$

$$v = v_c \quad (13b)$$

This situation is illustrated in Figure 2a.

All of the points which lie on this curve are critical points in the usual mathematical sense of the term, and these are the only critical points with $v < 1$ in the problem. Accordingly, we shall call the curve defined by (13) the "critical curve." Note that (13a) causes all of the numerators in (3) to vanish if $v = v_c$.

We have already noted that integral curves have $dr = 0$ on the surface $v = v_c$. From (3d) it is easy to show that r attains a local maximum at $v = v_c$ if $\mathcal{L} < C$ there and that r attains a local minimum at $v = v_c$ if $\mathcal{L} > C$ there. Integral curves of this sort are shown in Figure 2b [the curves x-x and y-y in the figure].

It is obvious that integral curves such as these are of no use to us: $v(r)$ and $\hat{L}(r)$ are double-valued for some values of r and are not even defined for other values of r . The fix is equally obvious: we must choose an integral curve which passes through the surface $v = v_c$ with $\mathcal{L} = C$, i.e., it must pass through the critical curve.

Actually, through each critical point there pass two different integral curves [see Appendix C for proof]. This also is illustrated in Figure 2b. The integral curve labelled b-c-d in the figure is of no interest in the accretion problem; the one we want is the one labelled a-c-e.

Our boundary condition on the velocity at the horizon of the black hole [equation (10a)] defines a straight line in $[r \times v \times \hat{L}]$:

$$v = 1 \tag{14a}$$

$$r = 2M \tag{14b}$$

hereafter called the "inner boundary line". On this line, equation (3d) reads simply

$$v' = - \frac{1}{4MY^2} \quad (15)$$

Since this is always negative, all integral curves coming off the inner boundary line (14) point into the physical region $v < 1$, $r > 2M$. [They continue on into the equally physical region $v > 1$, $r < 2M$, of course.]

5. Quasi-Exponential Behavior of the Luminosity

Equation (3e) reveals a crucial feature of the behavior of the system (3d,e). Because \hat{L}' appears on the left-hand side and \hat{L} (via \mathcal{L}) appears on the right, we may suspect that this equation will cause the luminosity \hat{L} to behave in a quasi-exponential fashion. [Indeed, this is the quasi-exponential behavior that has bedeviled all who have attempted numerical solution of this problem - cf. Tamazawa, et al. (1975), Kafka and Meszaros (1976), Gillman and Stellingwerf (1980). The possibility of quasi-exponential behavior of the luminosity in simplified models was also noted by Begelman (1979).] The exponential rate implied by equation (3e) is

$$k = - \frac{v^2 - v_s^2}{v^2 - v_c^2} \frac{\dot{HYM}_o}{qr} \frac{\mathcal{L}}{\hat{L}} \quad (16)$$

This rate k may be reexpressed in a variety of useful ways [see Appendix D]. In its most general form, it is

$$k = - \frac{v}{\chi} \frac{v^2 - v_s^2}{v^2 - v_c^2} \frac{v_c^2}{v_s^2} \frac{1}{Y(1+v^2)} \quad (17)$$

where χ is the "thermal diffusivity" of the accreting material [cf. (D3) and (D4)]. This form is valid regardless of the physical mechanism underlying χ . For the case at hand, where the energy transport is due to photons diffusing in local energy equilibrium, we have

$$\chi = \lambda_{\gamma} \frac{4PR}{\rho_0} \frac{g}{H} \frac{A}{b} \frac{v_c^2}{v_s^2} \quad (18a)$$

[cf. (B9) and (D7)] where

$$\lambda_{\gamma} \equiv \frac{l}{\rho_0 K_1} \quad (18b)$$

is the photon mean free path.

Note that k changes sign by passing through a zero at $v = v_s$ and by passing through a pole at $v = v_c$. Because k is negative for $v > v_s$ and for $v < v_c$ but is positive for $v_c < v < v_s$, the luminosity \hat{L} has the qualitative behavior shown in Figure 3 in these three different velocity regimes.

When this quasi-exponential behavior of \hat{L} is sufficiently pronounced, it is clear that it serves to select a certain $\hat{L}(r, v)$,

which we shall denote by $\hat{L}_0(r,v)$, which has the property that the integral curves of (3d,e) relax with rate k toward the surface $\hat{L} = \hat{L}_0(r,v)$. In this case it is also clear from equation (3e) that $\hat{L}_0(r,v)$ is approximately equal to the luminosity which causes \hat{L}' to vanish, i.e.,

$$\hat{L}_0(r,v) \approx \hat{L}_s \equiv \frac{\hat{L}}{\alpha} \alpha_s \quad (19)$$

[cf. (4b) & (11b)].

These ideas can be put on a firm footing [see Appendix E for details] by defining a parameter τ along integral curves of (3d,e) by

$$d\tau = k dr \quad (20)$$

[cf. (E2)]. Then one can just integrate (3e) along each integral curve to obtain

$$\hat{L}(\tau) = \hat{L}(\tau_0) e^{\tau-\tau_0} + \int_{\tau}^{\tau_0} \hat{L}_s(\tau') e^{\tau-\tau'} d\tau' \quad (21)$$

[cf. (E4)]. Now it is easy to see that the surface $\hat{L} = \hat{L}_0$ is defined by those integral curves which have $\hat{L}(\tau_0)$ bounded as $\tau_0 \rightarrow \infty$. For such integral curves we have

$$\hat{L}(\tau) = \int_{\tau}^{\infty} \hat{L}_s(\tau') e^{\tau-\tau'} d\tau' \quad (22)$$

[cf. (E5)].

It is clear enough even now--and we shall discuss it in detail in the next section--that only these integral curves with bounded luminosity are relevant to the solution of our problem. Hence the equation (22) which characterizes them will prove to be extremely important to us.

From (22) we can derive [see Appendix E] an accurate version of (19):

$$\begin{aligned}\hat{L} &= \sum_{n=0}^{\infty} \left(\frac{1}{k} \frac{d}{dr} \right)^n \hat{L}_s \\ &= \hat{L}_s + \frac{1}{k} \hat{L}'_s + \dots\end{aligned}\tag{23}$$

along those integral curves which define the surface $\hat{L} = \hat{L}_0$. The series (23) is by no means guaranteed to converge everywhere. For example, it will certainly not converge for $v \sim v_s$ where k vanishes and where \hat{L}_s has a pole. When (23) does converge, and converges rapidly, we have pronounced quasi-exponential behavior in \hat{L} ; this condition is sometimes referred to as "stiff" behavior [cf. Gear (1971), §11.1]. In this case, (23) tells us that \hat{L}_0 will be close to \hat{L}_s . This slight "offset" of \hat{L}_0 from \hat{L}_s is illustrated in Figure 4.

6. Construction of Solutions

We are now ready to begin the construction of a solution to the optically-thick accretion problem.

First, return to the "critical curve" of equation (13) and Figure 2. It is clear that we have a one-parameter family of acceptable integral curves of the type labelled "ace" in Figure 2b,

each of which passes through the critical curve at a different critical point. Now the parameter τ defined in equation (20) diverges to $+\infty$ along these integral curves as they approach their critical point [cf. equation (E8) and accompanying discussion in Appendix E]. This, together with the fact that \hat{L} is finite on the critical curve, means that the one-parameter family of integral curves which passes acceptably through the critical curve is the same as the one-parameter family of integral curves which defines the surface $\hat{L} = \hat{L}_0$ in the region $v < v_s$.

Now turn to the horizon of the black hole and to the "inner boundary line" of (14). Since $v = 1 > v_s$ at the horizon, k is negative there and the luminosity behaves as in Figure 3a. Now if we choose an integral curve with $\hat{L} \neq \hat{L}_0$ at the horizon, then $|\hat{L}|$ will grow as $\exp \tau$ where $\tau \rightarrow +\infty$ as $r \rightarrow 0$ [cf. (21) and Appendix E]. Nor will rapid quasi-exponential behavior of \hat{L} set in only at some $r \ll 2M$: from (14), (17), (18), and (D8) we have

$$|k| \approx 1/\lambda_r \quad \text{at } r = 2M \quad (24)$$

Hence the quasi-exponential behavior of \hat{L} is already very stiff at the horizon, and it remains so all the way down to $r = 0$. Since integral curves with exponentially unbounded luminosity do not represent physical solutions, they must be ruled out. Hence we have the boundary condition

$$\hat{L} = \hat{L}_0 \quad \text{at } r = 2M \quad (25)$$

Now the thoughtful reader may object that in the argument leading to (25) we are using information about the behavior of the solution in the region $r < 2M$ to partially determine the solution in the region outside the black hole--which is supposed to be causally disconnected from the region inside the horizon. This objection would indeed be valid if we were considering a completely hyperbolic problem with the fastest characteristic velocity equal to the speed of light. But in fact we are making use of the "parabolic" diffusion approximation to describe energy transport in our equations, and this introduces into our problem the well-known "infinite-velocity characteristics" typical of parabolic systems. For this reason, the solution in the region $r > 2M$ can, and indeed must, depend on conditions inside the horizon, and if (25) does not hold, the solution inside the horizon will not be physical.

While it must be conceded that it is a bit of an embarrassment in principle to have information propagating out from behind the horizon of a black hole, the important question is, "Does it matter in practice?". The answer is "No": if we perturb \hat{L} away from \hat{L}_0 by some amount at some $r < 2M$, we cause an enormous change in the solution for smaller r , but an exponentially insignificant change in the solution for larger r . Indeed, by rapidly damping the information trying to propagate outward, the diffusion approximation is doing the best it can to atone for its "acausal" nature. [For a discussion of "causal" heat equations, see Israel (1976) and references cited therein.]

Because (14) and (25) fix r , v , and \hat{L} at the horizon, it might seem that these conditions would serve to select a unique integral

curve coming out from the horizon. Actually this is not the case: there is a remaining degree of freedom at the horizon in the variable Y because (14) fails to determine Y there [cf. (2d)]. Equivalently, from (15) we may regard this remaining degree of freedom as residing in dv/dr at the horizon. Hence we have a one-parameter family of integral curves coming out from the horizon which satisfy our boundary conditions (14) and (25).

Because \hat{L} has very stiff quasi-exponential behavior at the horizon, (23) converges rapidly there, and its leading term, \hat{L}_s , provides a good approximation to \hat{L} . But if \hat{L} is anywhere near \hat{L}_s in the region $v > v_s$, $r < r_s$, it is easy to see from (3d) that \hat{L} is irrelevant to the determination of v' there, as

$$\frac{M}{rY^2} > |(1-v^2) \mathcal{L}_s| \quad \text{for } v > v_s, r < r_s \quad (26)$$

[cf. (11b) and (9a)]. Hence we have, to a very good approximation,

$$\frac{r}{v} v' \approx -\frac{M}{rY^2 v^2} \quad \text{for } v > v_s, r < r_s \quad (27)$$

whose solution is

$$Y = \text{constant} \quad (28a)$$

or
$$v^2 = \frac{1}{Y^2} \left[\frac{2M}{r} - (1-Y^2) \right] \quad (28b)$$

$$\approx \frac{2M}{r} \quad \text{if } Y \approx 1 \quad (28c)$$

So as r increases along our one-parameter family of integral curves satisfying (14) and (25) at the horizon, v decreases in accordance with (28) until $v \sim v_s$ or $r \sim r_s$.

The behavior of v in the region $v_c < v < v_s$ is not so easy to determine, even though we can limit our attention to those integral curves with $\hat{L} = \hat{L}_0$, which pass acceptably through the critical curve. Certainly, if we consider very optically thick cases, where k becomes arbitrarily large, we can cause (23) to converge as fast as we please and can make the leading term approximation, $\hat{L} = \hat{L}_s$, as good as we like. In such cases, v' is well described by the adiabatic limit of (3d), equation (7d), which can be rewritten as

$$\frac{r}{v} v' = -\frac{2}{\gamma^2} \left[\frac{1 - r_s/r}{1 - v^2/v_s^2} \right] \quad (29)$$

[cf. (9a)]. But for $v < v_s$, $r > r_s$, this equation gives

$$\frac{r}{v} v' \approx -2 \quad (30)$$

Indeed, from (3d), this conclusion is valid [for $v < v_s$, $r > r_s$] as long as

$$|\mathcal{L} - \mathcal{L}_s| < |v^2 - v_c^2| \quad (31)$$

Hence we are assured, in some cases at least, that integral curves which proceed inward from the critical curve will have v increasing

and will eventually encounter the surface $v = v_s$. The big remaining question then is, "What happens at $v = v_s$?"--the subject of the next section.

7. Behavior Near the Sonic Surface

In this section we shall investigate the behavior of integral curves of (3d,e) near the "sonic surface" $v = v_s$. First we need to determine the important qualitative features of this behavior. Then we can proceed later on to a mathematical treatment.

We have already seen how \hat{L} behaves as in Figure 3a for $v > v_s$ and as in Figure 3b for $v < v_s$, and we have seen how \hat{L}_0 and \hat{L}_s are related as in Figure 4. Now at $v = v_s$, \hat{L}_s has a pole, whose sign and strength are determined by the sign and magnitude of C there [cf. (11b)]. But k vanishes at $v = v_s$. Hence \hat{L} has no tendency to behave quasi-exponentially there, (23) fails utterly to converge, and integral curves with $\hat{L} = \hat{L}_0$ "decouple" from \hat{L}_s for $v \sim v_s$. Also, from (3e), \hat{L}' is independent of \hat{L} at $v = v_s$ and depends only on the value of C there. From these ideas alone, we can readily sketch the generic behavior of integral curves of (3d,e) in the neighborhood of the surface $v = v_s$. Figures 5a and 5b show two examples.

In Figure 5a, C is positive for $v \sim v_s$, and so \hat{L}_s has a pole at $v = v_s$ of the sign shown in the figure. The integral curves with $\hat{L} = \hat{L}_0$ are fairly close to \hat{L}_s for $v \gg v_s$ and for $v \ll v_s$, but they gradually decouple from \hat{L}_s as they approach the sonic surface $v = v_s$. Still, the pole in \hat{L}_s is sufficiently strong so as to cause these two integral curves with $\hat{L} = \hat{L}_0$ to miss each other at $v = v_s$, with the

one coming from the horizon passing below the one coming from the critical curve.

Figure 5b shows another case. Here C is negative for $v \sim v_s$, and so \hat{L}_s has a pole of the sign shown in the figure. Again the pole in \hat{L}_s is strong enough to cause the two integral curves with $\hat{L} = \hat{L}_0$ to miss each other at $v = v_s$, but this time the one coming from the horizon passes above the one coming from the critical curve.

But now it is clear that, if we can adjust C in the region $v \sim v_s$, then we ought to be able to effect a meeting at the sonic surface of an integral curve with $\hat{L} = \hat{L}_0$ coming from the horizon and an integral curve with $\hat{L} = \hat{L}_0$ coming from the critical curve. Figure 5c shows such a case.

From (4a) we see that, for $v \sim v_s$, adjusting C basically amounts to adjusting r . From this, and from the Figures 5, we can deduce that integral curves with $\hat{L} = \hat{L}_0$ intersect the sonic surface as shown in Figure 6. Integral curves with $\hat{L} = \hat{L}_0$ which come from the horizon intersect the sonic surface along the curve labelled BSD in the figure, while integral curves with $\hat{L} = \hat{L}_0$ coming from the critical curve intersect the sonic surface along the curve labelled ASE. Only the integral curve which passes through the point S of Figure 6 has $\hat{L} = \hat{L}_0$ on both sides of the sonic surface, and hence only this integral curve satisfies both our boundary conditions (14) and (25) at the horizon and the condition (13) at the critical curve. This integral curve, then, is our solution!

Now that we understand the behavior of integral curves near the sonic surface, we can proceed to an analytic treatment of the situation there. From equation (22), all integral curves which satisfy our boundary conditions (14) and (25) at the horizon and which pass through the sonic surface arrive at the sonic surface with a luminosity given by

$$\hat{L}(ss) = \int_0^{\infty} \hat{L}_s(\tau) e^{-\tau} d\tau \quad . \quad (32a)$$

Here we have adjusted the "constant of integration" left unspecified by (20) so that

$$\tau = 0 \quad \text{at} \quad v = v_s \quad . \quad (32b)$$

Near the sonic surface it is advantageous to use (20), (16), and (11b) to rewrite (32a) as

$$\hat{L}(ss) = \dot{M}_0 \int_{r=0}^{ss} \frac{H\gamma}{g} \frac{v_s^2 - v_c^2}{v^2 - v_c^2} [-C] e^{-\tau} d \ln r \quad (33)$$

Similarly, from (22), all integral curves which pass acceptably through the critical curve and which pass through the sonic surface arrive at the sonic surface with a luminosity given by equation (32a) provided we again make use of (32b). Using (20), (16), and (11b) then yields

$$\hat{L}(ss) = M_0 \int_{ss}^{cc} \frac{HY}{g} \frac{v_s^2 - v_c^2}{v^2 - v_c^2} C e^{-\tau} d \ln r \quad (34)$$

But if we are able to join at the sonic surface an integral curve which satisfies boundary conditions (14) and (25) at the horizon and an integral curve which passes acceptably through the critical curve (13), then certainly \hat{L} will be continuous across the sonic surface and the right-hand sides of (33) and (34) will be equal. This gives us the very interesting result

$$\int_{r=0}^{cc} \frac{HY}{g} \frac{v_s^2 - v_c^2}{v^2 - v_c^2} C e^{-\tau} d \ln r = 0 \quad (35)$$

Equation (35) says that, along our solution, C must vanish, at least once, somewhere between $r = 0$ and the critical curve. But since τ is a minimum at $v = v_s$ along integral curves which pass through the sonic surface with $d(v - v_s)/dr < 0$ [see Appendix E], the factor $\exp[-\tau]$ is peaked at $v = v_s$ and, in order to satisfy equation (35), C will have to vanish somewhere near the sonic surface. Indeed, from (20), (32b), and (17),

$$e^{-\tau} = \exp \left\{ - \int_0^x \frac{1}{X} \frac{v(v+v_s)}{2(v^2 - v_c^2)} \frac{v_c^2}{v_s^2} \frac{1}{Y(1+v^2)} \left[-\frac{dx}{dr} \right]^{-1} dx^2 \right\} \quad (36a)$$

$$= \exp \left\{ - \left[\frac{1}{\chi} \frac{v_c^2}{v_s^2 - v_c^2} \frac{1}{Y(1 + v_s^2)} \left(- \frac{dx}{dr} \right)^{-1} \right]_{x=0} x^2 + O(x^3) \right\} \quad (36b)$$

where

$$x \equiv v - v_s \quad . \quad (36c)$$

Now if we consider progressively optically thicker, and hence more adiabatic, cases by, e.g., letting χ become smaller and smaller, we see that the factor $\exp [-\tau]$ "squeezes down" tighter and tighter around the point where our solution crosses the sonic surface. And in the adiabatic limit, $\chi \rightarrow 0$, equation (35) requires

$$C = 0 \quad \text{at} \quad v = v_s \quad (37)$$

--just as in equations (8) of §3! Thus equation (35) is the generalization of the well-known "sonic point condition" of adiabatic accretion theory to the present problem where the photons are allowed to diffuse. Just why the "sharp" adiabatic constraint (37) should become transformed into the "spread out" constraint of equation (35) will be explored in §9.

8. Behavior at Large Radius: The Region $v < v_c$

In this section we examine the behavior of our solution in the region $v < v_c$. First, since \hat{L} must be finite at $r = \infty$, we have from

(4b) that $\mathcal{L} \rightarrow 0$ like $1/r$ there. Hence from (3d)

$$\frac{r}{v} v' \sim -2 \quad \text{for } r \rightarrow \infty. \quad (38)$$

Thus our last boundary condition, (10b), is satisfied.

The behavior of v closer to the critical point is not so easy to determine. We have already noted in §6 that, if conditions are sufficiently optically thick so as to enforce (31), then our solution will have

$$\frac{r}{v} v' \approx -2 \quad (39)$$

throughout the region $v < v_c$. Otherwise, we may expect some modification of (39) near the critical point.

Now let us consider the behavior of \hat{L} along our solution in the region $v < v_c$. We have already noted that, at its critical point, our solution has $\hat{L} = \hat{L}_s$ [cf. (12) and (13)]. As our solution proceeds away from its critical point toward larger r , it will have $\hat{L} \approx \hat{L}_s$ by virtue of (23) because $|k|$ is so large near the critical point. Since our solution passes through the critical curve, it satisfies equation (22) throughout the region $v < v_c$. Hence, in particular, \hat{L} at $r = \infty$ is given by

$$\hat{L}_\infty = \int_0^\infty \hat{L}_s(\tau) e^{-\tau} d\tau \quad (40)$$

where we have adjusted the "constant of integration" left unspecified

by (20) so that

$$\tau = 0 \quad \text{at} \quad r = \infty \quad (v = 0) \quad (41)$$

[cf. (E11, E12)], and where, recall, $\tau = \infty$ at our solution's critical point [cf. (E8)].

Now if we let $x = \exp(-\tau)$, (40) becomes

$$\hat{L}_\infty = \int_0^1 \hat{L}_S(x) dx \quad . \quad (42)$$

So \hat{L}_∞ is just an average of \hat{L}_S between our solution's critical point and $r = \infty$, with most of the weight in the average lying in the region where $x \sim 1/2$ or $\tau \sim 1$. Hence we have, to a first approximation,

$$\hat{L}_\infty \approx L_S(\tau \sim 1) \quad . \quad (43)$$

But from (11b), (4a), and (4b),

$$\hat{L}_S = \frac{A}{b} \frac{4P_R}{\rho_0} \frac{4\pi M}{\kappa_1} Y(1+v^2) \frac{v_s^2 - v_c^2}{v_s^2 - v^2} \left[1 - 2v^2 Y^2 \frac{r}{M} \right] \quad (44)$$

which, from (38), is just a constant at large r :

$$\hat{L}_S \sim \frac{A}{b} \frac{4P_R}{\rho_0} \frac{4\pi M}{\kappa_1} \left(1 - \frac{v_c^2}{v_s^2} \right) \equiv \hat{L}_{S\infty} \quad \text{for} \quad r \rightarrow \infty \quad . \quad (45)$$

Indeed, in many cases \hat{L}_S is virtually constant along our solution throughout the region $v < v_c$. In such cases it is not necessary to make much of a fuss over the integral (40), we just have the simple and useful result that

$$\hat{L}_\infty \approx \hat{L}_{S\infty} . \quad (46)$$

Significant modifications of (46) can arise only if: (i) \hat{L}_S is still varying appreciably along our solution for some distance outside the critical point, and (ii) the factor $\exp(-\tau)$ fails to cut this region off in the integral (40). One can imagine cases where both of these conditions might be satisfied. For example, if conditions are sufficiently optically thin, then the width of the constraint (35) is great, and C could change sign rather close to [but, of course, inside of] the critical point--in which case the factor in square brackets in (44) would be somewhat less than unity for some distance outside the critical point, and, if $x \sim 1/2$ in this region, then the value of \hat{L}_S there will dominate the integral (42). In such a case, \hat{L}_∞ would be less than $\hat{L}_{S\infty}$.

On the other hand, it is clear that, for sufficiently optically thick cases, we can cause the factor $\exp[-\tau]$ to cut off the integral (40) as far out in radius as we please, and hence that, in this limit, because of (45), the approximation (46) becomes arbitrarily accurate.

From (4f) and (B8a), we have, for a nonrelativistic, perfect gas,

$$\frac{A}{b} \frac{4P_R}{\rho_0} = \frac{\rho_G}{\rho_0} \frac{4P_R}{4P_R + P_G} \quad (47)$$

and if we define

$$L_1 \equiv \frac{4\pi M}{\kappa_1} \quad (48)$$

--which is just the "Eddington luminosity" defined with the actual first-moment opacity κ_1 rather than the electron-scattering opacity, then we can re-express (45) as

$$\tilde{L}_{s\infty} = \frac{\rho_G}{\rho_0} \frac{4P_R}{4P_R + P_G} \left(1 - \frac{v_c^2}{v_s^2}\right) L_1 \quad (49)$$

9. Theory of Critical and Subcritical Points

Why does the adiabatic accretion problem of §3 have a critical point when $v = v_s$? Why does the present problem, where the photons are allowed to diffuse, have a critical point where $v = v_c$, and why does it have the "spread-out" constraint of equation (35) as a remnant of the adiabatic description? This section is concerned with the answers to these questions. A discussion of this sort seems especially important because the concept of a critical point has been subjected to a good deal of abuse in the astrophysics literature.

If we take the basic conservation equations and the diffusion equation which underlie the equations (1) and "linearize" them in

flat spacetime and then combine them by suitable acts of differentiation, we obtain the equation governing small perturbations of our medium:

$$\chi v_s^2 \phi_{xxxx} - \chi \frac{v_s^2}{v_c^2} \phi_{ttxx} + \phi_{ttt} - v_s^2 \phi_{txx} = 0 \quad (50)$$

[See Appendix F for derivation]. In this equation ϕ stands for the perturbation in any quantity [density, pressure, velocity...], subscript t denotes a time derivative, and subscript x denotes a space derivative [for simplicity, only one space dimension has been retained, the generalization to three is straightforward and adds no insights]. Equation (50) may be factored to

$$\begin{aligned} & \chi \frac{v_s^2}{v_c^2} (\partial_t + v_c \partial_x)(\partial_t - v_c \partial_x)(\partial_t + \partial_x)(\partial_t - \partial_x) \phi \\ & + (\partial_t + v_s \partial_x)(\partial_t - v_s \partial_x)(\partial_t + 0) \phi = 0 \end{aligned} \quad (51)$$

[the remarkable resemblance of equation (17) will be explained in due course!].

Consider first the adiabatic description of our problem, where χ is zero in equation (51). Then the low order term of (51) gives us three velocities, which are just the characteristic velocities in an adiabatic gas:

$$-v_s, 0, +v_s \quad (52)$$

Let us call these three characteristics S^- , O , and S^+ , respectively. Of course, the characteristics S^\pm correspond physically to adiabatic sound waves, and the characteristic O arises because entropy perturbations are "frozen into" an adiabatic gas and hence must move with the same velocity as the gas. Now these characteristics play their usual role of propagating information about the solution through the gas from one spacetime point to another and thus tell us where we must specify boundary conditions in order to set well-posed physical problems.

Now consider a solution of the adiabatic, steady-state, spherical accretion problem, and identify the $+x$ direction with the direction of increasing r . Then it is easy to see that O characteristics carry their information from $r = \infty$ down to $r = 0$ and that the S^- characteristics do the same, only faster. But the situation is quite different for the S^+ characteristics: because their net outward velocity is $v_s - v$, which is negative inside the sonic point, they behave as shown in Figure 7a. But then from the figure it is obvious that the surface $r = r_s$ acts as the "source" of the S^+ characteristics, and indeed it is easy to show that, going backward in time, each S^+ characteristic approaches r_s as

$$r \sim r_s + s e^{\alpha t} \quad (53)$$

where

$$\alpha \equiv \left[- \frac{d(v - v_s)}{dr} \right]_{v=v_s} > 0 \quad (54)$$

along our solution and where s selects the characteristic. The situation becomes somewhat more clear if we switch for a moment from the coordinates r and t to:

$$\sigma \equiv \tanh (s/r_s) \quad (55a)$$

$$\tau \equiv \tanh (\alpha t) \quad (55b)$$

Then Figure 7a becomes transformed to Figure 7b, and now it is quite clear that we must specify a boundary condition on the surface $\tau = -1$, $-1 < \sigma < 1$, in order to determine a solution in the future. But this entire "surface" lies at $r = r_s$ ($t = -\infty$), and the fact that we must specify a boundary condition here shows up in the steady-state problem as the constraint (8) of §3. From this example, it is clear that we can expect to find critical points in equations describing stationary flow whenever the flow velocity equals a characteristic velocity.

Now when we improve upon the adiabatic description of our problem by allowing photon diffusion, χ is no longer zero in equation (51). Because the characteristic velocities are given by the highest-order derivative terms in the perturbation equation, these are no longer given by (52) but are instead

$$-\infty, -v_c, +v_c, +\infty . \quad (56)$$

Let us call the corresponding characteristics ∞^- , C^- , C^+ , and ∞^+ , respectively. The characteristics C^\pm correspond physically to isothermal sound waves, and it is easy to see on physical grounds that short wavelength acoustic perturbations must be isothermal. The characteristics ∞^\pm , because they actually coalesce to form one double characteristic, reveal the parabolic aspect of our system of equations. Though this parabolic quality derives from our adopting the diffusion approximation to describe energy transport, it is the equation of energy conservation which cannot be put into characteristic form. For our present purposes, however, it will be adequate to think of this double characteristic as propagating information in both directions at an infinite velocity (i.e., everywhere perpendicular to the gas four-velocity).

Now consider a solution of the steady, spherical accretion problem including the effects of photon diffusion. Then the ∞^- and C^- characteristics carry their information from $r = \infty$ down to $r = 0$. The C^+ characteristics, because they have a net outward velocity of $v_c - v$, which is negative inside the critical point, behave just like the S^+ characteristics did in the adiabatic case; and where $v = v_c$ there is a surface $r = r_c$ which acts as the source of the C^+ characteristics just as in Figures 7a,b drawn for S^+ in the adiabatic case. Again, because we must specify a boundary condition on this surface, our solution has a critical point there. The ∞^+ characteristics propagate their information from $r = 0$ out to $r = \infty$. Indeed we saw in §6 how our solution depended, albeit insignificantly, on conditions inside the horizon of the black hole, and there we

identified the ∞^+ characteristics as the culprit responsible for this "acausal" dependence.

At this point, it is natural to wonder what has become of S^- , 0 , and S^+ . Since these correspond to the low-order wave operators in Eqn. (51), they have lost their status as characteristics and are known instead as "subcharacteristics" [cf. Cole (1968), §4.1]. The fact that the low-order, subcharacteristic wave operators are present along with the high-order, characteristic wave operators in the perturbation equation (51) suggests that the subcharacteristics S^- , 0 , and S^+ will have some role to play in our problem--a role which should somehow pass over smoothly to their role as characteristics when we take the adiabatic limit $\chi \rightarrow 0$.

In order to understand the differing roles played by the characteristics and subcharacteristics in our problem, it is helpful to investigate the physical nature of the waves which propagate along them. Such a "wave hierarchy" analysis can be carried out by considering the signalling problem corresponding to equation (51), using Laplace transforms to obtain exact solutions, and then making appropriate asymptotic expansions to follow the waves of interest--or by means of a much simpler technique which will be employed here [cf. Witham (1974), §10, for an excellent discussion].

The basic idea behind the simplified technique can be put as follows. A roughly steady wave profile propagating with velocity v satisfies

$$(\partial_t + v \partial_x) \phi = 0 \quad (57)$$

to zeroth-order. A more refined approximation to the true behavior of this wave can then be obtained by substituting this zeroth-order approximation into the full perturbation equation in all of the wave operators save the critical one, which is retained as a directional derivative in order to follow the wave.

Thus, to follow the isothermal sound waves with $v = v_c$, we use $\partial_t = -v_c \partial_x$ in (51) and obtain

$$2\chi \frac{v_s^2}{v_c^2} (\partial_t + v_c \partial_x) \phi_{xxx} + (v_s^2 - v_c^2) \phi_{xxx} = 0 \quad (58)$$

The three x-derivatives in this equation are remnants of the other waves and can thus be integrated out without loss. We have then

$$(\partial_t + v_c \partial_x) \phi = - \frac{v_c^2}{2\chi} \left(1 - \frac{v_c^2}{v_s^2}\right) \phi \quad (59)$$

An elementary solution of (59) is

$$\phi = e^{-\gamma_c t} \int (x - v_c t) \quad (60a)$$

where

$$\gamma_c = \frac{v_c^2}{2\chi} \left(1 - \frac{v_c^2}{v_s^2}\right) \quad (60b)$$

Thus the isothermal sound waves $v = v_c$ are damped at the rate γ_c given by equation (60b).

Now let us follow the adiabatic sound waves with $v = v_s$. We use $\partial_t = -v_s \partial_x$ in (51) and obtain, after integrating out two x -derivatives,

$$\left(\partial_t + v_s \partial_x\right) \phi = \frac{\chi}{2} \left(\frac{v_s^2}{v_c^2} - 1\right) \phi_{xx} \quad (61)$$

An elementary solution of (61) is

$$\phi = \frac{1}{\sqrt{4\pi\nu_s t}} \exp \left\{ -\frac{(x - v_s t)^2}{4\nu_s t} \right\} \quad (t > 0) \quad (62a)$$

where

$$\nu_s \equiv \frac{\chi}{2} \left(\frac{v_s^2}{v_c^2} - 1\right) \quad (62b)$$

Thus the adiabatic sound waves with $v = v_s$ are diffused, so that an initial δ -function disturbance has a gaussian width σ given by

$$\sigma^2 = 2\nu_s t \quad (63)$$

at a time t later.

Now, physically, it is obvious that it is this diffusion of the adiabatic sound waves which is responsible for the transformation of the sharp adiabatic sonic point condition (8) into the spread-out constraint (35) which we found in §7. Indeed, when χ is small, the weighting function $\exp(-\tau)$ in (35) is, to an excellent approximation, just the gaussian

$$\exp \left\{ - \frac{\alpha z^2}{2 v_s^2} \right\} \quad (64)$$

where
$$z \equiv r - [r]_{v = v_s} \quad (65)$$

[cf. (54)] and where v_s is the same as in (62b). [Here we have neglected the relativistic correction factor $\gamma(1+v_s^2)$ in keeping with the simple, non-relativistic analysis of this section.]

We can understand the result (64) quite simply in terms of the propagation of the diffusing adiabatic sound waves near the sonic point of our solution.

First, it must be pointed out that the full perturbation equation describing the propagation of these waves is quite complicated. It contains, for example, terms arising from the spherical geometry and terms arising from gradients in the unperturbed solution, effects which (50), and hence (61), do not take into account. Here, however, we aim only to understand the limit form (64), and if

$$\sqrt{\frac{v_s}{\alpha}} \ll [r, \text{ scale heights}] \quad (66)$$

at the sonic point

then we can safely ignore the terms which are absent from (61) and can use it as it stands to investigate the propagation of the diffusing adiabatic sound waves near the sonic point.

First we must transform (61) to Schwarzschild coordinates t and r - or, more conveniently, z . We obtain

$$\left(\partial_t + (v_s - v) \partial_z \right) \phi = v_s \phi_{zz} \quad (67)$$

Near the sonic point we have

$$v_s - v = \alpha z \quad (68)$$

and so we want to study the behavior of ϕ obeying

$$\left(\partial_t + \alpha z \partial_z \right) \phi = v_s \phi_{zz} \quad (69)$$

With the coordinate transformation

$$s = z e^{-\alpha t} \quad (70a)$$

$$\tau = \frac{1}{2\alpha} [1 - e^{-2\alpha t}] \quad (70b)$$

[Note that s is constant along each subcharacteristic S^+], equation (69) becomes simply the heat equation

$$\phi_\tau = \nu_s \phi_{ss} \quad (71)$$

from which we can deduce the usual Green function for the initial-value problem:

$$G[s, s_0; \tau] = \frac{1}{\sqrt{4\pi\nu_s\tau}} \exp\left\{-\frac{(s-s_0)^2}{4\nu_s\tau}\right\} \quad (72)$$

$$(\tau > 0)$$

or, in terms of z and t ,

$$G[z, z_0; t] = \frac{1}{\sqrt{2\pi\frac{\nu_s}{\alpha}[1-e^{-2\alpha t}]}} \exp\left\{-\frac{(ze^{-\alpha t} - z_0)^2}{2\frac{\nu_s}{\alpha}[1-e^{-2\alpha t}]}\right\} \quad (73)$$

$$(t > 0)$$

Now, because we are studying the steady-state accretion problem, we are interested in the ultimate fate of perturbations, i.e., the limit of G as $t \rightarrow \infty$:

$$G_\infty[z, z_0] = \frac{1}{\sqrt{2\pi\frac{\nu_s}{\alpha}}} \exp\left\{-\frac{\alpha z_0^2}{2\nu_s}\right\} \quad (74)$$

This is independent of z , but depends on z_0 exactly as in (64). Equation (74) is telling us that points in a finite region around $[r]_{v=v_s}$ are effective in determining our solution in the future. It is for this reason that our generalized sonic point constraint (35) averages over these points and does so with the weights given by (74). Thus it seems that we can speak of our sonic point as being a "diffused" critical point. Perhaps better, since this diffusion results from the action of the higher-order terms in (51) and since the presence of these terms also converts the S^+ from characteristics to subcharacteristics, it seems appropriate to call our sonic point a subcritical point.

It is worth pointing out that if, proceeding as before, we follow the $v = 0$ waves of (51), which generate the subcharacteristics 0, we obtain the simplified equation

$$\phi_t = \chi \phi_{xx} \quad (75)$$

Again, these low-order waves are diffused, and the relevant diffusion coefficient for these waves is just χ itself. These diffusing subcharacteristic "waves" correspond physically to isobaric entropy perturbations.

Now we can deliver on the promise made immediately following equation (51) and can explain why k , the local growth rate for \hat{L} in our steady-state equation (3e), has the form shown in equation (17). We can derive (17) from the basic perturbation equation (51); the essential step is to impose the steady flow requirement on the perturbations ϕ we will consider. We then have [cf. equation (4) of paper 1]

$$\phi_t = -v \Upsilon \phi' \quad (76a)$$

$$\phi_x = \Upsilon \phi' \quad (76b)$$

where, as before, a prime denotes differentiation with respect to Schwarzschild radius r . Since the conditions (76) require that $\phi_t + v\phi_x = 0$, by imposing them we are abandoning any consideration of physical perturbations [sound waves, entropy perturbations,...] and are studying instead the response of our steady-state system (3d,e) to perturbations. Inserting (76) into (51) we obtain, after integrating out three primes,

$$\phi' = k_0 \phi \quad (77a)$$

where

$$k_0 = -\frac{v}{\chi} \frac{v^2 - v_s^2}{v^2 - v_c^2} \frac{v_c^2}{v_s^2} \frac{1}{\Upsilon} \quad (77b)$$

is evidently the local growth rate (in radius r) of perturbations ϕ which satisfy the steady flow conditions (76). [The rate k of equation (17) is virtually the same as k_0 except for an additional factor of $(1+v^2)^{-1}$ which arises because k refers specifically to the behavior of \hat{L} in our steady-state system whereas k_0 refers to the behavior of local quantities such as density, pressure, etc. [cf. (2m)].] Thus the somewhat bizarre form of equation (17) for k is in fact a natural consequence of imposing the steady-flow requirement on equation (51), which describes the way our fluid wants to behave when it is perturbed.

10. Example of Numerical Solution

Numerical solutions and detailed discussion of their physical properties are the province of paper III of this series. Nevertheless, we include one example here in order to assure the patient reader that all of the considerations in the preceding sections do in fact lead to actual solutions! The numerical technique, which will also be described more fully in paper III, basically amounts to patching together the three kinds of pieces shown in Figure 3, making appropriate joins at the critical and subcritical points, and taking care to observe our boundary conditions at the horizon. The accreting gas has been taken to be ionized hydrogen obeying the perfect gas equation of state; opacity is due to electron scattering and free-free absorption. Figure 8 shows the run of v , ρ_0 , T , and \hat{L} versus r ; Table 1 summarizes some of the important parameters of this particular solution. Note that the rest-mass accretion rate \dot{M}_0 is about one order of magnitude greater than the adiabatic accretion rate

$$2 \sqrt{2} \pi M^2 \rho_{0,\infty} / v_{s,\infty}^3 = 2.716 \times 10^{-6} \frac{M_\odot}{yr} \quad (78)$$

of a $\Gamma = 4/3$ gas [cf. Bondi (1952)]. The luminosity \hat{L}_∞ is indistinguishable from $\hat{L}_{s,\infty}$ in accordance with (46), and both are within .06% of $L_1 = L_{Ed}$ in accordance with (49).

11. Conclusion

Stationary, spherically-symmetric, optically thick accretion flows into black holes possess critical points where the inflow velocity equals the isothermal sound speed and subcritical points where the inflow velocity equals the adiabatic sound speed. The critical point corresponds to the existence of a stationary characteristic surface, and the subcritical point corresponds to the existence of a stationary subcharacteristic surface.

Critical and subcritical points will arise in any steady flow problem in which both characteristics and subcharacteristics are present--i.e., they will arise whenever the basic perturbation equation describing the time-dependent behavior of the system contains both high- and low-order wave operators. In particular, all hydrodynamics problems with radiative transfer treated in the diffusion approximation with LTE will have the characteristics and subcharacteristics discussed in this paper. If such problems involve steady flow in one dimension, then the ideas and techniques used here will carry over directly. In particular, the crucial issues of which boundary conditions one can specify and where one can specify them are made completely clear in this approach.

As regards the roles played by the critical and subcritical points in the optically thick accretion problem, the following heuristic picture can be given. First, in the adiabatic accretion problem, as we have seen, the sonic point constraint determines the rest-mass accretion rate. Now when we seek to improve upon this description by allowing photon diffusion, we necessarily introduce

a new variable into the problem, namely the luminosity. Thus, roughly speaking, we need some new constraint to determine a unique solution to the problem. The (isothermal) critical point provides this. Indeed we saw how the luminosity at infinity was intimately connected with this critical point. But we have also seen that, if conditions are very optically thick, the adiabatic sonic point, now a subcritical point, plays much the same role as it does in the strictly adiabatic case, so we can still think of it as determining the rest mass accretion rate. Finally, as conditions become progressively optically thinner, this neat division of labor between the critical and subcritical points no longer applies, and their action in determining the accretion rate and the luminosity becomes more mutual.

With the basic theory of optically thick accretion into black holes now firmly in hand, it is possible to move on with some confidence to consider some of the possible astrophysical applications. Two opposite limits immediately suggest themselves. In the first, the accretion solution is followed sufficiently far out into the hydrostatic region beyond the subcritical and critical points so that the self-mass of the accreting material becomes comparable with the mass of the central black hole. From this point on, the problem becomes one of standard, Newtonian stellar-model building, all of the very highly developed lore of that field can be brought to bear.

At the opposite extreme, there is the case where the accretion flow becomes optically thin at some finite radius. Here one must consider the details of radiative transfer in a "photosphere" with

large fluid velocities and significant steady-state compression [Cf. Payne and Blandford (1981) for a discussion of this situation in a particular limit.]. Beyond this photospheric transition region, one would join on to an optically thin accretion solution.

Because it can easily produce luminosities up to the usual Eddington limit, spherical optically thick accretion into black holes would seem to be a promising mechanism for powering the enormous light output of quasars. When more work is done along the lines sketched above, it will be possible to put this idea to a real test.

Acknowledgements

It is a pleasure to thank Kip Thorne who suggested a variant of this problem to me and whose questions during the later stages of this work greatly sharpened my understanding of some of the basic issues involved. I would also like to acknowledge a helpful conversation with G. B. Whitham. Richard Price and the referee made valuable comments on the manuscript.

References

- Begelman, M. C., 1978. Mon. Not. R. astr. Soc., 184, 53.
- Begelman, M. C., 1979. Mon. Not. R. astr. Soc., 187, 237.
- Birkhoff, G., and Rota, G.-C., 1969. Ordinary Differential Equations,
Blaisdell Publishing Co.
- Blumenthal, G. R., and Mathews, W. G., 1976. Astrophys. J., 203, 714.
- Bondi, H., 1952. Mon. Not. R. astr. Soc., 112, 195.
- Cole, J. D., 1968. Perturbation Methods in Applied Mathematics,
Blaisdell Publishing Co.
- Cox, J. P., and Giuli, R. T., 1968. Principles of Stellar Structure,
Vol. 1. Physical Principles, Gordon & Breach.
- Flammang, R. A., 1982. Mon. Not. R. astr. Soc., in preparation.
- Gear, W. C., 1971. Numerical Initial Value Problems in Ordinary
Differential Equations, Prentice-Hall, Inc.
- Gilden, D. L., and Wheeler, J. C., 1980. Astrophys. J., 239, 705.
- Gillman, A. W., and Stellingwerf, R. F., 1980. Astrophys. J., 240, 235.
- Israel, W., 1976. Ann. Phys. (N.Y.), 100, 310.
- Kafka, P., and Mészáros, P., 1976. Gen. Rel. Grav., 7, 841.
- Maraschi, L., Reina, C., and Treves, A., 1974. Astr. Astrophys., 35, 389.
- Mészáros, P., 1975. Astr. Astrophys., 44, 59.
- Michel, F. C., 1972. Astrophys. Space Sci., 15, 153.
- Payne, D. G., and Blandford, R. D., 1981. Mon. Not. R. astr. Soc.,
in press.
- Shvartsman, V. F., 1971. Sov. Astron.-A.J., 15, 377.
- Shapiro, S. L., 1973a. Astrophys. J., 180, 531.
- Shapiro, S. L., 1973b. Astrophys. J., 185, 69.

Tamazawa, S., Toyama, K., Kaneko, N., and Ono, Y., 1975.

Astrophys. Space Sci., 32, 403.

Tamm, R. E., Bodenheimer, P., and Ostriker, J. P., 1978.

Astrophys. J., 222, 269.

Thorne, K. S., Flammang, R. A., and Żytkow, A. N., 1981. Mon. Not.

R. astr. Soc., 194, 475.

Thorne, K. S., and Żytkow, A. N., 1977. Astrophys. J., 212, 832.

Vitello, P. A. J., 1978. Astrophys. J., 225, 694.

Whitham, G. B., 1974. Linear and Nonlinear Waves, John Wiley and
Sons, Inc.

Woosley, S. E., 1980. Private communication.

Appendix A

Here the equations (18) of paper 1 are reduced to the form (1) of the present paper. With (20) and (21) of paper 1 in force, the photons are diffusing and are in local energy equilibrium with the gas. Because they are diffusing, we have

$$w_1 \sim \frac{\bar{\lambda}}{\bar{\mathcal{L}}} w_0 \quad (\text{A1a})$$

and

$$w_2 \sim \left(\nu + \frac{\bar{\lambda}}{\bar{\mathcal{L}}}\right) \frac{\bar{\lambda}}{\bar{\mathcal{L}}} w_0 \quad (\text{A1b})$$

with

$$\frac{\bar{\lambda}}{\bar{\mathcal{L}}} \ll 1 \quad (\text{A2})$$

[cf. equation (20c) of paper 1]. Here $\bar{\lambda}$ stands for the photon mean free path, and $\bar{\mathcal{L}}$ stands for the smallest local macroscopic length scale [see equation (20a) of paper 1 for details]. Thus we may neglect w_2 in the radiation stress-energy tensor [equation (14) of paper 1] and write

$$P_R \equiv T_R^{\hat{r}\hat{r}} = T_R^{\hat{\theta}\hat{\theta}} = T_R^{\hat{\varphi}\hat{\varphi}} = \frac{1}{3} \rho_R \quad (\text{A3})$$

i.e., the radiation pressure is isotropic and equal to one third of the radiation energy density. With (A3), we may reexpress the equation of conservation of radial momentum [(18d) of paper 1] as in (1b) [cf. (2g,i)].

Similarly, we may reexpress the relativistic Bernoulli equation [(18c) of paper 1] as in (1c) [cf. (2j,m)]. In this equation, w_2 has been neglected. This point requires some discussion. The contributions of the first three moments of the photon distribution to the Bernoulli equation are in the ratios

$$\frac{4}{3}vw_0 : -(1+v^2)w_1 : vw_2 \quad (\text{A4a})$$

Using (A1) and ignoring signs and factors of order unity, these become

$$v : (1+v^2) \frac{\bar{\lambda}}{\bar{z}} : v \left(v + \frac{\bar{\lambda}}{\bar{z}} \right) \frac{\bar{\lambda}}{\bar{z}} \quad (\text{A4b})$$

Thus for $v \ll 1$, the w_2 term is small compared to both of the others; but for $v \sim 1$, as is the case near the horizon of the black hole [cf. equation (19d) of paper 1], the w_2 term is comparable to the w_1 term - though both of these are then small compared to the w_0 term. This means that ignoring w_2 will lead to substantial errors in calculated values of w_1 near the horizon. Fortunately, we shall see that the precise value of w_1 at the horizon has an insignificant influence on the rest of the solution. For this reason, retaining w_2 in the Bernoulli equation, which would require adding the second moment of the radiative transfer equation [(18g) of paper 1] to our system, is a refinement which in the end would not carry its own weight.

Because the photons are in local energy equilibrium with the gas, we have

$$\rho_R = aT^4, \quad (\text{A5})$$

where T is the gas temperature, from the zeroth moment of the radiative transfer equation [(18e) of paper 1]. From (A5), the first moment of the radiative transfer equation [(18f) of paper 1] becomes

$$L = -4\pi r^2 \frac{\frac{4}{3} a T^3}{\rho_0 K_1} (TY)' \quad (\text{A6})$$

which, with (2m), gives (1d).

The equation of "rest mass" conservation [(18b) of paper 1] appears here unchanged as (1a).

Appendix B

Here the basic equations of structure (1) are solved for the first-order derivatives of various quantities of interest.

By making use of (1a) and (2d), the equation of conservation of radial momentum (1b) can be expressed as

$$(v^2 - a) \frac{r}{\rho_0} \rho_0' - b \frac{r}{T} T' = C \quad (\text{B1})$$

[Cf. (4a), (4e), (4f)]. By using (1a) and (2d) and also (B1), the transport equation (1d) can be written as

$$\frac{a}{1-b} \frac{r}{\rho_0} \rho_0' - \frac{r}{T} T' = \frac{1}{b} Z \quad (\text{B2})$$

[Cf. (4b), (4e), (4f)]. Equations (B1) and (B2) can be solved for the pair (3a) and (3c). In these equations, the quantity $a/(1-b) \equiv v_c^2$ is the isothermal sound speed squared. To show this, we need the "reciprocity relation"

$$T \left(\frac{\partial \rho}{\partial T} \right)_{\rho_0} + \rho_0 \left(\frac{\partial T}{\partial \rho_0} \right) = \rho + P \quad (\text{B3})$$

[Cf. Cox & Giuli (1968), §9.11]. Then we have

$$v_c^2 \equiv \frac{a}{1-b} = \frac{\rho_o \left(\frac{\partial P}{\partial \rho_o} \right)_T}{\rho + P - T \left(\frac{\partial P}{\partial T} \right)_{\rho_o}} = \frac{\left(\frac{\partial P}{\partial \rho_o} \right)_T}{\left(\frac{\partial \rho}{\partial \rho_o} \right)_T} = \left(\frac{\partial P}{\partial \rho} \right)_T \quad (\text{B4})$$

The last quantity in this equation is the square of the isothermal sound speed.

Equation (3b) is easily derived from (1a), (1b), (2d), and (3a); then (3d) is easily obtained from (1a), (3a), and (3b).

Equation (3e) can be obtained by first differentiating (1c) with respect to r . Then, by subtracting off (1b) and using the first law of thermodynamics

$$d\rho = H d\rho_o + \rho_o T ds \quad (\text{B5})$$

we obtain the important result

$$(HY)' = (YT)S' \quad (\text{B6})$$

So the derivative of the redshifted enthalpy is just the redshifted temperature times the entropy derivative. Finally, by differentiating (1c) and subtracting off (1b), one can obtain

$$\frac{r}{H\gamma M_0} \hat{L}' = B \frac{r}{T} T' - (1-A) \frac{r}{\rho_0} \rho_0' \quad (\text{B7})$$

where
$$A \equiv \frac{\rho_0}{\rho+p} \left(\frac{\partial \rho}{\partial \rho_0} \right)_T \quad (\text{B8a})$$

and
$$B \equiv \frac{T}{\rho+p} \left(\frac{\partial \rho}{\partial T} \right)_{\rho_0} = \frac{\rho_0 T}{\rho+p} C_v \quad (\text{B8b})$$

Note that the reciprocity relation (B3) guarantees that

$$A + b = 1 \quad (\text{B9})$$

From (B7), (3a), and (3c), the remaining part of equation (3e) is readily derived. In this equation, q is given by any of the following expressions

$$q = \frac{1-A}{B} = \frac{b}{B} = \left(\frac{\partial p}{\partial \rho} \right)_{\rho_0} = \Gamma_3 - 1 \quad (\text{B10})$$

and the quantity $qb+a \equiv v_s^2$ is the adiabatic sound speed squared.

To show this, use the first law of thermodynamics to write

$$H = \left(\frac{\partial p}{\partial \rho_0} \right)_s = \left(\frac{\partial p}{\partial T} \right)_{\rho_0} \left(\frac{\partial T}{\partial \rho_0} \right)_s + \left(\frac{\partial p}{\partial \rho_0} \right)_T \quad (\text{B11a})$$

From this and (B10) it follows that

$$g = \frac{\rho_0}{T} \left(\frac{\partial T}{\partial \rho_0} \right)_s \quad (\text{B11b})$$

Then we have

$$\begin{aligned} v_s^2 &\equiv g b + a = \frac{1}{H} \left[\left(\frac{\partial p}{\partial T} \right)_{\rho_0} \left(\frac{\partial T}{\partial \rho_0} \right)_s + \left(\frac{\partial p}{\partial \rho_0} \right)_T \right] \\ &= \left(\frac{\partial \rho_0}{\partial p} \right)_s \left(\frac{\partial p}{\partial \rho_0} \right)_s = \left(\frac{\partial p}{\partial \rho} \right)_s \end{aligned} \quad (\text{B12})$$

The last quantity in this equation is the square of the adiabatic sound speed.

Appendix C

Here we show that two different integral curves pass through each critical point. By eliminating \mathcal{L} from equations (3d,e) and performing some algebra, we can obtain the very useful result

$$(v^2 - v_s^2) Y^2 \frac{r}{v} v' + \left(1 - \frac{2M}{r}\right) q_{\text{HYM}_0} \hat{L}' = 2v_s^2 \left(1 - \frac{r_s}{r}\right) \quad (\text{C1})$$

where r_s is as defined in equation (9a).

Because of (C1) it suffices to expand only equation (3d) about the critical point. Carrying out this expansion yields

$$\frac{r_c}{v_c} (v')_{\text{cp}} = \left(\frac{1 - v_c^2}{2v_c}\right) \left(\frac{\mathcal{L}}{\hat{L}}\right)_{\text{cp}} \left[\frac{\left[\left(\frac{\partial \hat{L}_v}{\partial r}\right)_{\text{cp}} + \left(\frac{\partial \hat{L}_v}{\partial v}\right)_{\text{cp}} (v')_{\text{cp}} + \left[\left(\frac{\partial \hat{L}_v}{\partial \hat{L}}\right)_{\text{cp}} - 1\right] (\hat{L}')_{\text{cp}}\right]}{\left[\left(\frac{\partial v_c}{\partial r}\right)_{\text{cp}} + \left[\left(\frac{\partial v_c}{\partial v}\right)_{\text{cp}} - 1\right] (v')_{\text{cp}} + \left(\frac{\partial v_c}{\partial \hat{L}}\right)_{\text{cp}} (\hat{L}')_{\text{cp}}\right]} \right] \quad (\text{C2})$$

where

$$\hat{L}_v \equiv \frac{\hat{L}}{Z} Z_v \quad (\text{C3})$$

[Cf. (4b) and (11a)]. Substituting from (C1) for $(\hat{L}')_{\text{cp}}$ then yields a quadratic equation for $(v')_{\text{cp}}$ with two solutions.

Appendix D

In this appendix we discuss the local growth rate k of §5. First, by making use of (1a) and (4b) in (16) we obtain

$$k = - \frac{1}{\lambda_\gamma} \left[\frac{H}{f} \frac{b}{A} \frac{\rho_0}{4P_R} \right] \frac{v (v^2 - v_s^2)}{v^2 - v_c^2} \frac{1}{\gamma (1 + v^2)} \quad (D1)$$

where

$$\lambda_\gamma \equiv \frac{1}{\rho_0 K_1} \quad (D2)$$

is the photon mean free path. Thus the fundamental length scale underlying k is λ_γ .

Equation (D1) may be reexpressed more conveniently as

$$k = - \frac{v}{\chi} \left(\frac{v^2 - v_s^2}{v^2 - v_c^2} \right) \frac{v_c^2}{v_s^2} \frac{1}{\gamma (1 + v^2)} \quad (D3)$$

Here χ is the "thermal diffusivity" defined as

$$\chi \equiv \frac{\kappa}{\rho_0 C_p} \quad (D4)$$

where κ is the thermal conductivity and C_p is the specific heat at constant pressure. Equation (D3) is valid regardless of the particular physical mechanism which provides energy transport.

When this role is played by photons diffusing in local energy equilibrium, we have from (A6)

$$\kappa = \kappa_\gamma \equiv \lambda_\gamma \frac{4}{3} a T^3 \quad (\text{D5})$$

The specific heat at constant pressure is

$$C_p = \gamma C_v = \frac{v_s^2}{A v_c^2} \frac{\rho + P}{\rho_0 T} B \quad (\text{D6})$$

So χ is given by

$$\chi = \lambda_\gamma \frac{4P_R}{\rho_0} \frac{A}{b} \frac{\gamma}{H} \frac{v_c^2}{v_s^2} \quad (\text{D7})$$

From (D7) it follows that

$$\chi < \lambda_\gamma \frac{v_c^2}{v_s^2} \quad (\text{D8})$$

Appendix E

In this appendix we develop a method for translating the idea of Figures 3 and 4 into equations. First, use (16) and (19) to rewrite equation (3e) as

$$\hat{L}' = k (\hat{L} - \hat{L}_s) \quad (\text{E1})$$

Now pick some arbitrary integral curve \mathcal{C} of the equations (3d, e). Along \mathcal{C} , all of the variables in our problem are a function of a single parameter--for example, radius r . But it is very useful to define a new parameter τ along \mathcal{C} by

$$d\tau = k dr \quad . \quad (\text{E2})$$

Then (E1) becomes

$$\hat{L}(\tau) - \frac{d}{d\tau} \hat{L}(\tau) = \hat{L}_s(\tau) \quad (\text{E3})$$

which we can just integrate along \mathcal{C}

$$\hat{L}(\tau) = \hat{L}(\tau_0) e^{\tau - \tau_0} + \int_{\tau}^{\tau_0} \hat{L}_s(\tau') e^{\tau - \tau'} d\tau' \quad (\text{E4})$$

Now all integral curves of (3d,e) satisfy equation (E4). But the surface $\hat{L} = \hat{L}_0(r, v)$ is characterized by those integral curves which have the property that $\hat{L}(\tau_0)$ remains bounded as $\tau_0 \rightarrow \infty$. For such integral curves we have

$$\hat{L}(\tau) = \int_{\tau}^{\infty} \hat{L}_s(\tau') e^{\tau - \tau'} d\tau' \quad (E5)$$

From (E5) we can obtain a useful series. Represent $\hat{L}_s(\tau')$ by its Taylor series about τ :

$$\begin{aligned} \hat{L}(\tau) &= \sum_{n=0}^{\infty} \frac{1}{n!} \left(\frac{d}{d\tau} \right)^n \hat{L}_s(\tau) \int_{\tau}^{\infty} (\tau' - \tau)^n e^{\tau - \tau'} d\tau' \\ &= \sum_{n=0}^{\infty} \left(\frac{d}{d\tau} \right)^n \hat{L}_s(\tau) \end{aligned} \quad (E6)$$

So

$$\hat{L}(r) = \sum_{n=0}^{\infty} \left(\frac{1}{k} \frac{d}{dr} \right)^n \hat{L}_s(r) \quad (E7)$$

This series converges when $|k|$ is large compared to the rates at which \hat{L}_s and k itself are varying.

Now, we need a few results concerning the behavior of the parameter τ defined in (E2). First consider the integral curves which pass acceptably through the critical curve of equation (13). Along these we have

$$\begin{aligned} \tau &= \int k \, dr = \int k \left[\frac{d(v - v_c)}{dr} \right]^{-1} d(v - v_c) \\ &= \int -\frac{v}{\chi} \frac{v_s^2 - v^2}{v + v_c} \frac{v_c^2}{v_s^2} \frac{1}{Y(1 + v^2)} \left[-\frac{d(v - v_c)}{dr} \right]^{-1} \frac{d(v - v_c)}{v - v_c} \end{aligned} \quad (\text{E8})$$

which diverges to $+\infty$ like $\ln \left| \frac{1}{v - v_c} \right|$ for $v \rightarrow v_c$ because $v_s^2 > v_c^2$ and because $d(v - v_c)/dr$ is finite (and negative) at $v = v_c$ for those integral curves which pass acceptably through the critical curve.

It turns out that our solutions have $k \sim -\frac{1}{r}$ as $r \rightarrow 0$. Hence τ diverges to $+\infty$ like $\ln \frac{1}{r}$ there.

Now consider an integral curve \mathcal{C} which passes through the surface $v = v_s$. From (E2), since k vanishes at $v = v_s$, τ is stationary there. To find out if τ is a maximum or a minimum there, let $x \equiv v - v_s$ along \mathcal{C} . Then $d\tau/dx = k (dx/dr)^{-1}$, and

$$\left[\frac{d^2 \tau}{dx^2} \right]_{x=0} = \left[\frac{dk}{dx} \right]_{x=0} \left[\frac{dx}{dr} \right]_{x=0}^{-1} \quad (\text{E9})$$

Since $k(x) = f(x)x$ where $f(0) < 0$ [cf. (17)], $(dk/dx)_{x=0}$ is negative. Hence $[d^2\tau/dx^2]_{x=0}$ has the sign of

$$- \left[\frac{d(v - v_s)}{dr} \right]_{v=v_s} .$$

Only those integral curves which pass through the surface $v = v_s$ with this quantity positive are relevant to the solution of the accretion problem. Hence τ achieves a minimum at $v = v_s$ along such integral curves. It will be convenient to choose the "constant of integration" left unspecified by (E2) so that

$$\tau = 0 \quad \text{at} \quad v = v_s \quad (\text{E10})$$

along these integral curves.

Finally, consider the behavior of τ along an integral curve which satisfies our boundary condition (10b) at $r = \infty$:

$$\begin{aligned} \tau &= \int k \, dr + \text{constant} \\ &= \int \frac{1}{\chi} \frac{1 - v^2/v_s^2}{1 - v^2/v_c^2} \frac{1}{Y(1 + v^2)} (vr^2) \, d\left(\frac{1}{r}\right) + \text{constant} \end{aligned} \quad (\text{E11})$$

Hence from (38) $\tau \sim \text{constant}$ for $r \rightarrow \infty$, and again it is convenient to set the "constant" equal to zero so that

$$\tau = 0 \quad \text{at} \quad r = \infty \quad . \quad (\text{E12})$$

Appendix F

The basic physical laws underlying equations (1) are conservation of baryon number

$$\vec{\nabla} \cdot (n\vec{u}) = 0 \quad (\text{Fla})$$

conservation of energy and momentum

$$\vec{\nabla} \cdot \mathbb{T} = 0 \quad (\text{Flb})$$

and the photon diffusion equation

$$\dot{\vec{q}} = -\kappa_\gamma \mathbb{P} \cdot (\vec{\nabla} T + \dot{\vec{a}} T) \quad (\text{Flc})$$

Here \vec{u} and \vec{a} are the baryon four-velocity and four-acceleration, \vec{q} is the photon energy flux as measured by observers moving with the baryons, \mathbb{T} is the stress-energy tensor, and \mathbb{P} projects orthogonal to \vec{u} . The conductivity κ_γ for photons diffusing in LTE is given by (D5). In this appendix we shall use n , the number density of baryons, rather than ρ_0 in order to avoid the awkward subscript.

Specialized to the case of flat spacetime and small velocities \underline{v} , the basic equations (F1) become

$$\frac{d}{dt} n + n \underline{\nabla} \cdot \underline{v} = 0 \quad (\text{F2a})$$

$$(\rho + p) \frac{d}{dt} \underline{v} + \underline{\nabla} p = 0 \quad (\text{F2b})$$

$$\frac{d}{dt} \rho - \frac{\rho + p}{n} \frac{d}{dt} n + \underline{\nabla} \cdot \underline{q} + \underline{q} \cdot \frac{d}{dt} \underline{v} = 0 \quad (\text{F2c})$$

$$\underline{q} + K \gamma [\underline{\nabla} T + T \frac{d}{dt} \underline{v}] = 0 \quad (\text{F2d})$$

where

$$\frac{d}{dt} \equiv \partial_t + \underline{v} \cdot \underline{\nabla} \quad (\text{F3})$$

These are not quite the usual Newtonian equations because we have not assumed small accelerations, nor have we assumed that the fluid is non-relativistic.

When linearized upon a uniform background with $\underline{v} = 0$, $\underline{q} = 0$, the equations (F2) become in turn:

$$n_t + n \nabla \cdot \underline{v} = 0 \quad (\text{F4a})$$

$$(\rho + p) \underline{v}_t + \nabla p = 0 \quad (\text{F4b})$$

$$\rho_t - \frac{\rho + p}{n} n_t + \nabla \cdot \underline{q} = 0 \quad (\text{F4c})$$

$$\underline{q} + K_\gamma [\nabla T + T \underline{v}_t] = 0 \quad (\text{F4d})$$

In these equations, differentiated quantities are perturbation values, and undifferentiated quantities are unperturbed (background) values.

In order to simplify subsequent manipulations it is convenient to "scalarize" the equations (F4) as well by considering only one space dimension; the generalization back to three is always trivial. Then we have finally,

$$n_t + n v_x = 0 \quad (\text{F5a})$$

$$(\rho + p)v_t + p_x = 0 \quad (\text{F5b})$$

$$\rho_t - \frac{\rho+P}{n} n_t + g_x = 0 \quad (\text{F5c})$$

$$g + K_g [T_x + T v_t] = 0 \quad (\text{F5d})$$

It remains only to combine these four first-order equations into one fourth-order equation. Using (F5a), we can combine (F5c) and (F5d) as

$$\rho_t - \frac{\rho+P}{n} n_t = K_g [T_{xx} - T \frac{n_{tt}}{n}] \quad (\text{F6})$$

Combining (F5a) and (F5b) we obtain

$$\frac{n_{tt}}{n} = \frac{P_{xx}}{\rho+P} \quad (\text{F7a})$$

$$= a \frac{n_{xx}}{n} + b \frac{T_{xx}}{T} \quad (\text{F7b})$$

[cf. (4e) and (4f)], whence

$$T_{xx} = \frac{T}{bn} [n_{tt} - a n_{xx}] \quad (\text{F7c})$$

Using this in (F6) we have

$$\rho_t - \frac{\rho+p}{n} n_t = K_\gamma \frac{T}{n} \frac{A}{b} \left[n_{tt} - v_c^2 n_{xx} \right] \quad (\text{F8})$$

[cf. (4c) and (B9)]. Using (B8a,b) and (B9) we can re-express the left-hand side of (F8):

$$(\rho+p) \left[B \frac{T_t}{T} - b \frac{n_t}{n} \right] = K_\gamma \frac{T}{n} \frac{A}{b} \left[n_{tt} - v_c^2 n_{xx} \right] \quad (\text{F9})$$

To eliminate the T derivative we differentiate (F9) twice with respect to x (Laplacian) and use (F7c) again. After some rearrangements, this gives

$$n_{ttt} - v_s^2 n_{txx} = \frac{K_\gamma TA}{(\rho+p) B} \left[n_{ttxx} - v_c^2 n_{xxxx} \right] \quad (\text{F10})$$

[cf. (4d) and (B10)]. Using (E6) and (E4) it is easy to check that the factor multiplying the expression in brackets on the right is $\chi v_s^2 / v_c^2$, so we have finally

$$\chi v_s^2 \phi_{xxxx} - \chi \frac{v_s^2}{v_c^2} \phi_{ttxx} + \phi_{ttt} - v_s^2 \phi_{txx} = 0 \quad (\text{F11})$$

-- as in equation (5) of the text. Here we have replaced n by the general symbol ϕ , which stands for the perturbation in any quantity describing the state of our fluid. This is permissible of course because all such perturbations are linearly related to one another.

Table 1

M	$3M_{\odot}$
\dot{M}_O	$2.954 \times 10^{-5} M_{\odot}/\text{yr}$
\hat{L}_{∞}	$9.795 \times 10^4 L_{\odot}$
$\hat{L}_{S,\infty}$	$9.795 \times 10^4 L_{\odot}$
$\rho_{O,\infty}$	$1.878 \times 10^{-9} \text{ g/cm}^3$
T_{∞}	$4.313 \times 10^5 \text{ }^{\circ}\text{K}$
$v_{S,\infty}$	$8.308 \times 10^{-3} [\text{c}]$
$v_{C,\infty}$	$2.814 \times 10^{-4} [\text{c}]$
$[P_G/P_R]_{\infty}$	1.532×10^{-3}

Figure Captions

- Fig. 1. Integral curves of equation (7d); r is Schwarzschild radius and v is locally measured inflow velocity. The curves are labelled by their value of S , entropy per unit rest mass, in arbitrary units. The unique accretion solution is shown by the dark curve.
- Fig. 2. These figures are drawn in the three dimensional space $[r \times v \times L]$. Figure 2a shows the mutual intersection of the three surfaces $\mathcal{L} = \mathcal{L}_v$, $\mathcal{L} = \mathcal{L}_S$, and $v = v_c$ [equations (11a,b,c) of §4]. The "critical curve" in which all three intersect [equation (13) of §4] is a one-parameter family of "critical points" of the differential equations (3d,e). Figure 2b shows two integral curves, xx and yy , which pass through the surface $v = v_c$, but not through the critical curve. These integral curves have extremal values of r in the surface $v = v_c$. Also shown in Figure 2b are the two integral curves, bcd and ace , which pass through the critical curve at the critical point c . See §4 for discussion.
- Fig. 3. This figure shows the qualitative behavior of the luminosity \hat{L} as a function of radius in the three different velocity regimes $v > v_s$ (Fig. 3a), $v_c < v < v_s$ (Fig. 3b), and $v < v_c$ (Fig. 3a). The quasi-exponential behavior shown here is governed by the rate k of §5 which changes sign at $v = v_s$ and at $v = v_c$.

Fig. 4. This figure shows the relationship between \hat{L}_O and \hat{L}_S discussed in §5. The "offset" shown here between \hat{L}_O and \hat{L}_S arises, in a first approximation, because $\hat{L}_S' > 0$ [cf. equation (23)].

Fig. 5. These figures show the qualitative behavior of integral curves of equations (3d,e) near the "sonic surface" $v = v_s$. All three figures are drawn so that r increases to the right and v increases to the left. Figure 5a shows a case where C is positive for $v \sim v_s$ and so \hat{L}_S has a pole at $v = v_s$ of the sign shown. The integral curve with $\hat{L} = \hat{L}_O$ in the region $v < v_s$ passes through the sonic surface at the point A, while the integral curve with $\hat{L} = \hat{L}_O$ in the region $v > v_s$ does so at the point B. Figure 5b shows a case where C is negative for $v \sim v_s$ and so \hat{L}_S has a pole at $v = v_s$ of the sign shown. The integral curve with $\hat{L} = \hat{L}_O$ in the region $v > v_s$ passes through the sonic surface at the point D, while the integral curve with $\hat{L} = \hat{L}_O$ in the region $v < v_s$ does so at point E. Figure 5c shows a case where C has been adjusted so as to join the two integral curves with $\hat{L} = \hat{L}_O$ on either side of the sonic surface. These two integral curves meet at the point S on the sonic surface.

Fig. 6. This figure shows how integral curves with $\hat{L} = \hat{L}_0$ intersect the sonic surface $v = v_s$. Integral curves with $\hat{L} = \hat{L}_0$ coming from the horizon intersect the sonic surface along the curve BSD. Integral curves with $\hat{L} = \hat{L}_0$ coming from the critical curve intersect the sonic surface along the curve ASE. The arrow along the bottom of the surface shows the direction of increasing C on the sonic surface. The points A, B, S, D, E are the same as the ones in Figures 5.

Fig. 7. These figures show the behavior of the S^+ characteristics of the adiabatic accretion problem. Figure 7a shows this behavior in terms of Schwarzschild coordinates r and t . In Figure 7b, the transformation of equation (55) of the text has been applied so that each characteristic is a straight, vertical line (transformation to characteristic coordinate) and so that the infinite future and the infinite past are brought in to where we can look at them.

Fig. 8. This figure shows the run of velocity, density, temperature, and luminosity versus radius for the solution with the parameters given in Table 1. The units for these quantities are the speed of light, grams/cm^3 , degrees Kelvin, and solar luminosities, respectively. The crosses mark the critical point; the circles mark the subcritical point.

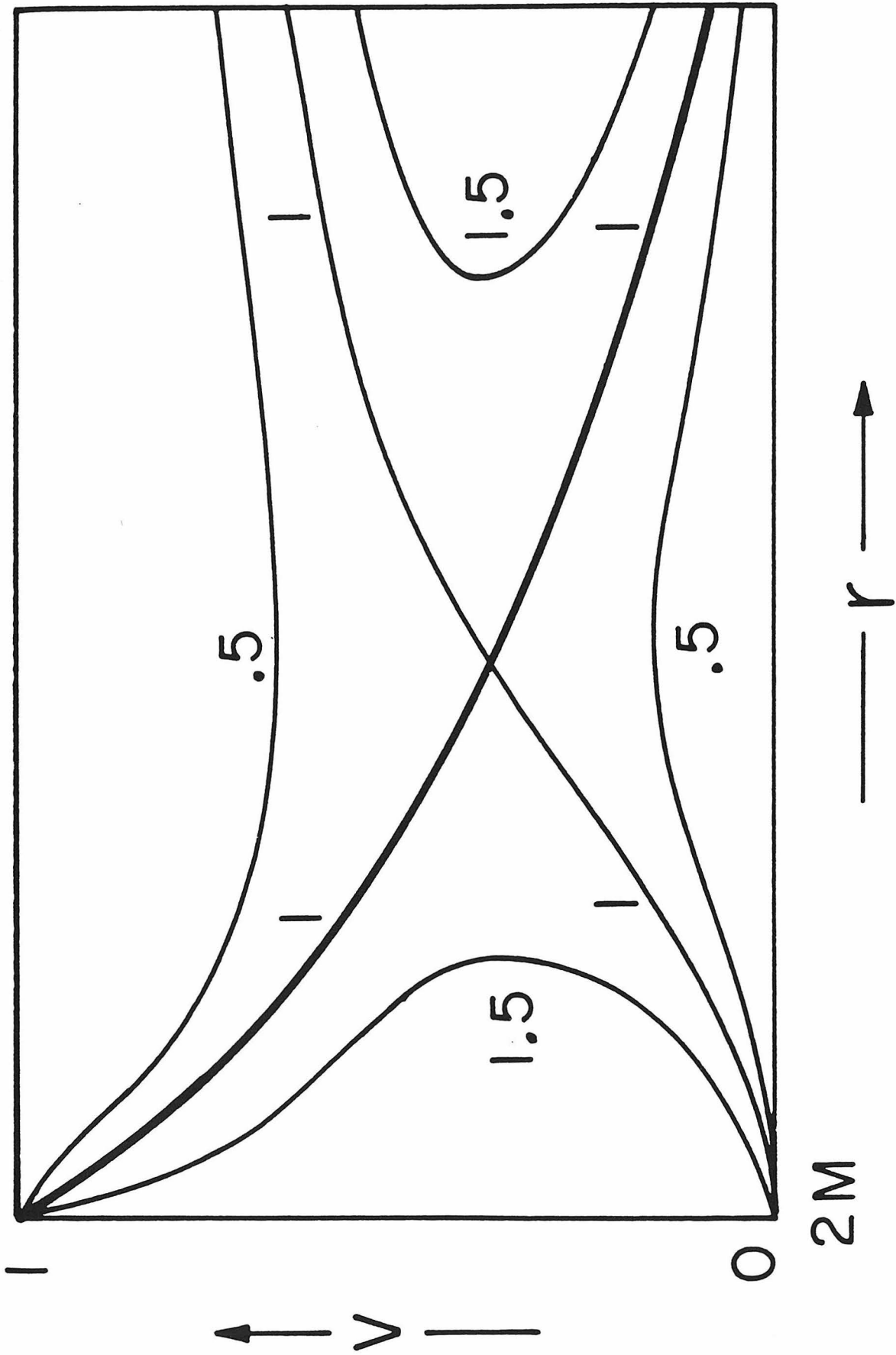
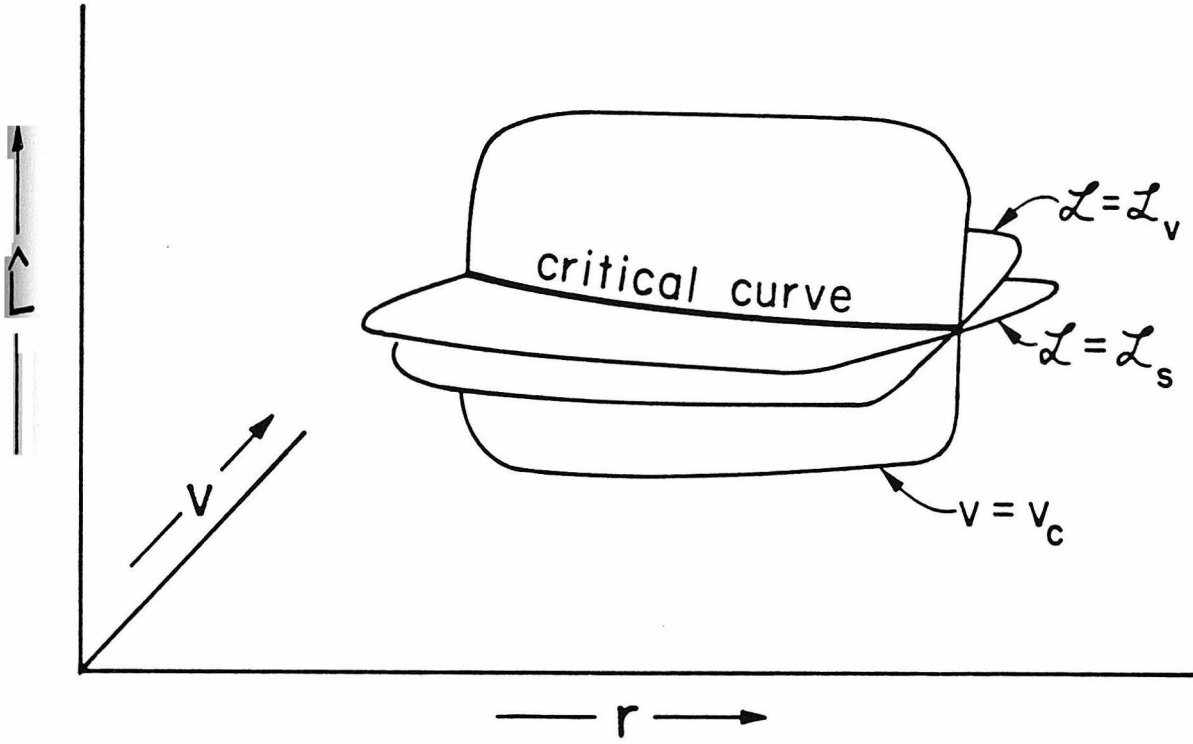
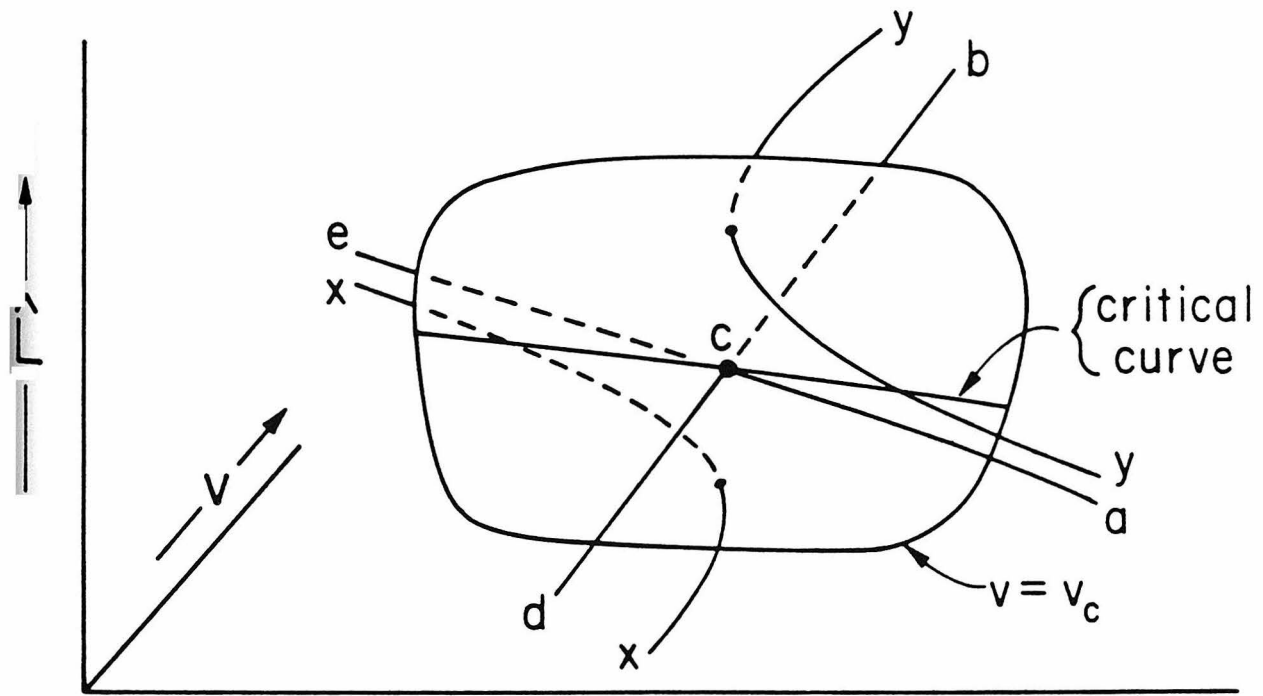


Fig. 1



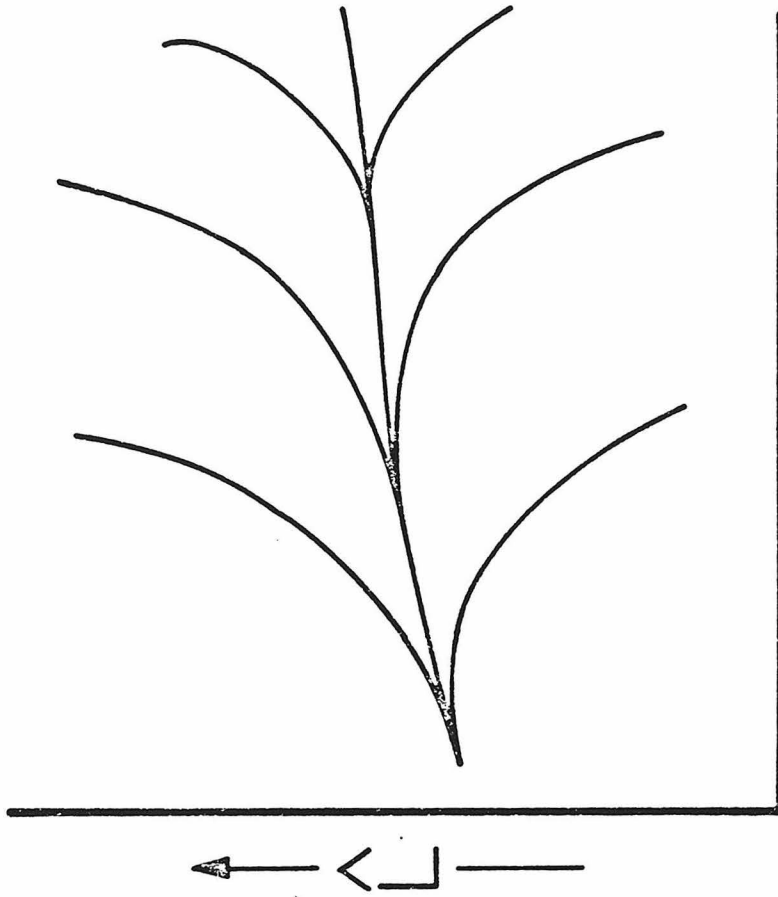
(a)



(b)

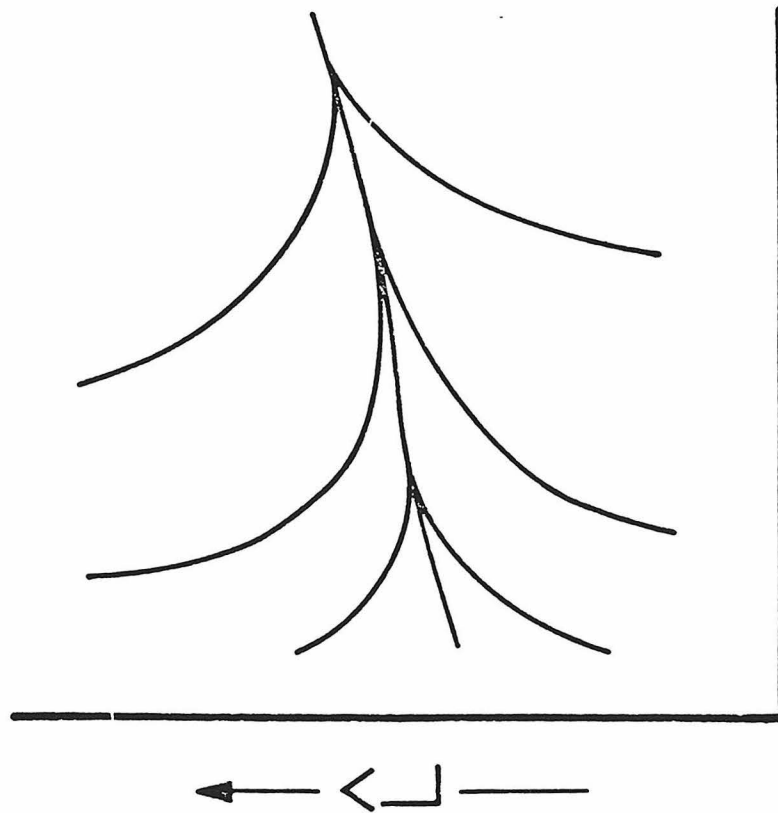
Fig. 2

$$V_C < V < V_S$$



(b)

$$V > V_S \text{ or } V < V_C$$



(a)

Fig. 3

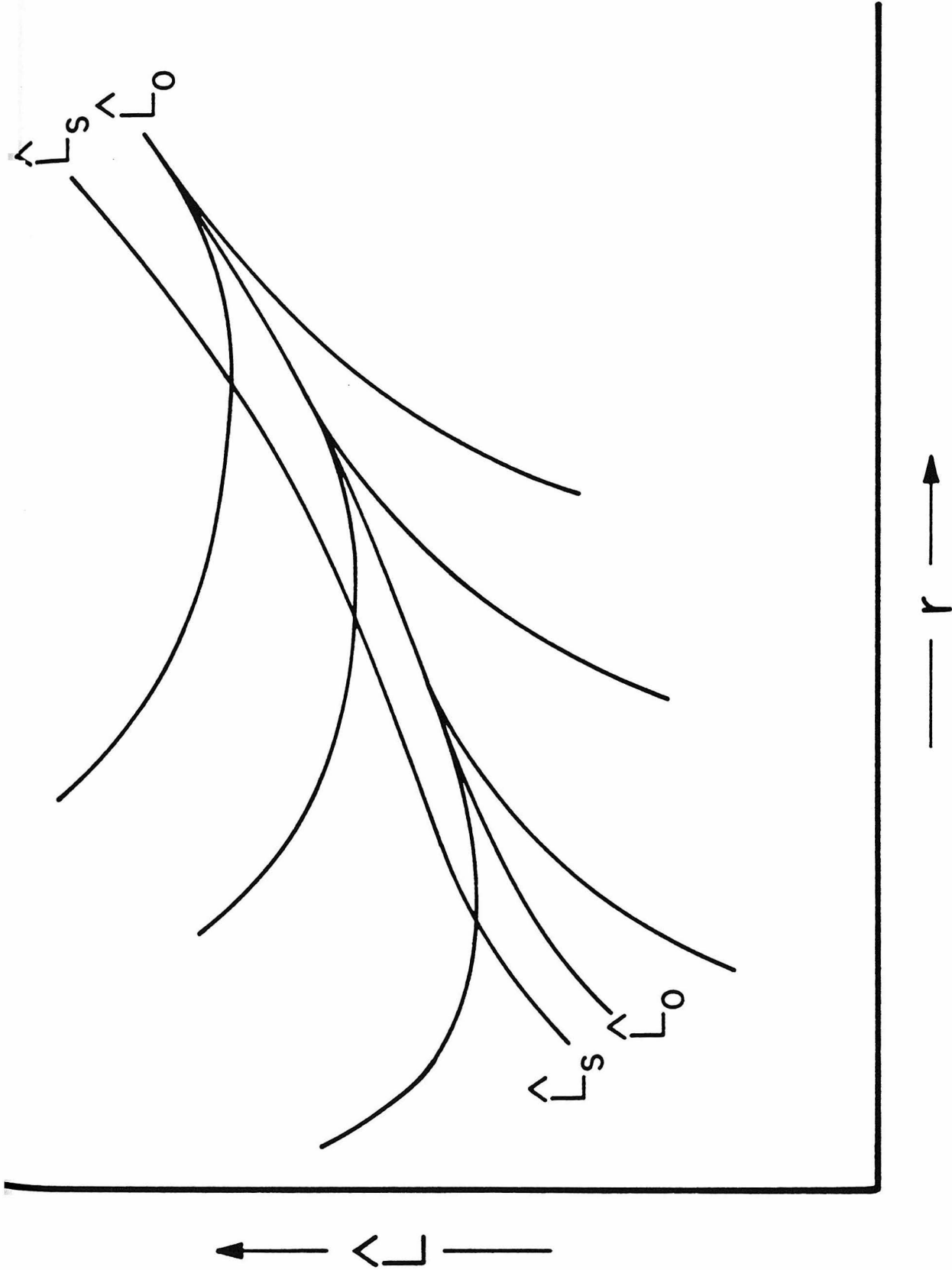


Fig. 4

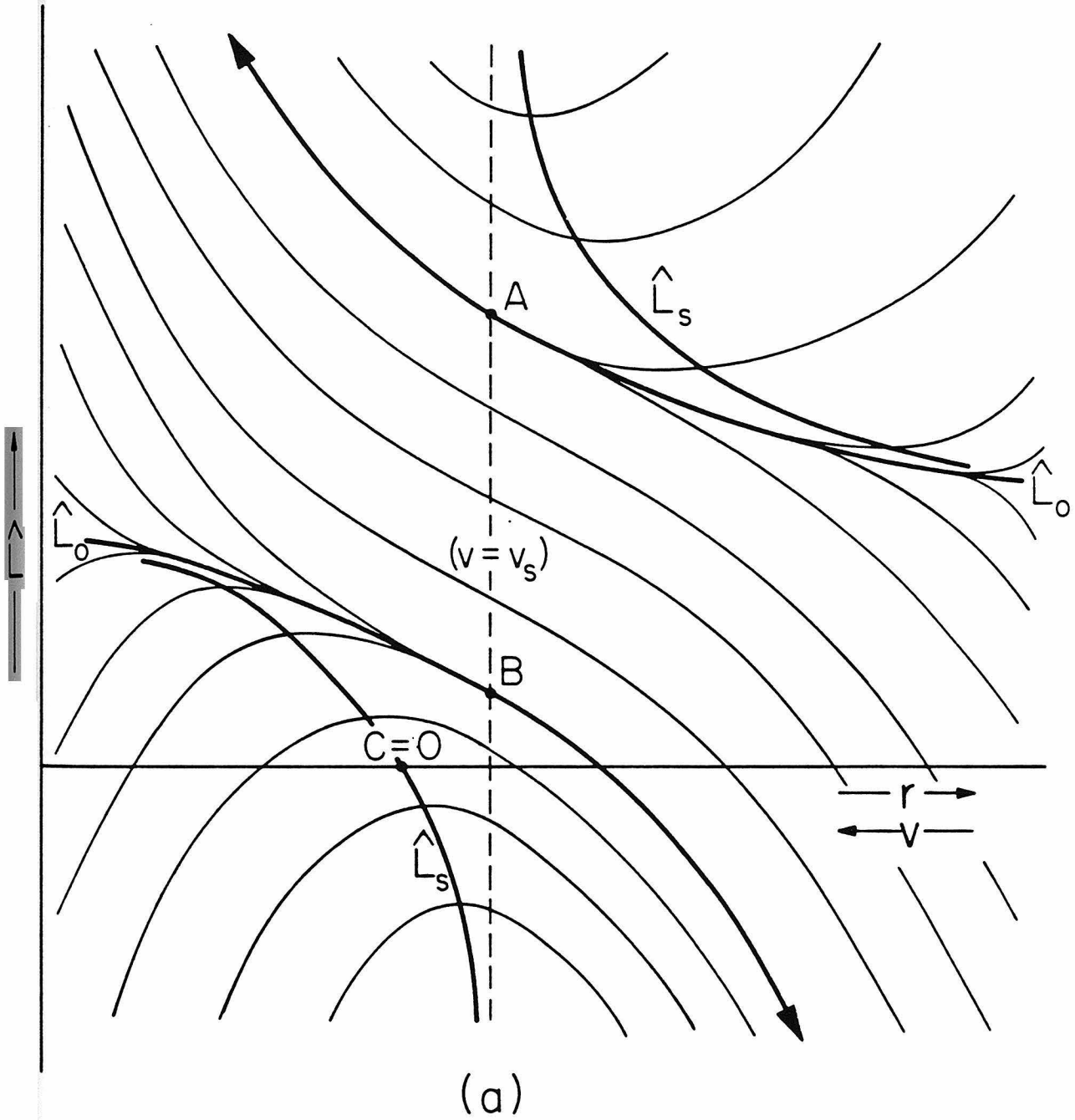


Fig. 5a

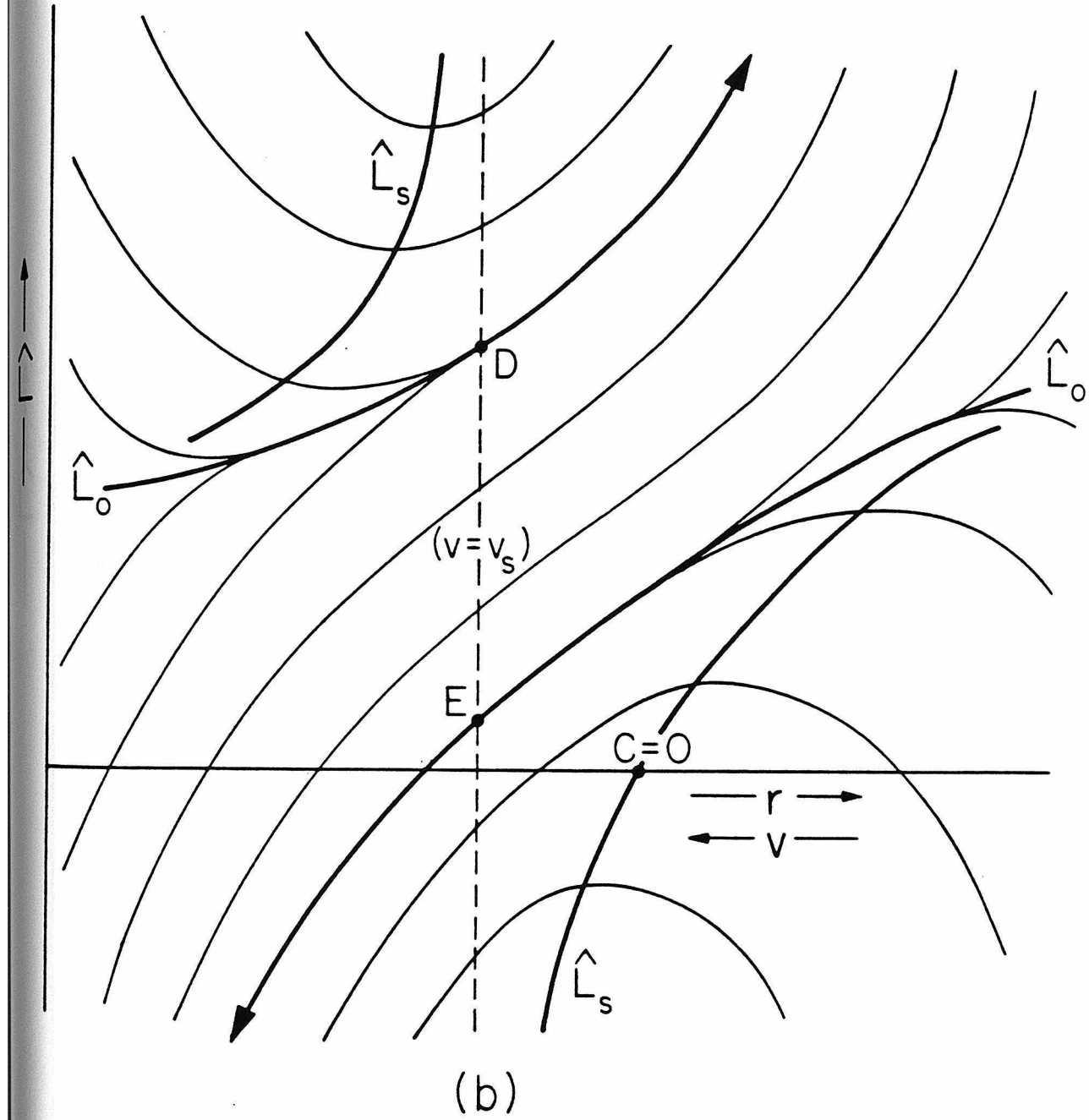


Fig. 5b

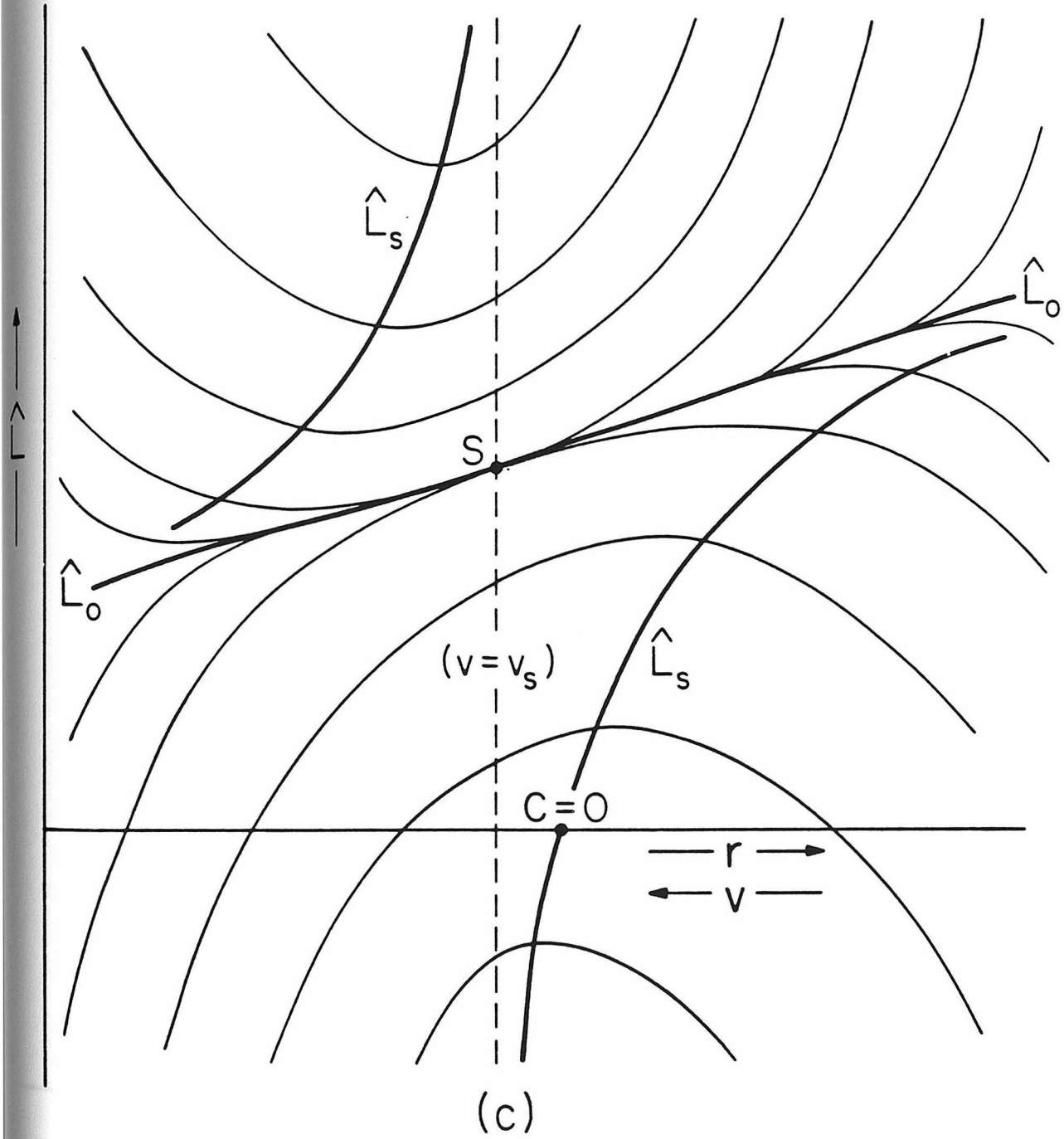


Fig. 5c

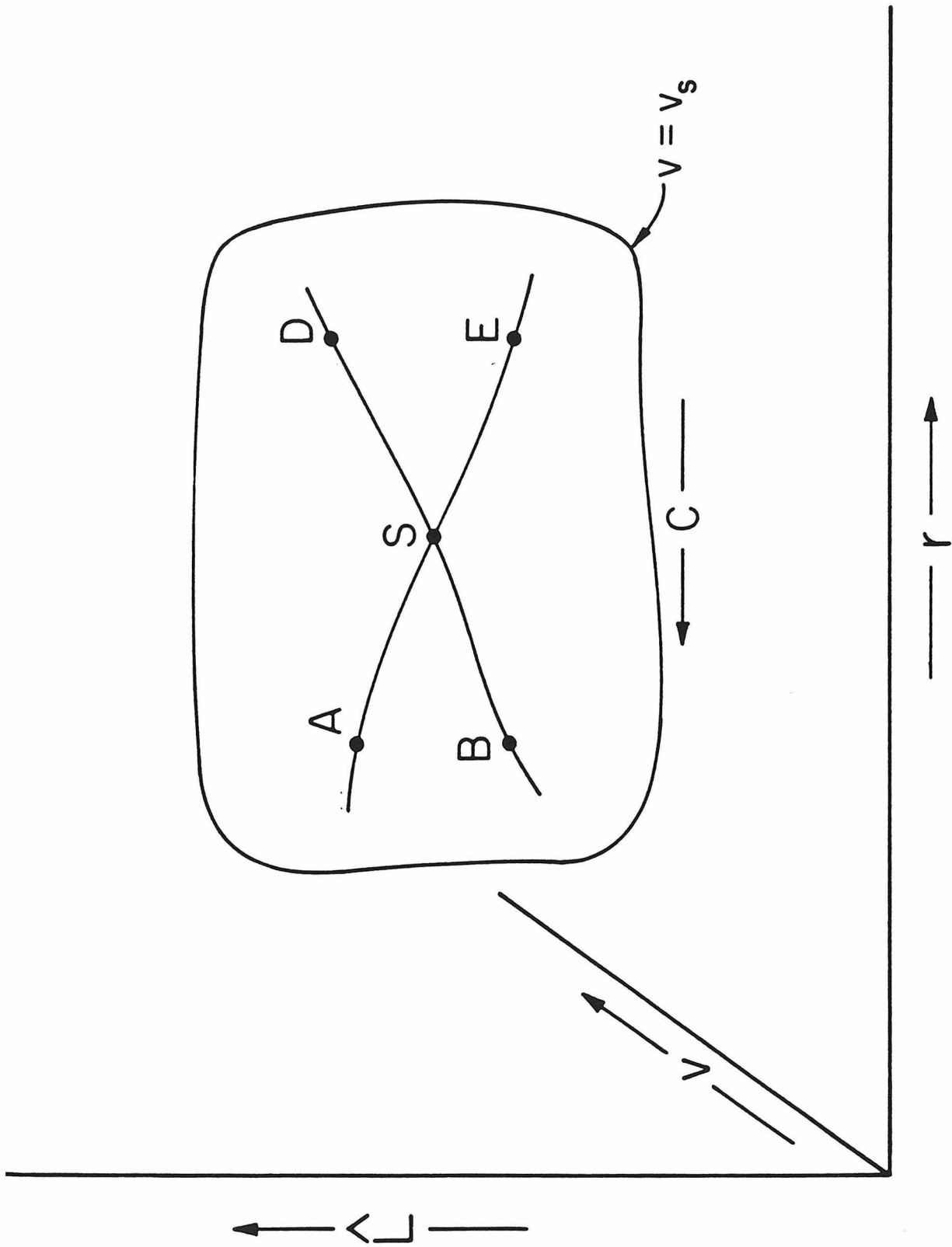


Fig. 6

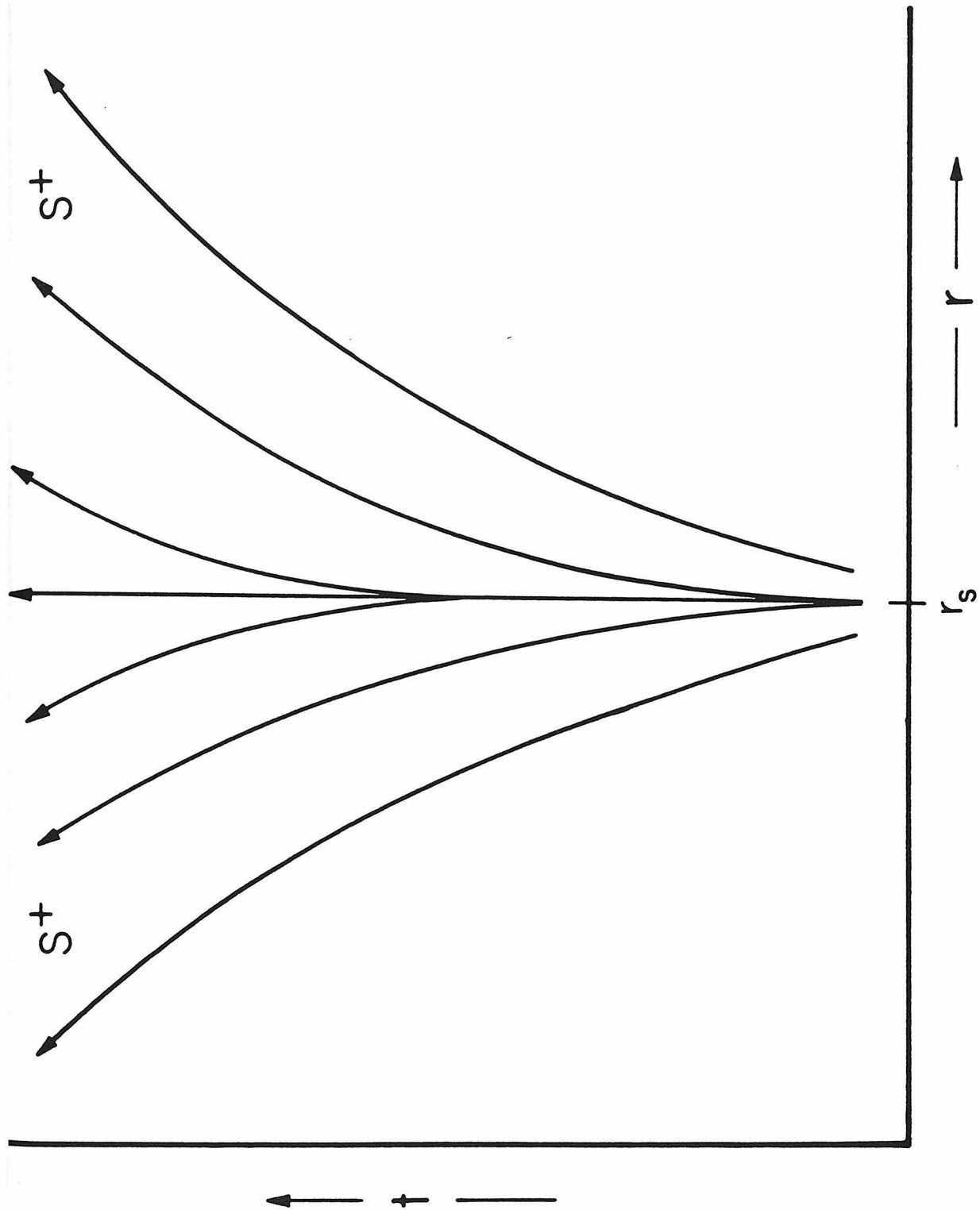


Fig. 7a

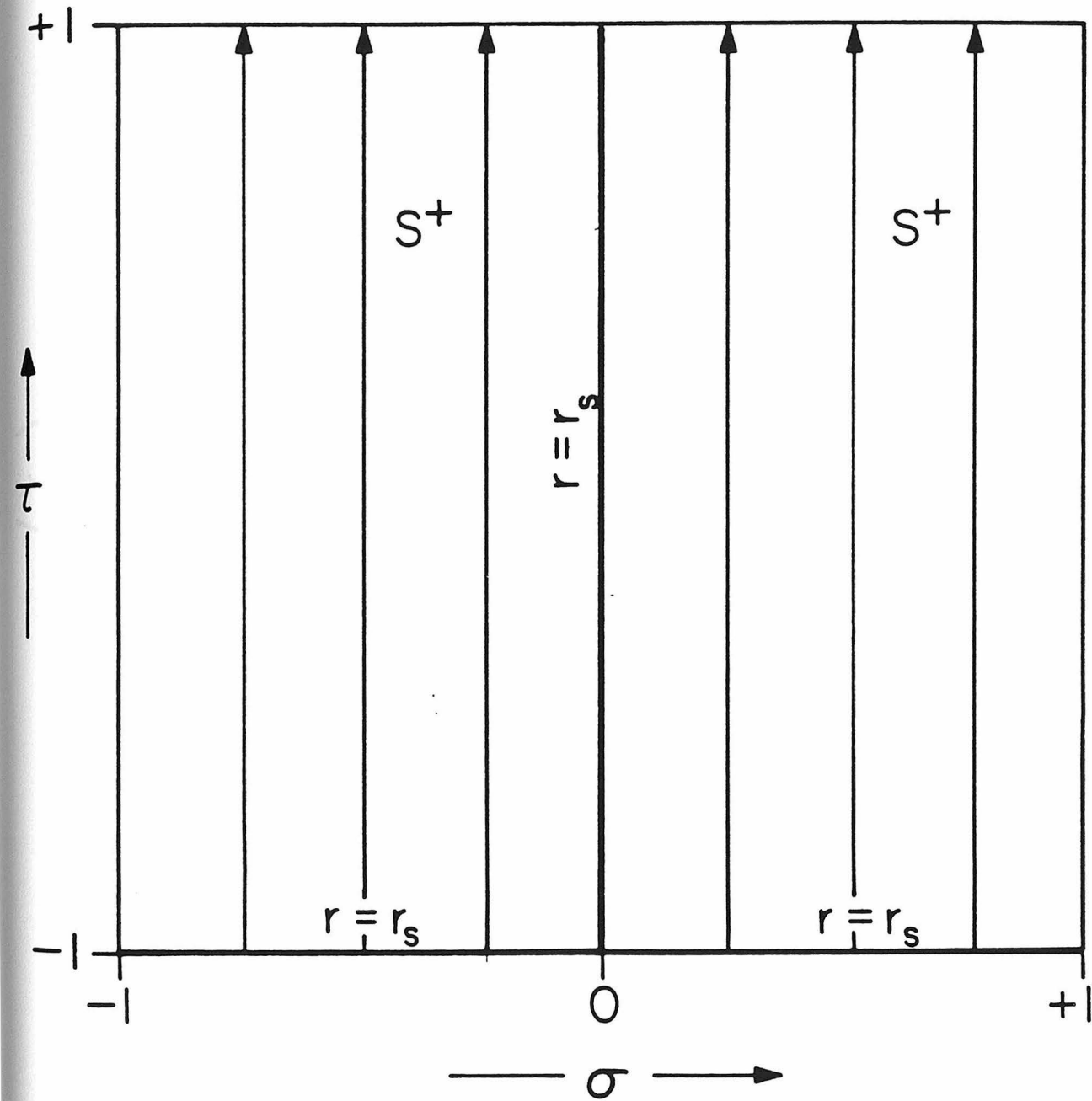


Fig. 7b

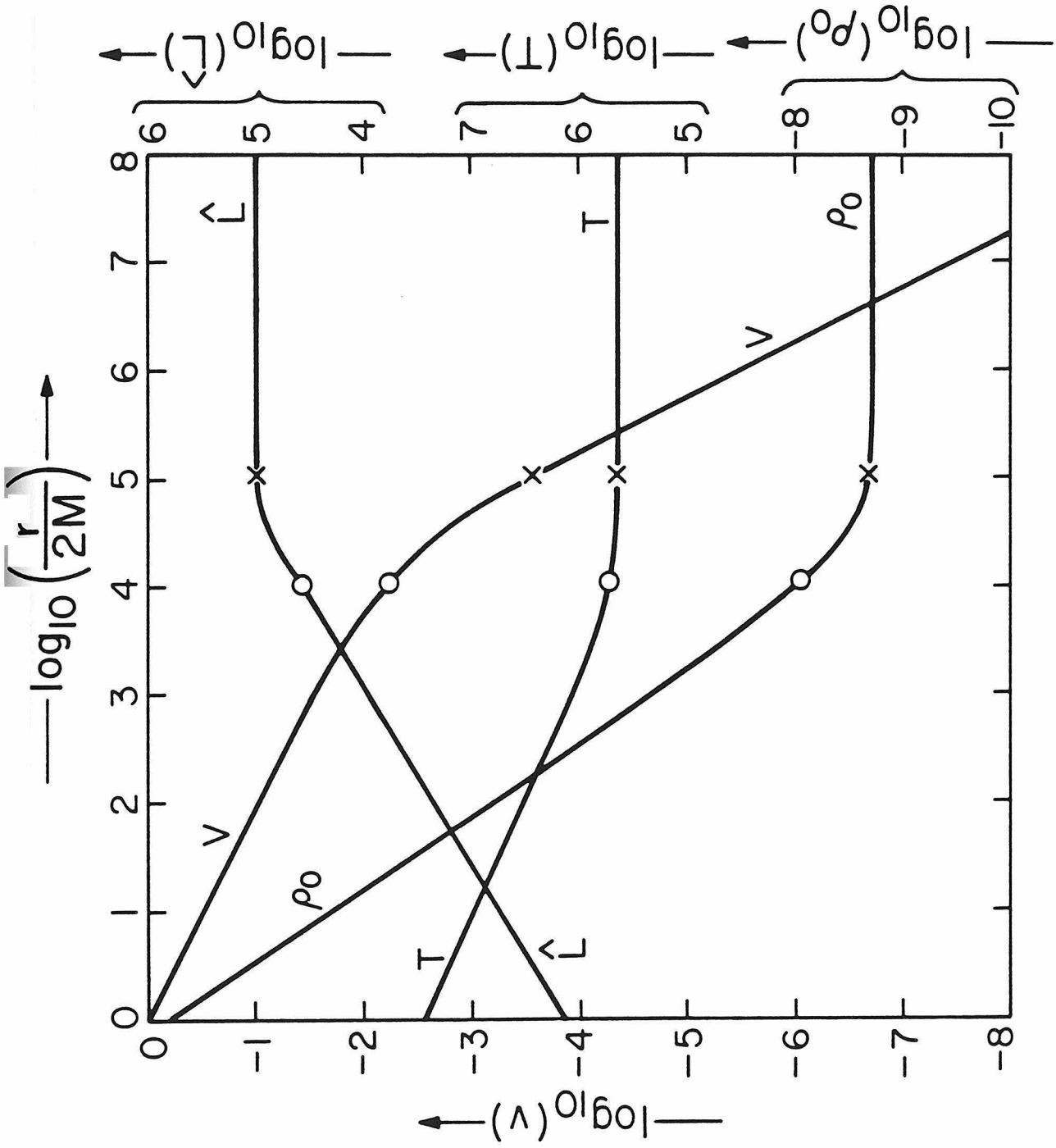


Fig. 8

Chapter 3

Optically Thick Accretion in Specific Cases

This chapter is a paper submitted for publication to the Monthly Notices of the Royal Astronomical Society.

Abstract

In this paper we apply the theory of stationary, spherical, optically thick accretion developed in paper II of this series (Flammang 1982). For this theory to be applicable, it is necessary that the photons be everywhere diffusing through and in local energy equilibrium with the accreting gas particles. We investigate this class of solutions over a wide range of physically different accretion regimes. Numerical solutions are presented and their physical properties are discussed. For solutions in which radiation pressure P_R dominates gas pressure P_G , but in which gas energy density (including its rest-mass) ρ_G dominates radiation energy density ρ_R , we pay particular attention to the adiabaticity of the flow. Our quantitative results in this regime agree very well with Begelman's (1978) theory. We find the dimensionless number which governs the importance of heat diffusion in our problem and show that it reduces to the idea of "trapping of photons" and to the Péclet number in the appropriate limits. We find that solutions with $P_R > P_G$ and $\rho_R > \rho_G$ are always essentially adiabatic, owing in part to a relativistic suppression of heat flux which becomes important in this regime. The diffusive luminosity at infinity for these solutions is the Eddington limit of the black hole; with the adiabatic accretion rate, "efficiencies" of up to order unity are possible. We give preliminary consideration to the question of the stability of our solutions against convection and conclude that the Schwarzschild criterion is applicable, even for our non-static accretion flows. We show that solutions with $P_R > P_G$ are everywhere stable against convection. On the other hand, solutions which start out at radial infinity with $P_G > P_R$ are unstable to convection (if the adiabatic index of the gas γ_G exceeds 17/12) from

radial infinity down to the point where $P_R \sim P_G$ and the radiation-gas mixture has attained an adiabatic index of $17/12$. Inside this point, the solution is stable against convection. The diffusive luminosity at infinity for these solutions is reduced from the Eddington limit of the black hole by the factor $(\gamma_G - 1)4P_{R\infty}/\gamma_G P_{G\infty}$; it is further reduced by the ratio of the electron scattering opacity to the actual opacity at infinity, if this differs from unity. In most cases, energy diffusion has a negligible effect on the accretion rate of these solutions.

1. Introduction

In a previous paper, Flammang (1982), hereafter paper II, we set forth the complete mathematical theory of stationary spherical accretion into black holes with radiative transfer treated in the diffusion approximation with LTE. In this paper, a sequel, we shall investigate in detail the properties of the resulting solutions over a very wide range of physically different accretion regimes. Whereas the emphasis in paper II was on generality and completeness, the emphasis here will be on simple physical description of specific cases.

We restate here the principal assumption of both paper II and this paper. (1) The diffusion approximation is applicable; that is, the photon mean free path must be small compared to local macroscopic length scales. It turns out that the relevant local macroscopic length scale is always greater than or of order r , the local value of the radius. (2) The photons are in local energy equilibrium with the gas particles, which in turn are in thermal equilibrium with one another at some temperature T . (3) Photon viscosity is negligible. This assumption is actually nugatory: its validity is guaranteed by assumption (1) above. (4) No "chemical" effects are considered (ionization reactions, e^+e^- pair production, nuclear reactions, ...). A model gas free of these complications would be ionized hydrogen ($10^4 \text{ }^\circ\text{K} < T \ll 10^9 \text{ }^\circ\text{K}$), but others could equally well be considered. (5) Magnetic fields are not considered.

The relevant parameter space for the problem being considered here is three-dimensional. A convenient set of parameters is $\{M, \rho_{\infty}, T_{\infty}\}$, the black hole mass and the rest-mass density and temperature at radial

infinity. Another convenient set is $\{M, \rho_{0\infty}, v_{s\infty}\}$, where $v_{s\infty}$ is the adiabatic sound speed at infinity. Since M provides only gravity, which is simple, whereas $\rho_{0\infty}$ and T_∞ determine the accretion flow's microphysics, which can be quite complicated, we shall employ Figure 1, which shows the $\rho_{0\infty} - T_\infty$ plane, to organize our discussion of results, always bearing in mind that there is also a third parameter, M , which has to be taken into account as well.

We begin in section 2 with a brief discussion of certain aspects of the numerical technique used to generate the solutions discussed in this paper. This information will be useful to anyone faced with the task of numerically integrating equations similar to the ones considered here, but the general reader can skip over it. In section 3 we consider solutions whose pressure is dominated by radiation, but whose energy density is still dominated by rest mass (region Ia of Figure 1). We pay particular attention to the question of the adiabaticity of the flow and to the effect of energy diffusion on the rest mass accretion rate \dot{M}_0 . In section 4 we find the dimensionless number which governs the importance of energy diffusion in our problem. We show that this dimensionless number reduces to the idea of "trapping of photons" and to the Péclet number of standard fluid mechanics in the appropriate limits. Section 5 is devoted to relativistic accretion: cases in which the energy density in the radiation exceeds that in rest mass (region Ib of Figure 1). Here we find that a "relativistic correction" to the heat transport equation (the first moment of the radiative transfer equation in the diffusion limit) is fully as important as — and in fact nearly cancels — the Newtonian term. The net effect is to render all solutions in this region of the figure essentially adiabatic.

Solutions in region Ib boast the highest "efficiencies" $\epsilon \equiv L_\infty / \dot{M}_O$, which can in fact approach unity in this region of the figure. In section 6 we consider the question of stability against convection and argue therein that the Schwarzschild criterion is the correct one, even for our non-static accretion solutions. From this we show that solutions with radiation pressure P_R dominating gas pressure P_G (region I of Figure 1) are stable against convection. In Section 7 we consider solutions which start out at radial infinity with gas pressure dominating radiation pressure (region II of Figure 1). We show that if the gas has an adiabatic index γ_G in excess of 17/12 then the solution is unstable to convection from radial infinity down to the point where P_R approaches P_G and the gas-radiation mixture has attained an adiabatic index of 17/12. Inside this point the solution is stable against convection.

Notation in this paper is the same as in paper II; in particular, unless otherwise noted, natural units ($G = c = 1$) are used.

2. Method

Because of the special mathematical character of the system of equations describing accretion with photon diffusion [equations (1) of paper II], certain rather special techniques must be employed to obtain good numerical representations of solutions on a computer. First, one must always integrate from critical points toward subcritical points. Otherwise, as one approaches a critical point, the solution will

inevitably diverge and become very unphysical [cf. Figures 3 of paper II]. [This was the problem encountered by Kafka and Mészáros (1976) in their numerical work.] Thus one must integrate outward from the horizon to the sonic (subcritical) point, inward from the critical point to the sonic point, and then outward again from the critical point to radial infinity.

Second, because our equations are stiff, and because the length-scale for this stiff behavior, k^{-1} , is a very sensitive function of v [cf. equation (17) of paper II], it is necessary to use an integrating routine with variable step size and to always keep the step size comfortably below $|k^{-1}|$.

Finally, when integrating stiff equations, it is necessary to use some form of an implicit scheme in order to obtain stable results. The "backwards Euler method"

$$y_{n+1} = y_n + y'_{n+1} h \quad (2.1a)$$

[cf. Gear (1971), §11.1] works, but the semi-implicit method

$$y_{n+1} = y_n + \frac{1}{2} (y'_n + y'_{n+1})h \quad (2.1b)$$

is far more accurate and just as stable [cf. Potter (1973), §II.6(d)]. In these equations, y stands for the dependent variable(s), h is the step size, subscripts denote the step number, and a prime denotes differentiation with respect to the independent variable (radius r , in our problem).

3. Solutions with $P_R > P_G$, $\rho_G > \rho_R$

Here we discuss solutions which lie in region Ia of Figure 1.

Figure 2 shows an example; Table 2 summarizes a few parameters of this solution. The velocity shown in the figure is that measured by local observers sitting at fixed radius r . As was discussed in paper I (Thorne, Flammang and Żytkow 1981), the inflow velocity so defined must equal unity (speed of light) at the horizon of the black hole. From this value it falls off smoothly with radius - as $r^{-1/2}$ in an inner ("free-fall") region and as r^{-2} in an outer ("hydrostatic") region. Also shown in the figure are the adiabatic and isothermal sound speeds, v_s and v_c respectively. As was discussed extensively in paper II, where the inflow velocity equals the isothermal sound speed, our solution passes through a critical point of the differential equations describing our problem, and where the inflow velocity equals the adiabatic sound speed, there is a sort of "diffused critical point" dubbed a subcritical point in paper II.

Corresponding to the power-law behavior of $v(r)$, the rest-mass density ρ_0 varies as $r^{-3/2}$ in the free-fall region and is roughly constant in the hydrostatic region. From the figure, the inflowing material is compressed by a factor of more than 10^5 by the time it crosses the horizon of the black hole. In response to this compression, the temperature rises inward; but the eye can discern that T starts rising at a radius smaller than that at which ρ_0 starts to rise. To see this effect more clearly, we define the local "adiabaticity"

$$\alpha \equiv \frac{\frac{\rho_o}{T} \frac{T'}{\rho_o'} - v_c^2}{q - v_c^2} \quad (3.1a)$$

where

$$q = \frac{\rho_o}{T} \left(\frac{\partial T}{\partial \rho_o} \right)_S \quad (3.1b)$$

where S is the entropy per unit rest mass (cf. equation B11b of paper II) and plot α on a linear scale at the top of the figure. This choice for α is uniquely determined by the requirements that α be linear in the temperature gradient, equal to unity if the flow is strictly adiabatic, and equal to zero if the flow is strictly isothermal - in the relativistic sense $(TY)' = 0$, rather than $T' = 0$ (cf. equation A6 of paper II). As the figure shows, the flow is nearly adiabatic at both small and large radii but deviates toward isothermal flow in an intermediate region.

Physically, the flow is nearly adiabatic at small radii because the velocity is so large there. Diffusion, though it is present, is unable to compete with the inward transport of energy due to the bulk fluid motion. Hence diffusion is not able to push the solution very far from adiabatic. This is the idea of "trapping photons" [cf. Rees (1978), Begelman (1978)]. The same idea finds its expression in the standard terminology of fluid mechanics in terms of the Péclet number, φ [cf. Landau and Lifshitz (1959), §53]. The Péclet number is just the heat - conduction analog of the Reynolds number -- it describes, in rough, dimensional analysis terms, the relative importance of energy transport by bulk fluid motion versus energy transport by diffusive processes. It turns out that the idea of "trapping of photons" is an appropriate estimator of adiabaticity only in region Ia of Figure 1 (the only region where it was meant to apply) and that the Péclet number is appropriate

only in region II of the same figure (where $P_G > P_R$). Accordingly, in §4 we shall generalize and reconcile these two dimensional-analysis approaches to the question of adiabaticity and shall find a dimensionless number which applies throughout Figure 1--and indeed which applies regardless of the specific form of the equation of state of a fluid or the specific mechanism responsible for heat conduction.

Physically, the solution shown in Figure 2 is nearly adiabatic at large radii because macroscopic length scales are so huge there. The fact that the quantities shown in Figure 2 all go flat at large radii shows that these macroscopic length scales have become very large compared to the local value of r there. For example, using the fact that the solution of Figure 2 is nearly adiabatic at large radius, it follows from equations (7a) and (38) of paper II that the density scale height has asymptotic value

$$\left| \frac{\rho_0}{\rho'_0} \right| \sim \frac{r^2}{M} v_s^2 \quad \text{as } r \rightarrow \infty . \quad (3.2)$$

More relevant to the issue of adiabaticity however, by making use of equations (E1), (23), (44), and (38) of paper II, it is possible to deduce that, for the solution shown in Figure 2, the asymptotic scale height for the luminosity \hat{L} is

$$\frac{\hat{L}}{\hat{L}'} \sim \frac{1}{6} \frac{M}{v^2} \quad (3.3)$$

which increases as r^4 at large radii.

Only in the middle region of Figure 2, where macroscopic length scales are becoming as short as r itself but where v is not yet too large, is diffusion able to relax the solution significantly away from

adiabatic flow.

Figure 2 also shows the behavior of the luminosity L [cf. equation 10 of paper I] and the quantity L_s defined as

$$L_s = \frac{A}{b} \frac{4P_R}{\rho_0} \frac{4\pi M}{\kappa_1} \frac{1}{Y} \left(1 - \frac{v_c^2}{v_s^2}\right) \left[\frac{1 - 2v^2 Y^2 \frac{r}{M}}{1 - v^2/v_s^2} \right] \quad (3.4)$$

[cf. equations (44) and (2m) of paper II]. In this expression A and b are given by

$$A \equiv \frac{\rho_0}{\rho + P} \left(\frac{\partial \rho}{\partial \rho_0} \right)_T \quad (3.5a)$$

$$= 1 - b \quad (3.5b)$$

$$b \equiv \frac{T}{\rho + P} \left(\frac{\partial P}{\partial T} \right)_{\rho_0} \quad (3.5c)$$

[cf. equations (B8a), (B9), and (4f) of paper II], P_R is the radiation pressure, κ_1 is the first-moment opacity [cf. equation (2f) of paper II], and Y is given by

$$Y \equiv \sqrt{\frac{1 - \frac{2M}{r}}{1 - v^2}} \quad (3.6)$$

[equation (2d), paper II]. The pole in L_s at the subcritical point is very much in evidence in Figure 2. As was emphasized in paper II, the luminosity L hugs L_s everywhere except in the neighborhood of the subcritical point. At the subcritical point itself, the strength of the pole in L_s has been adjusted so as to make L continuous across the subcritical point [cf. paper II, §§5 and 7, for a thorough discussion]. Note that the $r^{1/2}$

behavior of L and L_s at small radii can be deduced by using the free-fall approximation $v \propto r^{-1/2}$ and the adiabatic approximation $T^3 \propto \rho_0$ in equation (3.4) for L_s . This conclusion is valid however only for solutions which lie in region Ia of Figure 1. As was pointed out in paper II, the luminosity at infinity is given, to an excellent approximation, by the value of L_s there [see Table 2]. For solutions lying in region I of Figure 1, the value of L_s at infinity is very nearly equal to the usual Eddington limit [cf. paper II, §8 for discussion].

The solution of Figure 2 has a rest-mass accretion rate \dot{M}_0 which exceeds the adiabatic rate

$$(\dot{M}_0)_{\text{Ad}} = 2\sqrt{2} \pi M^2 \rho_{0,\infty} / v_{s,\infty}^3 \quad (3.7)$$

[Bondi (1952)] by roughly a factor of 7 [cf. Table 2]. Physically, this occurs because pressure builds up in the inward radial direction less rapidly than it would if the flow were strictly adiabatic. With smaller pressure gradients, there is less force to resist the tug of the black hole's gravity, and the resulting accretion rate exceeds that predicted by the Bondi adiabatic formula.

Figure 3 shows another solution lying in region Ia of Figure 1. Some of its properties are summarized in Table 3. It differs from the solution of Figure 2 in that the density at infinity is lower by about a factor of 4 and the temperature at infinity is a bit higher--resulting in an asymptotic adiabatic sound speed $v_{s,\infty}$ that is higher by about a factor of 3 [cf. Table 3].

As is immediately apparent from the figure, this solution deviates much farther from adiabatic flow than does the solution shown in Figure 2. The plot of $\alpha(r)$ now exhibits a deep, wide, nearly isothermal

trough. Physically, this occurs primarily because the photon mean free path, which in region I of Figure 1 is simply inversely proportional to the density, is longer than it was in the solution of Figure 2. Hence diffusion is more effective and is able to relax the solution to nearly isothermal flow over a decade and a half of radius. Because this solution is less adiabatic than the solution of Figure 2, its accretion rate exceeds the adiabatic rate (3.7) by an even greater amount--by about a factor of 86 in this case [cf. Table 3].

That photon diffusion could cause solutions in region Ia of Figure 1 to deviate from adiabatic flow in the manner shown in Figures 2 and 3 and that this, in turn, would cause the rest mass accretion rate to exceed the Bondi prediction was first correctly pointed out by Begelman (1978). In fact Begelman was able to deduce an expression for the accretion rate of solutions lying in region Ia in cases where diffusion is able to relax the solution significantly away from adiabatic flow. His result can be written as

$$\dot{M}_O \approx (\dot{M}_O)_{\text{Beg}} + (\dot{M}_O)_{\text{Ad}} \quad (3.8a)$$

where we have defined

$$(\dot{M}_O)_{\text{Beg}} \equiv \frac{4\pi}{3} \frac{M}{\kappa_{es} v_{s,\infty}^2} = \frac{L_{\text{Ed}}}{3 v_{s,\infty}^2} \quad (3.8b)$$

[Begelman (1978), equations (27) and (28)]. [Here κ_{es} is the electron-scattering opacity and L_{Ed} is the Eddington luminosity.] As Tables 2 and 3 show, the agreement between Begelman's prediction and our numerical results is very good --- especially if the (small) $(\dot{M}_O)_{\text{Ad}}$ term is dropped in (3.8a).

It is interesting that, from (3.8b), we have for the efficiency in the regime under discussion

$$\epsilon \equiv \frac{L_{\infty}}{\dot{M}_0} \approx \frac{L_{Ed}}{\dot{M}_0} \approx 3v_{s,\infty}^2 \quad . \quad (3.9)$$

4. The Dimensional-Analysis Approach to the Question of Adiabaticity

As we noted briefly in the previous section, the idea of "trapping of photons" has been used in the past to simplify the optically thick accretion problem in region Ia of Figure 1. In this approach, it is argued that the relevant dimensionless quantity to consider in deciding how adiabatic the flow will be is

$$\frac{rv}{\lambda_{\gamma}} \quad (4.1)$$

[Begelman (1978)] - a quantity we shall hereafter refer to as the "trapping parameter", φ_T . On the other hand, conventional fluid mechanics texts suggest the "Péclet number"

$$\varphi \equiv \frac{hv}{\chi} \quad (4.2)$$

for the same purpose [Landau and Lifshitz (1959), §53]. In these expressions, λ_{γ} is the photon mean free path

$$\lambda_{\gamma} \equiv 1/\rho_0 \kappa_1 \quad , \quad (4.3)$$

h is a local macroscopic length scale characteristic of the problem at hand, and χ is the "thermometric conductivity" [cf. Landau and Lifshitz (1959) §50]. When energy transport is due to photons diffusing in local energy equilibrium, χ is given by

$$\chi \equiv \lambda_\gamma \frac{4P_R}{\rho + P} \frac{A}{B} \frac{v_c^2}{v_s^2} \quad (4.4)$$

[cf. paper II, Appendix D]. In this expression for χ , ρ is the total energy density--including "rest mass energy", P is the total pressure--gas plus radiation, and B is given by

$$B \equiv \frac{T}{\rho + P} \left(\frac{\partial \rho}{\partial T} \right)_{\rho_0} \quad (4.5a)$$

$$= b/q \quad (4.5b)$$

[cf. (2i), (2g), (B8b), and (B10) of paper II]. It is easy to check that φ and φ_T are quite different from one another, even though they are obviously trying to get at the same idea. Accordingly, in this section we shall derive a dimensionless number which is an accurate estimator of adiabaticity in our problem, and then we will be able to comment on the applicability of φ and φ_T .

We seek a dimensionless number which is large when the flow is nearly adiabatic and which is small when diffusion has its maximum effect and produces isothermal flow. The quantity $\alpha/(1-\alpha)$ would seem to be ideally suited to the task. A bit of calculating then shows that

$$\frac{\alpha}{1-\alpha} = \frac{h_L v}{\chi} \frac{v_c^2}{v_s^2}, \quad (4.6a)$$

where

$$h_L \equiv \frac{\hat{L}}{(1+v^2)Y \hat{L}'} \quad (4.6b)$$

[see Appendix A]. This result is exact; accordingly, we propose that

$$\bar{\phi} \equiv \frac{h\nu}{\chi} \frac{v_c^2}{v_s^2} \quad (4.7)$$

is the relevant dimensionless quantity to consider when trying to estimate the importance of diffusive energy transport in general fluid flows. Here, as before, h stands for a macroscopic length-scale which characterizes the problem at hand.

From (4.4), the following approximate values of $\chi v_s^2/v_c^2$ can be deduced for the various regions of Figure 1:

$$\chi \frac{v_s^2}{v_c^2} \approx \begin{cases} \frac{1}{4} \frac{\rho_G}{\rho_R} \lambda_\gamma & \text{region Ib} & (4.8a) \\ \frac{1}{3} \lambda_\gamma & \text{region Ia} & (4.8b) \\ \frac{8}{3} \frac{P_R}{P_G} \lambda_\gamma & \text{region II} & (4.8c) \end{cases}$$

Here $\rho_R = 3P_R$ is the radiation energy density, ρ_G is the gas energy density (including "rest mass energy") and P_G is the gas pressure.

[For the numerical value shown in (4.8c), it has been assumed that the gas consists of single particles ($\gamma_G = 5/3$) like ionized hydrogen].

Thus $\chi v_s^2/v_c^2$ is of order λ_γ in region Ia of Figure 1 but is much smaller than λ_γ elsewhere in the figure.

From (4.8b), $\bar{\phi}$ reduces to

$$\bar{\phi} \approx 3 \frac{h\nu}{\lambda_\gamma} \quad (4.9)$$

in region Ia of Figure 1, in essential agreement with the trapping parameter ϕ_T --as long as $h \approx r$. We have already seen in the last section that h is indeed roughly equal to r in the inner, free-fall region of our solutions but that h greatly exceeds r in the outer, hydrostatic

region [cf. (3.2), (3.3)]. Thus φ_T is an appropriate estimator of adiabaticity in spherical accretion flows only for the inner regions of solutions which lie in region Ia of Figure 1.

From (4c) and (4d) of paper II, we have that

$$\frac{v_s^2}{v_c^2} = \frac{(1+q)P_G + q4P_R}{P_G} \frac{\rho_G}{\rho + p} \quad (4.10)$$

Consequently, the ratio v_s^2/v_c^2 in the various regions of Figure 1 is given approximately by

$$\frac{v_s^2}{v_c^2} \approx \begin{cases} \frac{1}{3} \frac{\rho_G}{P_G} & \text{region Ib} & (4.11a) \\ \frac{4}{3} \frac{P_R}{P_G} & \text{region Ia} & (4.11b) \\ \frac{5}{3} & \text{region II} & (4.11c) \end{cases}$$

[Here we have used the facts that $q \approx 1/3$ if $P_R \gg P_G$ and that $q \approx 2/3$ if $P_G \gg P_R$ - again assuming that the gas is non-relativistic and is composed of single particles like ionized hydrogen.] Thus v_s^2/v_c^2 is of order unity in region II of Figure 1 but greatly exceeds unity elsewhere in the figure. Hence Φ and φ agree in region II. Outside of region II however, the Péclet number φ is bound to be in serious error. As an extreme example, for the idealized equation of state with $P_G = 0$ [Maraschi et al., (1974); Kafka and Mészáros (1976); Begelman (1978)], χ vanishes because $v_c^2 = 0$ [cf. (4.4)], and this makes φ infinite! However it is certainly not true that diffusion becomes unimportant in the limit $P_G \rightarrow 0$. In this limit, $\chi v_s^2/v_c^2$ remains finite, and thus Φ continues to provide an accurate estimate of adiabaticity.

The critical reader may object that all of the dimensional-analysis approaches to the question of adiabaticity discussed in this section, including the Φ proposed here, are swindles inasmuch as, to obtain anything like accurate results in the outer, hydrostatic region of our solutions for example, one must be prescient enough to use the (a priori unknown) scale height for the luminosity in expression (4.7) for Φ -- rather than, say, the density scale height [cf. (3.2) and (3.3)]. This objection is of course entirely valid and merely underscores the tentativeness of any dimensional-analysis approach to physics: it is no substitute for actually solving equations.

5. Relativistic Accretion: The Case $\rho_R > \rho_G$

Here we discuss solutions which lie in region Ib of Figure 1. In this region, the adiabatic sound speed is nearly equal to its limiting value,

$$v_s^2 = \frac{1}{3} \quad (5.1a)$$

[cf. equation (4d) of paper II]. The corresponding sonic radius for the adiabatic accretion problem is

$$r_s = 3M \quad (5.1b)$$

[equation (9) of paper II]. Hence accretion in this regime is necessarily relativistic, and solutions will be approximately hydrostatic down to radii of the order given by (5.1b).

We have already seen in equation (4.8) that $\chi v_s^2/v_c^2$ is much smaller in region Ib of Figure 1 than it is in region Ia. This is due to the presence of the factor A in equation (4.4) for $\chi v_s^2/v_c^2$. From (3.5),

A is given by

$$A = \frac{\rho_G}{\rho + P} \approx \begin{cases} \frac{3}{4} \frac{\rho_G}{\rho_R} & \text{region Ib} \\ 1 & \text{elsewhere} \end{cases} \quad (5.2a)$$

$$(5.2b)$$

Thus solutions in region Ib of Figure 1 will be far more adiabatic than otherwise comparable solutions in region Ia. This effect has a simple physical explanation which we shall briefly describe here.

The first moment of the radiative transfer equation in the diffusion limit is

$$\frac{L}{4\pi r^2} = - \frac{4P_R}{\rho_0 \kappa_1} Y \left(\frac{1}{4} \frac{P'_R}{P_R} + \frac{Y'}{Y} \right) \quad (5.3a)$$

[equation (18f) of paper I]. The term Y' in the parentheses on the right is just the radial acceleration of the accreting gas [cf. equation (5) of paper I], and its presence in (5.3a) is a relativistic correction which takes into account the inertia of the energy which is being transported relative to the gas rest frame. This term is given by the momentum equation [(1b) of paper II]. Thus we have

$$\frac{L}{4\pi r^2} = - \frac{4P_R}{\rho_0 \kappa_1} Y \left(\frac{P'_R}{4P_R} - \frac{P'}{\rho + P} \right) , \quad (5.3b)$$

and now it is quite clear that, as $\rho + P \rightarrow 4P_R$ ($P \rightarrow P_R$) in region Ib, the "correction" largely cancels the entire effect! With LTE, the surviving piece is only

$$\frac{L}{4\pi r^2} = - \frac{4P_R}{\rho_0 \kappa_1} Y A \left(\frac{T'}{T} - v_c^2 \frac{\rho_0'}{\rho_0} \right) \quad (5.3c)$$

[cf. (4f,e,c) and (B9) of paper II] - hence the appearance of the factor A in (4.4).

This relativistic suppression of heat flux is sufficiently great to guarantee that all solutions in region Ib of Figure 1 will be essentially adiabatic. From (4.7) and (4.8a) we have

$$\bar{\phi} \approx 4 \frac{\rho_R}{\rho_G} \frac{h}{\lambda_\gamma} v \quad (5.4)$$

in region Ib. $\bar{\phi}$ will attain a minimum along a given solution for $v \lesssim v_s = 1/\sqrt{3} \sim 1$, whereas the other factors in (5.4) are large - ρ_R/ρ_G because we are considering region Ib and h/λ_γ because the diffusion approximation must hold.

Since solutions in region Ib of Figure 1 are essentially adiabatic, we can readily establish all the desired results analytically. First, the luminosity at infinity, as always, is given by the value of L_s there [cf. equation (3.4)]. Again, in region I of Figure 1, this value is essentially equal to the Eddington luminosity. The rest mass accretion rate $\dot{M}_0 = 4\pi r^2 \rho_0 v Y$ [equation (1a), paper II] can be evaluated at the sonic point (sp) using equations (5.1):

$$\dot{M}_0 = 4\pi(3M)^2 \rho_{0 \text{ sp}} \frac{1}{\sqrt{3}} Y_{\text{sp}} \quad (5.5)$$

From (3.6) and (5.1) we have $Y_{\text{sp}} = 1/\sqrt{2}$. To get $\rho_{0 \text{ sp}}$ in terms of $\rho_{0 \infty}$, use the relativistic Bernoulli equation

$$HY = \text{constant} \quad (5.6a)$$

[equation (5c) of paper II], where

$$H \equiv \frac{\rho + P}{\rho_0} \quad (5.6b)$$

is the total enthalpy, including rest mass, per unit rest mass. In region Ib of Figure 1, $H \approx 4 P_R/\rho_0$ which is proportional to $\rho_0^{1/3}$ for adiabatic flow. Hence $\rho_0 Y^3$ is constant and $\rho_{0 \text{ sp}} = 2\sqrt{2} \rho_{0 \infty}$. Thus we have

$$\dot{M}_0 = 4\pi 6\sqrt{3} M^2 \rho_{0 \infty} \quad (5.7)$$

It is quite a tribute to the robustness of Bondi's non-relativistic theory that his formula for the accretion rate (3.7) is only off by a factor of $1/2\sqrt{2}$ in this case. Combining our result for the luminosity at infinity with this result for the accretion rate, we have for the efficiency $\epsilon \equiv L_{\infty}/\dot{M}_0$

$$\epsilon = \frac{1}{3\sqrt{3}} \frac{\lambda_{\gamma\infty}}{2M} \quad (5.8)$$

where $\lambda_{\gamma\infty}$ is the photon mean free path at infinity [cf. equation (4.3)].

6. Stability Against Convection

In a static, chemically homogeneous star, the criterion for stability against convection is the well-known Schwarzschild criterion $|dT/dr| < |dT/dr|_{Ad}$ [Schwarzschild (1906)], which can be expressed more

simply as $dS/dr > 0$, where S is the entropy per unit rest mass. The direction dr appears in this formulation solely because, in a static star, the Newtonian "force of gravity" acts in the direction of decreasing r . By the equivalence principle, an accelerated blob of fluid will be unstable to convection if its entropy gradient points in a direction opposite to its acceleration. In our problem, this acceleration, including the Newtonian "gravitational acceleration", is given by the momentum equation [(1b) of paper II] which can be written as

$$a_{\hat{r}} = - \frac{\gamma P'}{\rho + P} \quad , \quad (6.1)$$

where $a_{\hat{r}}$ is the radial acceleration [cf. equation (5) of paper I]. Thus the acceleration is directed opposite to the pressure gradient, and we have the more general criterion for stability against convection

$$\frac{dS}{dP} < 0 \quad . \quad (6.2)$$

It might be thought that, even in this form, the simple criterion (6.2) cannot be applied to our problem because our solutions are not static. A careful analysis of the stability of our solutions, including non-convective instabilities, is an interesting and worthwhile task but is one which is well beyond the scope of this paper. In what follows we shall give a few simple but compelling heuristic arguments in favor of the validity of (6.2) as the appropriate criterion for stability against convection in our problem.

From (6.1), radially adjacent fluid elements will experience different outward radial accelerations if they happen to lie in regions with different YP' (pressure force) or if they have different values of $\rho + P$ (buoyancy effect). In either case, relative motion of the two fluid elements commences.

Consider a localized Lagrangian perturbation in the radial velocity of the form

$$v_1 \sim e^{ik_x x} \quad (6.3)$$

where subscript 1 denotes a perturbation value and where x is some coordinate perpendicular to r . The time scale to restore horizontal pressure equilibrium if it should be disturbed by (6.3) is $1/v_s k_x$, which is finite. The time scale on which (6.3) would try to drive horizontal pressure differences is h/v_1 where h is the pressure scale height. Since v_1 is infinitesimal this time scale is effectively infinite. Thus horizontal pressure equilibrium prevails.

Suppose, for the sake of definiteness, that our unperturbed solution has $P' < 0$ [as is always the case] and $S' < 0$ so that the stability criterion (6.2) is violated. Then the perturbation (6.3) will draw up high entropy material from below and place it radially adjacent to lower entropy material it has pulled down from above. With horizontal pressure equilibrium, the only source of relative acceleration in equation (6.1) is differences in ρ . Then, assuming only $(\partial\rho/\partial S)_p < 0$ [as is always the case], the material which has been uplifted experiences the greater outward radial acceleration, i.e., the perturbation is unstable and the

convective motion is driven. If we assume instead that $S' > 0$ in our unperturbed solution, the conclusion is reversed.

Processes taking place on the background Lagrangian time scales h_i/v , where h_i are scale heights, seem to be irrelevant here because the unperturbed solution is spherically symmetric, and thus these processes affect radially adjacent fluid elements equally. The horizontal compression of the fluid as it moves inward will cause k_x to vary as $1/r$, but this will not affect our conclusion. The vertical stretching of the fluid as it moves in ($v' < 0$) tends to reduce, but can never reverse, the horizontal entropy contrasts caused by (6.3). Similarly, horizontal heat flow can only reduce, but can never reverse, these entropy contrasts.

The result is a slowing down of the initial growth rate of the perturbation (6.3), but, again, not a change in the stability criterion (6.2). This is obvious physically; it also follows from a study of the roots of the appropriate limit ($\Omega \rightarrow 0$, $\nu \rightarrow 0$) of the dispersion relation given by Goldreich and Schubert (1967) [their equation (32)].

Still, it would be a mistake to regard (6.2) as the last word on stability against convection in our solutions. We have argued that there are localized Lagrangian perturbations which grow. A comprehensive analysis could conceivably turn up effects we've not anticipated. More likely, it might cause us to reinterpret, or interpret more carefully, what we mean by stability in an accretion flow. In the meantime, however, we shall presume that solutions which satisfy (6.2) are stable against convection and that those which violate it are not. We can take

considerable comfort in the fact that convection will be an important energy transport mechanism only when the convective velocity exceeds the inflow velocity. Hence it will only be important in the subsonic, quasi-hydrostatic region of our solutions, and it is very hard to imagine (6.2) being wrong in these regions.

We have already remarked that $P' < 0$ in all of our solutions. Hence, for our purposes, the stability condition (6.2) is equivalent to $S' > 0$. From equation (3e) of paper II, we have the fundamental relationship

$$\hat{L}' = \dot{M}_0 Y T S' \quad (6.4)$$

where $\hat{L} \equiv (1+v^2)Y^2 L$; so we can deduce the sign of S' just by looking at the run of \hat{L} versus r in our solutions.

Figures 2 and 3, which show solutions lying in region Ia of Figure 1, plot L rather than \hat{L} , but it's easy to check that the monotonic rise of L with radius shown in these figures is a property shared by \hat{L} as well. Thus these solutions have $S' > 0$ and are stable against convection. This same information is contained in the plots of $\alpha(r)$ of course. The fact that $\alpha < 1$ in these solutions means that the temperature gradient is subadiabatic [cf. equation (3.1)].

It is not necessary to have numerical solutions to find out whether \hat{L} is an increasing or a decreasing function of r . As was emphasized in paper II, \hat{L} is always very nearly equal to $\hat{L}_s \equiv (1+v^2)Y^2 L_s$ [except near the subcritical point ($v=v_s$) where \hat{L}_s has a pole], and it is easy to deduce the radial dependence of \hat{L}_s from equation (3.4) for L_s . We

have already pointed out in §3 how this procedure gives the correct $r^{1/2}$ dependence of L and L_s at small radii for solutions lying in region Ia of Figure 1. Thus, in this region of Figure 1, \hat{L} increases steadily with radius until it reaches its asymptotic value at infinity. Hence all solutions in region Ia of Figure 1 are stable against convection. A similar analysis of the supersonic asymptote of (3.4) for solutions in region Ib of Figure 1 yields the behavior $L_s \propto Yr$ at small radii, so again \hat{L} increases with radius to meet its asymptotic value at infinity. Hence all solutions in region Ib of Figure 1 are also stable against convection.

We have found that solutions throughout region I of Figure 1 are stable against convection. It is extremely interesting that the same conclusion does not hold for solutions lying in region II.

7. Solutions with $P_{G\infty} > P_{R\infty}$

In this section we discuss solutions which start out at radial infinity in region II of Figure 1. First, it needs to be pointed out that such solutions will not necessarily remain in region II as they proceed inward. For example, if the accreting gas has an adiabatic index γ_G of 5/3, like ionized hydrogen, then an adiabatic solution starting out in region II obeys

$$(\eta - \eta_\infty) + \ln \frac{\eta}{\eta_\infty} = \ln \frac{\rho_o}{\rho_{o\infty}}, \quad (7.1a)$$

where

$$\eta \equiv \frac{8P_R}{P_G}, \quad (7.1b)$$

as it proceeds inward. Hence, with η_∞ small, such a solution will attain $\eta = 1$ when

$$\frac{\rho_o}{\rho_{o\infty}} \approx \frac{e}{\eta_\infty} \quad (7.2)$$

and will actually cross over into region I when $\rho_o/\rho_{o\infty} \approx 8e^8/\eta_\infty$. We shall see below that diffusion will only hasten this approach to $\eta \sim 1$. Note that such a solution will be unable to attain $\eta \gg 1$ outside the horizon of the black hole.

Using the fact that an adiabatic solution has $\rho_o/\rho_{o\infty} \sim (r_o/r)^{3/2}$ for $r \ll r_o$, where $r_o = M/2 v_{s\infty}^2$ for $\gamma_G = 5/3$ (Bondi 1952), (7.2) is equivalent to $r/r_o \approx (\eta_\infty/e)^{2/3}$ or $r/2M \approx (\eta_\infty/e)^{2/3}/4 v_{s\infty}^2$. Hence an adiabatic solution with $\gamma_G = 5/3$ attains $\eta = 1$ outside the black hole's horizon if it starts out with

$$\left(\frac{T_4}{\rho_0^{2/3}} \right)_\infty \gtrsim .1 \quad (7.3)$$

(here T_4 is $T/10^4$ °K and ρ_0 is measured in g/cm^3). Since (7.3) holds good for the entirety of region II, it follows that for $\gamma_G = 5/3$ all solutions starting out in this region of the figure will attain $\eta = 1$ well outside the horizon of the black hole.

The principal result to be reported in this section is that solutions which start out at radial infinity with $P_G \gg P_R$ and $\gamma_G \geq 17/12$ are unstable to convection down to the point where $q = 5/12$. If $\gamma_G = 5/3$, this corresponds to the point where $\eta = 3$ or $8P_R = 3P_G$. Interior to this point, the solution is stable against convection.

First, consider that part of region II with $P_G \gg P_R$. There we have

$$\frac{A}{b} \frac{4P_R}{\rho_0} \approx \frac{4P_R}{P_G} \propto \frac{T^3}{\rho_0} \quad (7.4a)$$

and

$$v_s^2 \propto T \quad (7.4b)$$

Consequently, we have the following behavior of L_s on the two asymptotes of equation (3.4):

$$L_s \propto \frac{T^3}{\rho_0^{\kappa_1}} \quad \left\{ \begin{array}{ll} rT & v \gg v_s \quad (7.5a) \\ 1 & v \ll v_s \quad (7.5b) \end{array} \right.$$

[constant factors have been omitted]. Now assume for the moment that the solution is nearly adiabatic [relaxing this assumption only strengthens our conclusions!] and suppose, for the sake of definiteness, that $\gamma_G = 5/3$ so $T^3 \propto \rho_0^2$. Then, using the free-fall approximation $\rho_0 \propto r^{-3/2}$ in (7.5a), we have that

$$L_s \propto \rho_0 / \kappa_1 \quad (7.6a)$$

on both of its asymptotes, whence

$$L \propto \rho_0 / \kappa_1 \quad (7.6b)$$

everywhere. Since ρ_0 is everywhere a decreasing function of r , \hat{L} now decreases with radius, and this means our solution is unstable to convection. This is true in region IIa of Figure 1 where κ_1 is constant and equal to the electron scattering opacity, and in region IIb, where bremsstrahlung opacity dominates, the prospects for stability are even worse, as $\kappa_b \propto \rho_0 / T^{7/2}$; so in this region $L \propto T^{7/2}$, which falls off even faster with radius ρ_0 .

Now to determine the point where our solution makes the transition from the unstable region of Figure 1 to the stable region, note that by making use of the thermodynamic identity $(v_s^2 - v_c^2) = b(q - v_c^2)$ we have quite generally

$$L_s \propto r T^4 / \rho_0 \quad (7.7)$$

on the supersonic asymptote of equation (3.4) (here we have used the fact that $\kappa_1 \approx \kappa_{es} = \text{constant}$ for $P_R \sim P_G$ and have ignored constant or nearly constant factors). With $L \approx L_s$, or directly from equation (1d) of paper II, it is easy to see that L also will obey (7.7). Then with

$r \propto \rho_0^{-2/3}$ we see that L will be stationary when $T^4/\rho_0^{5/3}$ is constant, i.e., when $d \ln T/d \ln \rho_0 = 5/12$. But at this point, the solution is strictly adiabatic [cf. (6.4)]. Hence the solution makes the transition from instability to stability against convection when $q = 5/12$ [cf. (3.1b)].

Since our equations make no provision for convection, we cannot use them for a quantitative study of solutions which start out in region II of Figure 1. We can, however, gain considerable insight as to how such solutions will behave by means of certain simple considerations.

First, take the easiest case: forbid all diffusion and hold in check all convection. Then we have adiabatic flow, and, from equation (9a) of paper II, the accretion rate will be

$$\dot{M}_0 = \xi \pi M^2 \rho_{0\infty} / v_{s\infty}^3 \quad (7.8a)$$

(neglecting small relativistic corrections), where

$$\xi \equiv \frac{\left(\rho_0 v_s^{-3} \right)_{sp}}{\left(\rho_0 v_s^{-3} \right)_{\infty}} \quad (7.8b)$$

will lie in the range

$$1 < \xi < 2\sqrt{2} \quad (7.8c)$$

for $\gamma_G = 5/3$ (Bondi 1952), the exact value depending on η_{∞} .

Now turn on diffusion, but continue to artificially suppress convection. Then the diffusive luminosity at infinity is immediately given by the value of L_s there. Thus we have from equation (3.4)

$$L_{\infty} \approx \frac{8}{5} \left(\frac{P_R}{P_G} \right)_{\infty} \frac{4 \pi M}{\kappa_{1 \infty}} \quad (7.9)$$

in region II. This is much smaller than the Eddington luminosity of course. First, $\kappa_{1 \infty}$ can be dominated by bremsstrahlung (region IIb), an obvious effect. In addition, L_{∞} is down by the factor $8P_R/5P_G$, which arises physically because in region II the radiation pressure gradient provides only a small fraction of the total pressure gradient needed to support the outer nearly hydrostatic regions of our solutions. Indeed, equation (7.9) can be derived from the equation of approximate hydrostatic equilibrium and the equation of radiation force balance relating L to P'_R (to get the factor of $8/5$, use the adiabatic approximation $d \ln T / d \ln \rho_0 \approx q \approx 2/3$).

Turn now to the effect of diffusion on the accretion rate in region II. We have already seen that in region II, as long as $q > 5/12$, diffusion induces superadiabatic temperature gradients. Hence pressure will now increase inward more rapidly than is assumed by the adiabatic formula (7.8), and this will cause the accretion rate to be less than the adiabatic rate.

It is important to check whether diffusion will have an appreciable effect on the accretion rate. Note from equation (4.8) that $\chi v_s^2/v_c^2$ is much smaller in region II than it is in region Ia. First, λ_{γ} tends to be smaller because of the higher characteristic densities or, in region IIb, because bremsstrahlung opacity exceeds electron scattering opacity. In addition, $\chi v_s^2/v_c^2$ is down by the factor $8P_R/P_G$ compared to its value in region Ia. This factor is just the ratio of the heat capacities (at constant ρ_0) in the radiation and in the gas (for $\gamma_G = 5/3$). Physically, this factor appears in (4.8c) because in region II

the heat capacity of the fluid is dominated by the gas particles, while the vastly outnumbered photons still bear the burden of diffusively transporting the energy.

We can estimate whether or not energy diffusion will have a significant effect on the accretion rate by looking at $|\bar{\Phi}(r_0)|$, where $r_0 = M/2 v_{s\infty}^2$. If this quantity is large, diffusion will have a negligible effect on the accretion rate. From (4.7) and (4.8c), with $h \sim r_0$, $v \sim v_{s\infty}$, and other factors approximately equal to their values at infinity, we have

$$|\bar{\Phi}(r_0)| \sim \frac{3}{16} M \left(\frac{P_G}{P_R} \frac{\rho_0 \kappa_1}{v_s} \right)_\infty \quad (7.10a)$$

$$\approx 4 \times 10^{12} \frac{M}{M_\odot} \left(\frac{\rho_{02}^2}{T_7^{7/2}} \frac{\kappa_1}{\kappa_{es}} \right)_\infty \quad (7.10b)$$

[In equation (7.10b), ρ_{02} is ρ_0 measured in units of 100 g/cm^3 and T_7 is temperature in units of 10^7 Kelvin - values characteristic of the sun's center.] From (7.10b) it follows that, for $M \gtrsim M_\odot$ diffusion will not have a significant effect on the accretion rate of a solution which starts out in region II of Figure 1.

Now, finally, we must allow convection to proceed. Convection will provide an additional luminosity and will change the temperature gradient of our solutions. In a static star, the effect of convection is always to push the temperature gradient back down towards its adiabatic value. Not so here. With convection, equation (6.4) will be modified to

$$\hat{L}'_d + \hat{L}'_c = \dot{M}_0 Y T S' \quad (7.11)$$

where L_d and L_c are now the diffusive and convective luminosities, respectively. \hat{L}_c will be positive, but there is no a priori reason for \hat{L}_c' to be positive - any more than there is an a priori reason for \hat{L}_d' to be positive. If \hat{L}_c' is positive, convection will reduce the magnitude of the temperature gradient and will thus increase the accretion rate; if \hat{L}_c' is negative, convection will steepen the temperature gradient and reduce the accretion rate.

Convection will not be able to significantly perturb our solution away from adiabatic inflow at radial infinity. Hence the result (7.9) for the diffusive luminosity at infinity will remain valid even when convection is present.

8. Conclusion

From the discussions in the preceding sections, it is clear that the behavior of an accreting black hole depends very much on what it is being fed. In the different regions of Figure 1, a wide variety of different physical effects become important and each changes the accretion picture in a different way. In this report, we have tried to give a coherent account of why these effects arise, when they will be important, and how they will affect our accretion solutions.

Because of the wide diversity of accretion regimes considered in this paper, it is possible to give a comprehensive overview of diffusive accretion only by doing a certain amount of violence to the issues discussed in the preceding sections. Nevertheless it seems a good idea to emphasize in closing that the diffusive accretion problem has a characteristic accretion rate

$$(\dot{M}_o)_{Ad} = \xi \pi M^2 \rho_o \omega / v_s^3 \quad (8.1a)$$

where

$$\xi \equiv \frac{\left(\rho_o v_s^{-3} \right)_{sp}}{\left(\rho_o v_s^{-3} \right)_\infty} \sim 1 \quad (8.1b)$$

is given by Bondi's (1952) theory, and has the diffusive luminosity at infinity

$$L_{d\infty} = \left[\frac{\rho_G}{\rho_o} \frac{4P_R}{4P_R + P_G} \left(1 - \frac{v_c^2}{v_s^2} \right) \frac{4\pi M}{\kappa_1} \right]_\infty \quad (8.2a)$$

$$\approx \begin{cases} L_{\text{Edd}} & \text{region I} & (8.2b) \\ \frac{\gamma_G - 1}{\gamma_G} \left[\frac{4P_R}{P_G} \frac{\kappa_{es}}{\kappa_1} \right]_{\infty} L_{\text{Edd}} & \text{region II} & (8.2c) \end{cases}$$

given in paper II, and hence has a characteristic "efficiency"

$\epsilon \equiv L_{\infty} / \dot{M}_0$ given by

$$\epsilon \approx \frac{2}{\pi} \left[\left(1 - \frac{v_c^2}{v_s^2} \right) \frac{4P_R}{4P_R + P_G} \right]_{\infty} v_{s\infty} \left(\frac{\lambda \gamma}{M/2v_s^2} \right)_{\infty} . \quad (8.3)$$

The result (8.2) for the diffusive luminosity is ironclad. The result (8.1) for the accretion rate, on the other hand, is subject to modification by energy diffusion (region Ia), relativity (region Ib), and convection (region II).

ACKNOWLEDGEMENT

I am deeply indebted to Yekta Gürsel for his invaluable assistance with all phases of the computing involved in this project. Work supported in part by the National Science Foundation [AST79-22012].

References

- Begelman, M. C., 1978. Mon. Not. R. astr. Soc., 184, 53.
- Bondi, H., 1952. Mon. Not. R. astr. Soc., 112, 195.
- Flammang, R. A., 1982. Mon. Not. R. astr. Soc., in press.
- Gear, W. C., 1971. Numerical Initial Value Problems in Ordinary Differential Equations, Prentice-Hall, Inc.
- Goldreich, P. and Schubert, G., 1967. Astrophys. J., 150, 571.
- Kafka, P. and Mészáros, P., 1976. Gen. Rel. Grav., 7, 841.
- Landau, L. D. and Lifshitz, E. M., 1959. Fluid Mechanics, Pergamon Press, Oxford.
- Maraschi, L., Reina, C. and Treves, A., 1974. Astr. Astrophys., 35, 389.
- Potter, D., 1973. Computational Physics, John Wiley and Sons.
- Rees, M. J., 1978. Physica Scripta, 17, 193.
- Schwarzschild, K., 1906. Gesellschaft der Wiss. Göttingen Nach. Math.-Phys. Kl., 1, 41.
- Thorne, K. S., 1981. Mon. Not. R. astr. Soc., 194, 439.
- Thorne, K. S., Flammang R. A. and Żytkow, A. N., 1981. Mon. Not. R. astr. Soc., 194, 475.

Appendix A

Here, equation (4.6) of the text is derived. From (3.1), write

$$\frac{\alpha}{1-\alpha} = \frac{-\left(\frac{T'}{T} - v_c^2 \frac{\rho_o'}{\rho_o}\right)}{\frac{T'}{T} - q \frac{\rho_o'}{\rho_o}} \quad (\text{A1})$$

Next, observe that the numerator of this expression contains the combination of derivatives that determines \hat{L} while the denominator contains the combination which determines \hat{L}' . Thus, from (B2) and (B7) of paper II, we have

$$\frac{\alpha}{1-\alpha} = \frac{B}{A} \frac{\rho+P}{4P_R} v_{\rho_o}^k \frac{\hat{L}}{(1+v^2)Y\hat{L}'} \quad (\text{A2})$$

[where we have also used equations (1a), (2j), (4b,c), and (B9,10) of paper II to simplify the result]. Inserting (4.3) and (4.4) of the present paper into (A2) then yields equation (4.6), the desired result.

Table 2

M	$3M_{\odot}$
$\rho_{O,\infty}$	$7.81 \times 10^{-9} \text{ g/cm}^3$
T_{∞}	$.982 \times 10^6 \text{ }^{\circ}\text{K}$
$v_{s,\infty}$	$2.11 \times 10^{-2} \text{ [c]}$
$v_{c,\infty}$	$4.25 \times 10^{-4} \text{ [c]}$
\dot{M}_O	$4.65 \times 10^{-6} \text{ } M_{\odot}/\text{yr}$
$(\dot{M}_O)_{\text{Ad}}$	$6.90 \times 10^{-7} \text{ } M_{\odot}/\text{yr}$
$(\dot{M}_O)_{\text{Beg}}$	$4.98 \times 10^{-6} \text{ } M_{\odot}/\text{yr}$
L_{∞}	$.982 \times 10^5 \text{ } L_{\odot}$
$L_{s,\infty}$	$.982 \times 10^5 \text{ } L_{\odot}$

Table 3

M	$3M_{\odot}$
$\rho_{O,\infty}$	$1.96 \times 10^{-9} \text{ g/cm}^3$
T_{∞}	$1.24 \times 10^6 \text{ }^{\circ}\text{K}$
$v_{S,\infty}$	$6.68 \times 10^{-2} \text{ [c]}$
$v_{C,\infty}$	$4.77 \times 10^{-4} \text{ [c]}$
\dot{M}_O	$4.67 \times 10^{-7} M_{\odot}/\text{yr}$
$(\dot{M}_O)_{\text{Ad}}$	$5.45 \times 10^{-9} M_{\odot}/\text{yr}$
$(\dot{M}_O)_{\text{Beg}}$	$4.97 \times 10^{-7} M_{\odot}/\text{yr}$
L_{∞}	$.983 \times 10^5 L_{\odot}$
$L_{S,\infty}$	$.983 \times 10^5 L_{\odot}$

Figure Captions

Fig. 1. This figure shows the location, in the temperature-density plane, of the various different physical accretion regimes considered in the text. In region I, radiation pressure exceeds gas pressure; and, in region Ib, the energy density in radiation exceeds that in the rest mass of the gas. In region II, gas pressure exceeds radiation pressure; and, in region IIb, bremsstrahlung opacity dominates electron scattering opacity. In region III the electrons are degenerate. This region is not considered in this paper. In this figure the temperature T and the rest mass density ρ_0 are measured in cgs units.

Fig. 2. This figure shows the radial dependence of various quantities of interest for the solution with the parameters of Table 2. The velocities v , v_s , and v_c are the inflow velocity, the adiabatic sound speed, and the isothermal sound speed, respectively, all measured in units of the speed of light. The dark spot, where $v = v_c$, marks the critical point; the open circle, where $v = v_s$, marks the subcritical point. The rest mass density ρ_0 and the temperature T are in cgs units. The luminosities L and L_s are in solar units. The local adiabaticity α , which is plotted on a linear scale, is dimensionless. See §3 for definitions and discussion.

Fig. 3. This figure shows the radial dependence of various quantities of interest for the solution with the parameters of Table 3. Symbols and units are as in Figure 2. See §3 for discussion.

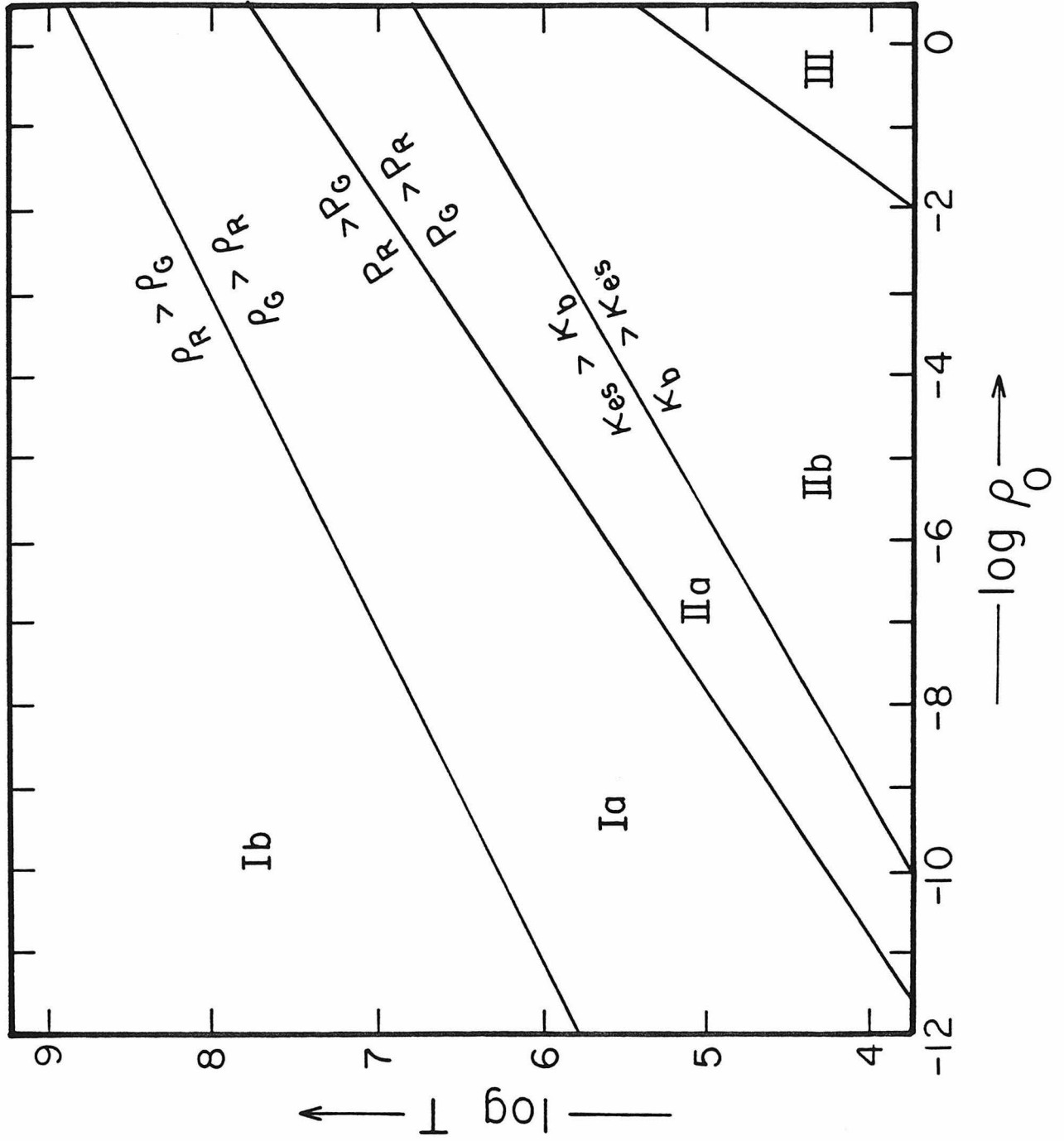


Fig. 1

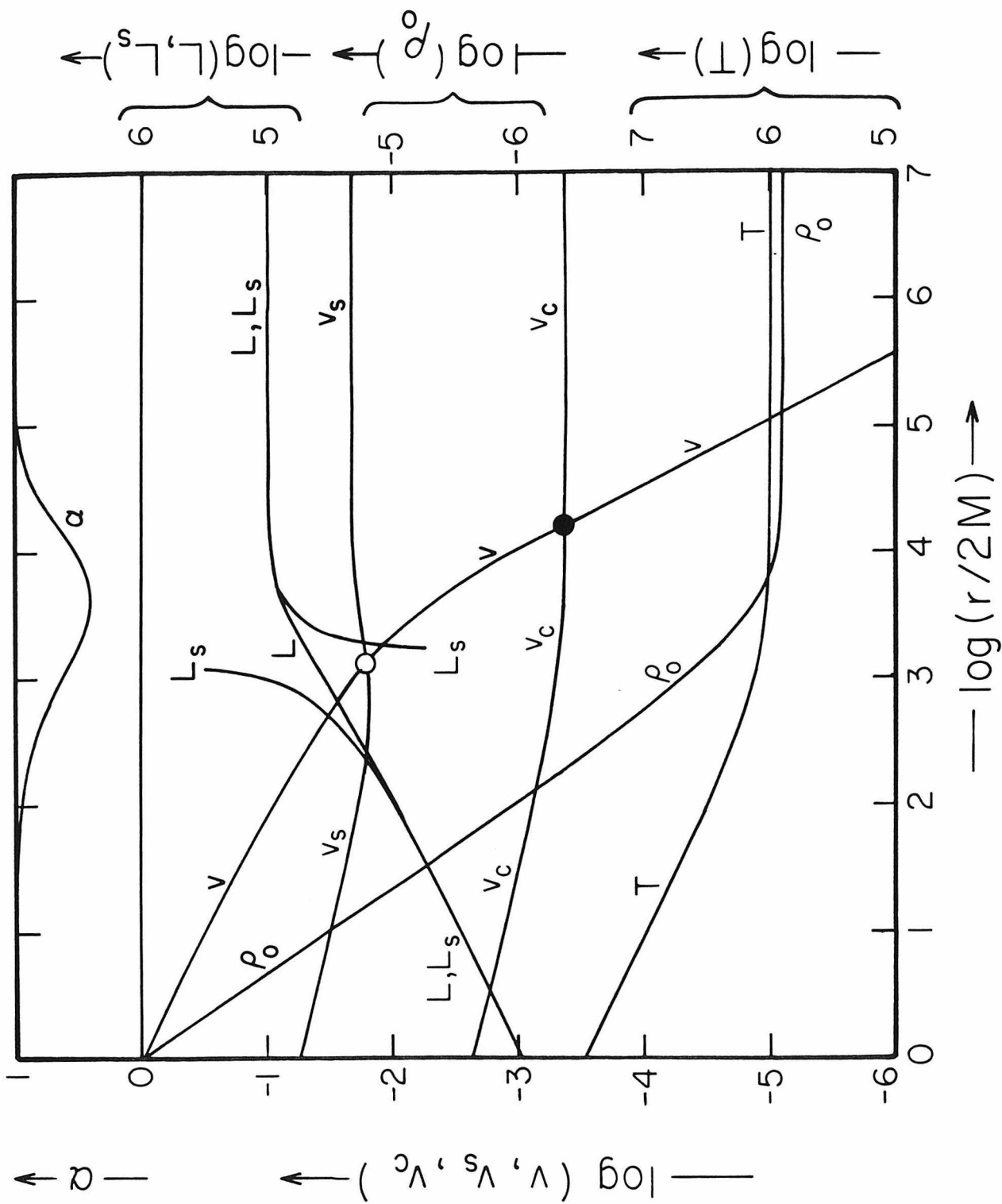


Fig. 2

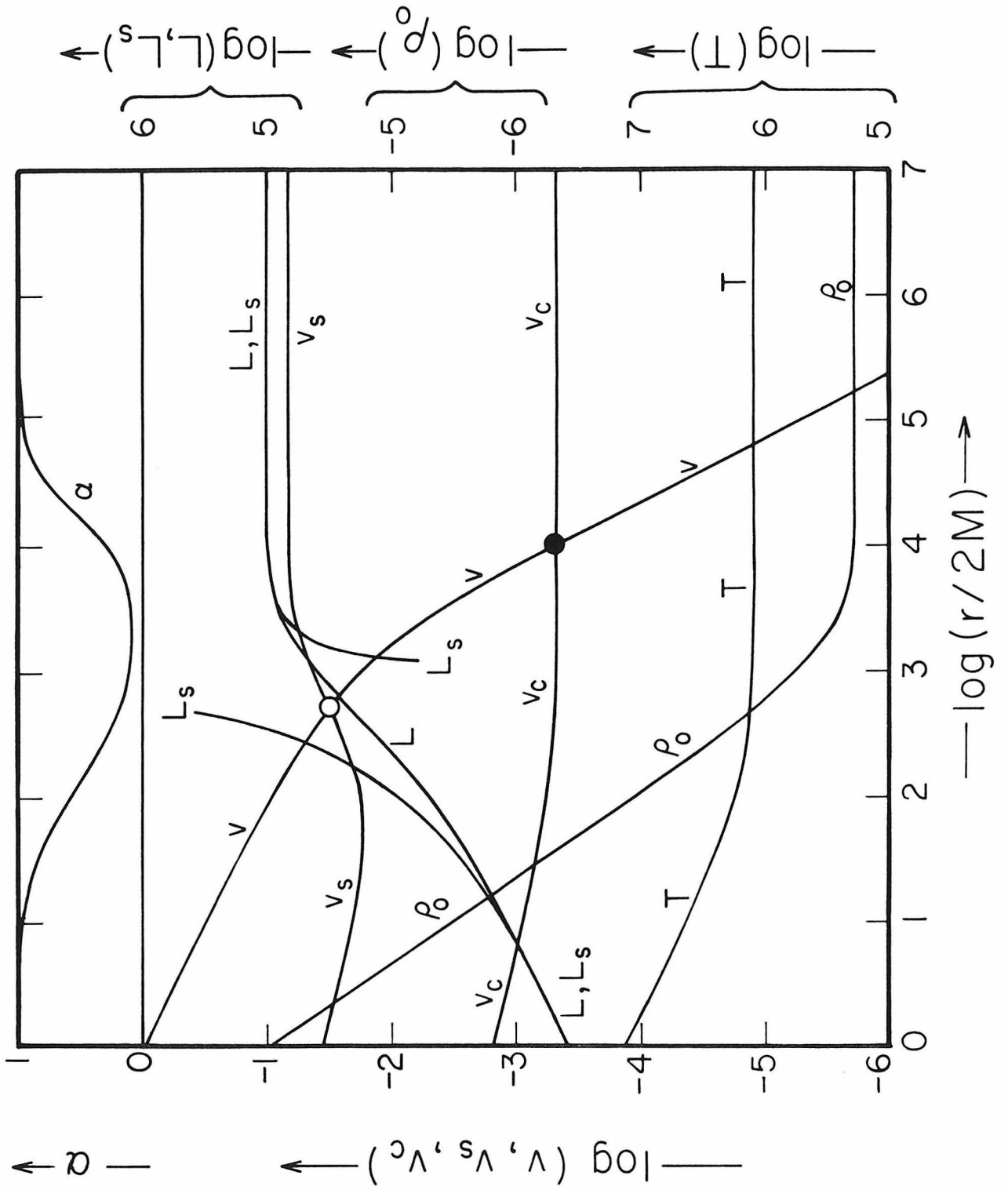


Fig. 3